





LIBRARY Michigan State University

This is to certify that the

dissertation entitled

THE DEVELOPMENT OF A TOUGHENING BINDER FOR GLASS FIBER REINFORCED UNSATURATED POLYESTERS

presented by

Hendrik Rintcius Jacob ter Veen

has been accepted towards fulfillment of the requirements for

PhD degree in Chemical Engineering

Date 5/8/97

MSU is an Affirmative Action/Equal Opportunity Institution

0-12771

Sawrence T. Dysl Major professor PLACE IN RETURN BOX to remove this checkout from your record. TO AVOID FINES return on or before date due.

DATE DUE	DATE DUE	DATE DUE
1000002		

MSU is An Affirmative Action/Equal Opportunity Institution ctoircidatedus.pm3-p.1

THE DE

THE DEVELOPMENT OF A TOUGHENING BINDER FOR GLASS FIBER REINFORCED UNSATURATED POLYESTERS

Ву

Hendrik Rintcius Jacob ter Veen

A DISSERTATION

Submitted to
Michigan State University
in partial fulfillment of the requirements
for the degree of

DOCTOR OF PHILOSOPHY

Department of Chemical Engineering

1997

THE D

Glass F manufact

is placed

The fiber

develop a

Statistica

design a

propertie

was no ca

in the firs

Since thi

ABSTRACT

THE DEVELOPMENT OF A TOUGHENING BINDER FOR GLASS FIBER REINFORCED UNSATURATED POLYESTERS

By

Hendrik Rintcius Jacob ter Veen

Glass Fiber Reinforced Unsaturated Polyesters (GFRUPs) are commonly manufactured by Resin Transfer Molding (RTM). In this method, a fiber preform is placed into a mold. Then, the resin is injected and cured to obtain a solid part. The fiber preform is kept together by a binder. The aim of this research was to develop a binder with toughening characteristics, the 'toughening binder'.

Statistical analysis of flexure test results is used to show that it is possible to design a binder that does not deteriorate the composite properties. The flexure properties correlate moderately to strongly with the fiber volume fraction. There was no correlation with the binder content.

In the first attempt to make a toughening binder, liquid silicone rubber was used.

Since the size of the silicone domains which phase separate from the

unsatural
silicone e

A rubber
commerc
possible t
binder has
The fractu
nubber bin
bridging b
rubber par
bridging fa
composite
The fractu

nbber-ma

acid treatr

resin rich

particles f

unsaturated polyester matrix, could not be controlled by the nature of the silicone end group, this research path was abandoned.

A rubber binder was made from recycled tire rubber by coating it with a commercial binder through a reverse antisolvent phase separation process. It is possible to cover 27 % of the rubber surface with commercial binder. This rubber binder has the same binding characteristics as the commercial binder.

The fracture toughness of the composite can increase by 75 % when 6 % of rubber binder is added to the glass fibers. The toughening mechanism is crack bridging by the rubber particles. The rubber-matrix adhesion is poor but the rubber particles are kept to the fracture surface by the fibers. The particle bridging fails when the fiber-particle interlocking fails. The flex properties of the composite did not change significantly.

The fracture toughness can be increased by an additional 25 % when the rubber-matrix adhesion is improved through a combined UV / ozone and oleic acid treatment. The improved rubber-matrix adhesion caused rubber particles in resin rich areas to participate in the crack bridging. Ultimately, these rubber particles fail through a cavitation mechanism.

Anybody that it is i cover. The The first setbacks Scranton me their i I appreci Research Herman I thank a Brian Ro We tsza and ES

treatme

little this

ACKNOWLEDGMENTS

Anybody who goes through the process of getting an advanced degree knows that it is impossible to do this work alone. Yet, only one name ends up on the cover. The acknowledgments are there to make up for this injustice.

The first person to thank is Dr. Drzal. He helped me through the numerous setbacks that are part of any research project. I am very grateful to Drs. Scranton, Jayaraman, Liu and Baker, the members of my committee, for giving me their time, support and constructive criticism.

I appreciate the financial support from MMPI and DSM Research. Within DSM Research, I have to mention Boudewijn Scholtens, Josephine Brackman, Herman Worries and Ton van der Ploeg for the advice they gave so freely.

I thank all the staff in the Composite Materials and Structures Center. Mike Rich, Brian Rook and Dan Hook taught me how to use the various instruments. Cara Weitszacker, Richard Schalek and Steven Rozeveld helped me with the ESCA and ESEM experiments. Rao Dontula told me all I needed to know about UV treatments. Jean Rooney, Jennifer Sweet and Arlene Klingbiel took care of many little things which I had taken for granted.

Four un Matthew

devoted

Ben and

prose. T

bridge sh

As with a

friends fo

some ped

of mine

India will

His weire

think. I wi

and hidde

a forgiving

Of course

the worrie

The last p

She is wh

to this dis

and emoti

Four undergraduate students have done part of the work for this dissertation.

Matthew Neumann, Michael Grad, Qingsong Liu and Thay Nguyen were devoted, creative, motivated and eager to learn.

Ben and Marie Bohnhorst contributed their share by proofreading this work of prose. They should also be mentioned as the people who showed me how bridge should be played.

As with any job, your colleagues can make or break it. At MSU, I have made friends for life. We had many scientific and philosophic discussions. There are some people whom I especially want to mention. Sanjay Padaki is a great friend of mine. He gave me something that few other people could have given me. India will always have a special place in my heart. Mark Wilenski is a great guy. His 'weirdness' reduces lots of stress, yet he is more normal than many would think. I wish him the very best. Sanjay Yedur's integrity, (apparent) calm, wisdom and hidden enthusiasm were always a good inspiration. He is a great friend and a forgiving bridge partner.

Of course, I thank my brother Jaco and my parents, for the encouragement and the worries: 'Bedankt voor alles.'

The last person to thank is Marketta. She had the patience to wait until the end. She is what I 've always dreamed of and never seemed to get. She contributed to this dissertation in a technical (antisolvent), practical (formatting and printing) and emotional (...) way. 'Kiitos!'

LIST OF

LIST OF

Chapter INTROE

> Chapte FRACT

Chapte THE IN PROPI UNSA

TABLE OF CONTENTS

LIST OF TABLES	ix
LIST OF FIGURES	xi
Chapter 1	
INTRODUCTION	1
Glass Fiber Reinforced Unsaturated Polyesters	1
Preforming	9
Research objective	11
This dissertation	12
References	13
Chapter 2	
FRACTURE AND FRACTURE TOUGHNESS	14
Stresses in the vicinity of a crack	15
The toughening of homogeneous thermosets	21
Toughening mechanisms in fiber reinforced thermoset composites	23
Toughening of random fiber reinforced composites	30
References	33
Chapter 3	
THE INFLUENCE OF COMMERCIAL BINDER ON THE FLEXURE	34
PROPERTIES OF UNIDIRECTIONAL GLASS FIBER REINFORCED	
UNSATURATED POLYESTERS	
Introduction	34
Experimental	35
Results and data treatment	35
Residual analysis	37
Multivariate analysis	43
Discussion	44
Conclusions	47
References	48

Chapter FEASIE TOUGH In E

> C R

Chapter PREPAI ANTISC

Chapte THE E PROP POLY

Chapter 4 FEASIBILITY STUDY FOR THE USE OF SILICONE RUBBER AS A	49
TOUGHENING BINDER	73
Introduction	49
Experimental	50
Results and discussion	50
Estimation of the interchange cohesive pressure	50
FTIR analysis	53
Particle size analysis	57
Conclusions	58
References	59
Chapter 5	
PREPARATION OF A RUBBER BINDER USING A REVERSE ANTISOLVENT PHASE SEPARATION METHOD	60
Introduction	60
Antisolvent processes	61
A thermodynamic model for antisolvent phase separation	63
of a polymer	
Experimental verification and discussion of the ternary mixing model	77
Manufacturing of a rubber binder with a reverse antisolvent phase separation process	78
Characterization of the rubber binder	81
Sieving	83
Surface analysis	83
Environmental Scanning Electron Microscopy	85
Testing of the binding capacity	91
Conclusions	91
References	93
Chapter 6	- 4
THE EFFECT OF THE RUBBER BINDER ON MECHANICAL	94
PROPERTIES OF GLASS FIBER REINFORCED UNSATURATED POLYESTERS	
Fracture toughness testing	94
Introduction	94
Experimental	99
Environmental Scanning Electron Microscopy of fracture surfaces	105
Flexure testing	109
Discussion	112
Conclusions	113
References	114

Chapter
THE EF
MECHA
UNSAT
In
S
F
C
C
Re

Chapter to CONCLU

Appendix Materials

Appendix Turbo Pa program

Appendix Data for

Appendi Data for

Append. Data for

Appendi Data for

Appenda Data for

Chapter 7	
THE EFFECT OF RUBBER SURFACE MODIFICATION ON THE MECHANICAL PROPERTIES OF GLASS FIBER REINFORCED	115
UNSATURATED POLYESTERS Introduction Surface modification Fracture toughness testing	115 115 119
Environmental Scanning Electron Microscopy of fracture surfaces Discussion Conclusions References	122 128 129 130
Chapter 8 CONCLUSIONS	131
Appendix I Materials and experimental procedures	134
Appendix II Turbo Pascal 7.0 source code for the fracture toughness calculation program	140
Appendix III Data for chapter 3	167
Appendix IV Data for chapter 4	170
Appendix V Data for chapter 5	171
Appendix VI Data for chapter 6	172
Appendix VII Data for chapter 7	173

Table 2.

Table 2

Table 3 properti

Table 3 depend the bind

Table 4 intercha

Table 5

Table 5 uncoate as dete

Table (Tubber by ESC

Table 7 determi

Table 7 determi

LIST OF TABLES

Table 2.1 Improvements in fracture toughness or impact strength of unidirectional composites by fiber coating [12]	29
Table 2.2 Improvements in impact strength of random fiber composites	31
Table 3.1 Regression coefficients for the linear regression of the flexure properties with fiber volume fraction	40
Table 3.2 Regression parameters for the multivariate analysis: The dependence of the flexure properties on the fiber volume fraction and the binder percentage, and the correlation coefficients ρ	42
Table 4.1 Dispersive (δ_d) and polar (δ_p) solubility parameters and the interchange cohesive pressure with styrene for the various end groups and styrene	52
Table 5.1 Input parameters used to calculate the solubility of polyester in mixtures of acetone and water (from [8])	73
Table 5.2 Surface elemental composition in atom percent of uncoated rubber particles, rubber binder and polyester powder as determined by ESCA	82
Table 5.3 Surface elemental composition in atom percent of uncoated rubber particles, rubber binder and polyester powder as determined by ESCA, assuming that silicon is present in the form of silica.	84
Table 7.1 Atomic compositions of rubber particle surfaces as determined by ESCA	117
Table 7.2 Atomic compositions of rubber particle surfaces as determined by ESCA, after correcting for silica	117

Table A

Table A flexure

Table A chapter

Table A chapter

Table A

Table A

Table A

Table A

Table A

Table A

Table /

Table Al.1 Composition of the resin mixture	135
Table Al.2 Sample dimensions and testing conditions for the 3 point flexure tests	138
Table AllI.1 0° Flexure data for statistical analysis as described in chapter 3	167
Table AllI.2 90° Flexure data for statistical analysis as described in chapter 3	168
Table AIV.1 Particle size data for Figure 4.2	170
Table AIV.2 Particle size data for Figure 4.3	170
Table AV.1 Miscibility data for Figure 5.3	171
Table AV.2 Sieve data for Figure 5.5	171
Table AVI.1 Fracture toughness data for Figures 6.4 and 6.5	172
Table AVI.2 Data for Figures 6.9 and 6.10	172
Table AVII.1 Fracture toughness data for Figures 7.1 and 7.2	173

Figure in the w

Figure

Figure The un maieic

Figure

Figure the use

Figure of a cr

Figure

Figure bndgi:

Figun

Figur

Figur of a fi

Figur

Figur

LIST OF FIGURES

Figure 1.1 The position of preformed composites, such as GFRUPs, in the world of composites	3
Figure 1.2 Schematic representation of the RTM process	4
Figure 1.3 Structural formulas of unsaturated polyester and styrene. The unsaturated polyester is a random copolymer of phthalic acid, maleic acid and ethylene glycol.	6
Figure 1.4 Reaction mechanism for a radical polymerization	8
Figure 1.5 Schematic process of the manufacturing of a preform with the use of a solid binder	10
Figure 2.1 Schematic representation of stress levels in the vicinity of a crack	16
Figure 2.2 Stress strain curve for an ideally elastoplastic material	19
Figure 2.3 Schematic picture of a craze. Polymeric fibrils are bridging the surfaces of the craze	21
Figure 2.4 Schematic picture of the occurrence of cavitation	22
Figure 2.5 The fibers fracture in the same plane as the matrix	24
Figure 2.6 Fiber pull-out can increase the fracture toughness of a fibrous composite	24
Figure 2.7 Schematic representation of Outwater-Murphy debonding	26
Figure 2.8 Schematic representation of Cook-Gordon debonding	26

Figure function

Figure fraction

Figure percer

Figure fractio calcul

> Figure perce

> > Figure and for

Figur mod:f betwe

> Figur of the

> free e case the to the s

Figu unsa

from The sepa

Figure 3.1 0° Flexure modulus averaged over each panel as a function of fiber volume fraction.	36
Figure 3.2 0° Flexure modulus plotted against the fiber volume fraction V _f	38
Figure 3.3 The residual of the 0° flexure modulus plotted against the percentage of binder on the fibers	40
Figure 3.4 90° Flexure modulus plotted against the fiber volume fraction V _f . The solid line represents the 90° Flexure modulus as calculated with equation 3.2	41
Figure 3.5 The residual of the 90° flexure modulus plotted against the percentage of binder on the fibers	42
Figure 4.1 FTIR spectra for unreacted silanol terminated PDMS and for the same PDMS after reaction with cresol	54
Figure 4.2 Number and volume average particle sizes of end group modified PDMS as a function of interchange cohesive pressure, A_{12} , between the end group and styrene	55
Figure 4.3 Silicone particle size as a function of the solubility parameter of the end group and of the relative mass of the end group	56
Figure 5.1 Example of a Gibbs free energy of mixing plot. The Gibbs free energy of mixing is given as a function of solute fraction. In this case, the mixture will separate into two phases. The composition of the two phases can be found from the points where the curve touches the straight line ($x_2 = 0.15$ and $x_2 = 0.78$).	68
Figure 5.2 Molecular formulas of dimethyl phthalate and unsaturated polyester.	74
Figure 5.3 Phase diagram for a mixture of polyester and acetone/water from calculations for T = 280 K (▲), T = 300 K (X) and T = 320 K (●). The graph also shows working data for the occurrence of phase separation (★). The working data may not represent thermodynamic equilibrium.	76

Figure 5.4 Schematic setup of the reverse antisolvent phase separation process	79
Figure 5.5 Weight based particle size distribution of the 40 mesh rubber particles	82
Figure 5.6 ESEM micrograph of untreated rubber particles. The box marks the field of view for Figure 5.7	86
Figure 5.7 ESEM micrograph of untreated rubber particles	87
Figure 5.8 ESEM micrograph of rubber binder particles	88
Figure 5.9 ESEM micrograph of rubber binder particles. The box marks the field of view for Figure 5.10	89
Figure 5.10 ESEM micrograph of rubber binder particles	90
Figure 6.1 DCB geometry for fracture toughness testing	95
Figure 6.2 ENF geometry for fracture toughness testing	95
Figure 6.3 A typical set of strain energy release rate curves. Different theories were used to calculate these curves: -▲- Modified Compliance Calibration theory, -X- Compliance Calibration theory, -■- Modified Beam Theory	100
Figure 6.4 Strain energy release rate as a function of rubber binder percentage (solid line to guide the eye)	101
Figure 6.5 Standard deviation in the strain energy release rate as a function of rubber binder percentage (solid line to guide the eye)	103
Figure 6.6 ESEM micrograph of a fracture surface after fracture toughness testing (a = glass fiber bundle, b = pull-out of rubber particle)	106
Figure 6.7 ESEM micrograph of a fracture surface after fracture toughness testing (a = pull-out of rubber particle, b = matrix side of fiber-matrix failure, c = fiber bundle)	107
Figure 6.8 ESEM micrograph of a fracture surface after fracture toughness testing (a = rubber particle, b = fiber bundle, c = brittle matrix failure)	108

Figure Reinford rubber

> Figure (Reinford rubber b

Figure 7 rubber to standar have be

Figure sample standa standa

> Figure tough

> > Figur toug!

Figu toug the v

Fig: toug

Fig tou

Fiç

Fig for the

Figure 6.9 Flexure modulus of Random Continuous Glass Fiber Reinforced Unsaturated Polyester, modified with different levels of rubber binder	110
Figure 6.10 Flexure strength of Random Continuous Glass Fiber Reinforced Unsaturated Polyester, modified with different levels of rubber binder	111
Figure 7.1 The fracture toughness of samples with surface modified rubber binder (x) compared with the fracture toughness of samples with standard rubber binder (♠). Error bars for the standard rubber binder have been removed for clarity.	120
Figure 7.2 The standard deviation in the fracture toughness of samples with surface modified rubber binder (x) compared with the standard deviation in the fracture toughness of samples with standard rubber binder (♦)	121
Figure 7.3 ESEM micrograph of a fracture surface after fracture toughness testing. (a = pull-out of rubber particle)	123
Figure 7.4 ESEM micrograph of a fracture surface after fracture toughness testing. (a = rubber particle, b = matrix)	124
Figure 7.5 ESEM micrograph of a fracture surface after fracture toughness testing. (a = fractured rubber particle) The box indicates the view area for the micrograph in Figure 7.6	125
Figure 7.6 ESEM micrograph of a fracture surface after fracture toughness testing. The box indicates the view area for the micrograph in Figure 7.7	126
Figure 7.7 ESEM micrograph of a fracture surface after fracture toughness testing	127
Figure Al.1 Reaction equation for the end group modification of PDMS	135
Figure Al.2 Cumulative distribution plot. The inverse of the error function of the cumulative distribution is plotted against the logarithm of the particle size, to obtain the distribution parameters σ and μ .	137

Glass I

This the

binder

• *I*t

• It

pr

е

Bind

this

ther

type

GFF

ענס

the

Chapter 1

INTRODUCTION

Glass Fiber Reinforced Unsaturated Polyesters

This thesis describes the development of a toughening binder, more specifically for Glass Fiber Reinforced Unsaturated Polyesters (GFRUPs). The toughening binder has two functions:

- It has to serve as a glass fiber binder, keeping the fibers together in a preform.
- It has to increase the fracture toughness of the composite part by adding an elastomeric phase to the matrix.

Binders are used for various types of composites, with various matrices. Though this research is limited to the development of a toughening binder for GFRUPs, there is no reason to assume that this concept would not be applicable to other types of composites where a binder is used.

GFRUPs are interesting materials for a number of reasons. In general, composite materials are very hi-tech materials. As hi-tech often implies hi-cost, the use of most composites has been limited to applications where extreme

mechan many ∞ GFRUP (far more applicat. body of : since the to manuf Figure 1 GFRUPs point of v Some of strong as is formed falture 7 to be imp The terr glass fit

GFRUP

(RTM).

GFRUP

mechanical properties need to be combined with a low density. That is why many composite materials are found in aerospace applications.

GFRUPs are more 'down to earth'. They are applied in aircraft, but their use is far more widespread. They are often used for automotive and recreational applications. A well-known example is the 'polyester' sailing boat. The whole body of the boat is made out of GFRUP. For this application, GFRUPs are used since they are stiff and strong, they are lightweight and they are relatively easy to manufacture.

Figure 1.1 briefly characterizes the place of preformed composites such as GFRUPs in the world of materials. Their properties are good. Yet, from a cost point of view their usage is still feasible in everyday applications.

Some of the properties of GFRUPs are better than others. GFRUPs are very strong and very stiff. On the other hand, they are also very brittle. Once a crack is formed, they are unable to absorb much energy, which leads to catastrophic failure. This is an area where GFRUPs, as well as many other composites, need to be improved.

The term glass fiber reinforced unsaturated polyester would imply that it covers glass fibers in any form (long, short, unidirectional or random). However most GFRUPs are random short fiber composites made by Resin Transfer Molding (RTM). The research described in this dissertation deals with this type of GFRUP.

Figure 1

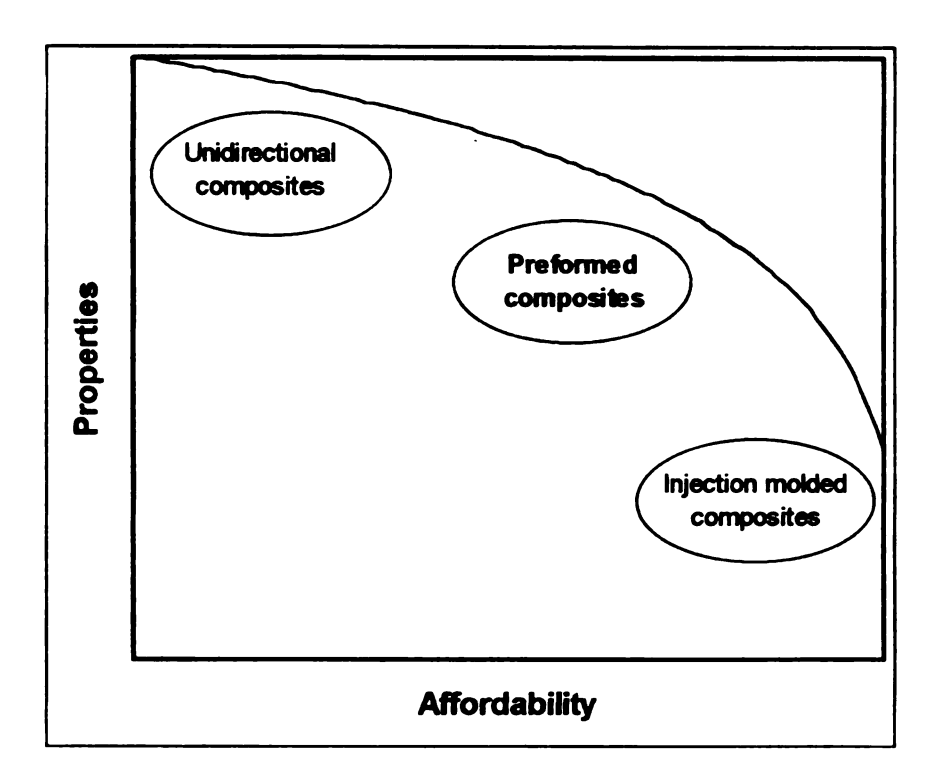


Figure 1.1 The position of preformed composites, such as GFRUPs, in the world of composites

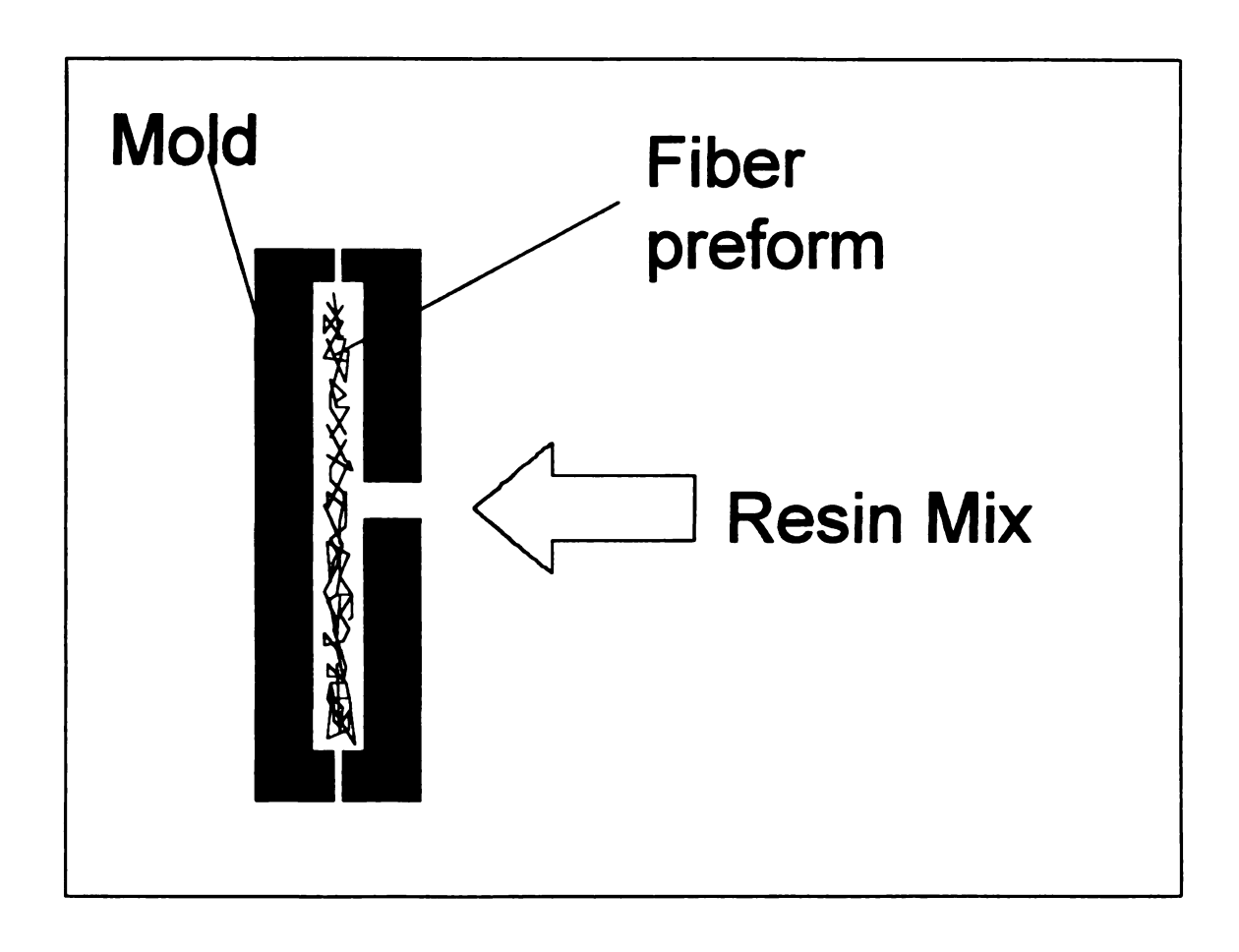


Figure 1.2 Schematic representation of the RTM process

The R placing reinford Then tr **tempe**ra part is resin ar contains formulas 50 % re agents a start the the deco regulate There is manufa:

manufa

stubbor

The RTM process is schematically depicted in Figure 1.2. The process starts by placing a fiber preform in the mold. The preform contains the fiber reinforcements. With the preform in the mold, the mold is closed and evacuated. Then the resin mixture is injected. The resin is cured (hardened) by raising the temperature and applying pressure. After that, the mold is opened and a solid part is obtained. This part can still undergo a postcure cycle to fully cure the resin and give the part its ultimate strength and stiffness. The resin mixture contains the unsaturated polyester resin dissolved in styrene. Their molecular formulas are given in Figure 1.3. A typical mixture would contain approximately 50 % resin and 50 % styrene. Apart from these components several curing agents are needed for the curing of the part. A peroxide initiator is needed to start the curing reaction. An accelerator is added as a homogeneous catalyst for the decomposition of the initiator. In addition, cocatalysts can be used to further regulate the curing rate.

There is some confusion between the scientific terms and the terms used in manufacturing. What is called an initiator in science is called a catalyst in manufacturing. Some scientific purists add to the confusion by correctly, but stubbornly referring to the accelerator as the catalyst.

Figure 1.3 Structural formulas of unsaturated polyester and styrene. The unsaturated polyester is a random copolymer of phthalic acid, maleic acid and ethylene glycol.

The cur mechan

two :

the s

electr

• In the

• In the

One

(reco

monom

very his

which i

thermo

ln⊐ea.

The curing reaction mechanism follows that of a radical polymerization [1,2]. The mechanism of a radical polymerization contains three steps (Figure 1.4):

- The first step is the initiation. In this step, the initiator molecule is split up in two radicals. After that the radical can react with the double bond of either the styrene or the unsaturated polyester to form a new radical. The free electron is shifted to the end of the molecule.
- In the propagation step, the radical is growing rapidly. This is where the molecular weight builds up.
- In the termination step, the free electron at the end of the chain is removed.
 One way for this to happen is for two radicals to react with each other (recombination).

During the first part of the reaction, when there is still a large amount of styrene monomer present, the molecular weight of the new formed polymer molecules is very high. Later in the reaction, the concentration of monomer has gone down, which means that only shorter chains are formed. This is much different from thermosets that cure via a step reaction mechanism, such as epoxies. In that case, the molecular weight of the reactive chains in the polymer network increases continuously.

Pro

Figure ·

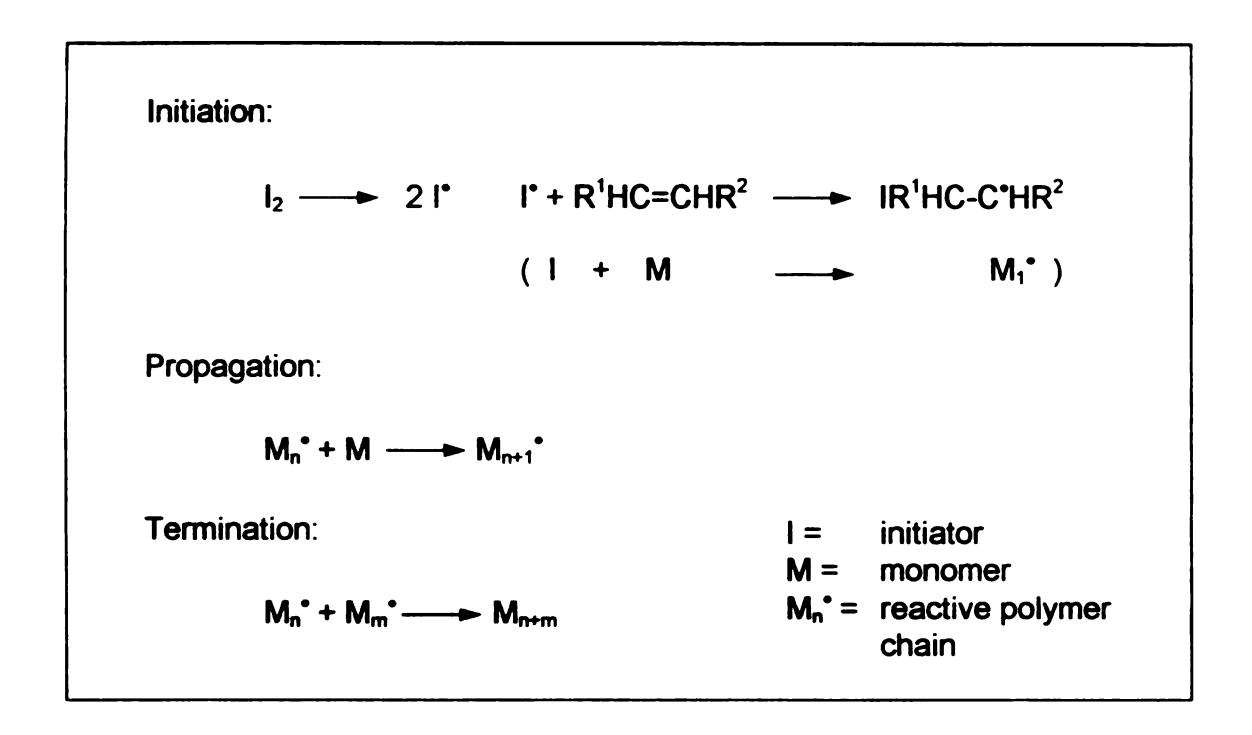


Figure 1.4 Reaction mechanism for a radical polymerization

Preform

As ment

a preformwanted :

that in c

part. Hov

done

There a

preform

technia

SWIT I

Figure

manuf

_...

fibers

vacuu

f:bers

Wr.e

*wo*lα

are I

îêş

بغي

Preforming

As mentioned before, in an RTM process, a fiber preform is used [3,4]. In theory, a preform contains the fibers in the locations and directions where the designer wanted them to be. In practice, many times, preforms are made in such a way that in critical areas the fiber volume fraction is higher than for the rest of the part. However, controlling the direction of fibers is expensive and is hardly ever done.

There are several ways to make a preform. Fibers can be knitted or woven into a preform. A widespread preforming technique is binding the fibers together. This technique is used to manufacture random continuous fiber mats (also called 'swirl' mats) and to make random short fiber preforms.

Figure 1.5 shows schematically one way in which a random short fiber preform is manufactured. A long glass fiber roving is chopped into short (1/8 to 1 inch) fibers. The fibers are blown onto a screen. On the other side of the screen a vacuum is pulled so that the fibers are sucked on the screen. Together with the fibers, a binder powder is blown towards the screen.

When all the fibers have been deposited on the screen, the other side of the mold is closed and the consolidation cycle starts. The temperature and pressure are raised. The binder can flow over the fibers. After cooling down, the binder has solidified and a rigid preform is obtained. Typically a fiber preform contains between 2 and 10 weight percent of binder.

Vac

Figure a scho

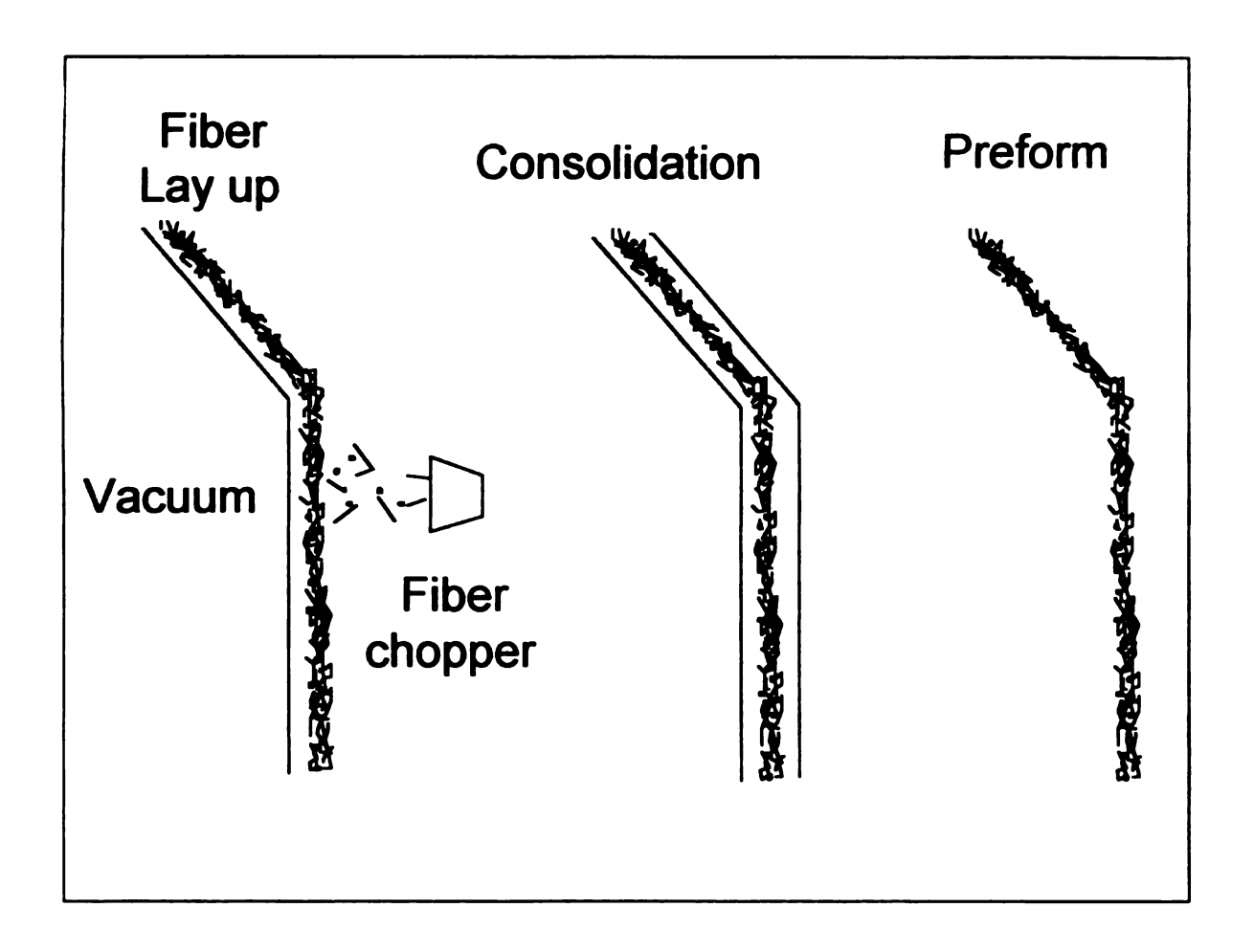


Figure 1.5 Schematic process of the manufacturing of a preform with the use of a solid binder

during adhesic compositions reaction can dissimatrix rules final compositions are constitutive final compositions.

Resea

more b

and a associated

not a

the co

In the final composite, this binder can cause problems. It can stay on the fibers during processing, which may have a negative influence on fiber-matrix adhesion. It can be dragged into the matrix material, causing a flaw in the composite or deteriorating the surface properties (such as gloss) of the composite part. It can dissolve into the matrix while inert to the cross-linking reaction. This may have a negative influence on the matrix properties. Finally, it can dissolve and take part in the cross linking reaction as if it were part of the matrix resin. In this case, the binder cannot be found as a separate entity in the final composite. Therefore, a binder that dissolves and takes part in the crosslinking reaction is considered an ideal binder.

For some systems, binders do behave ideally. For others, the ideal binder cannot be found. In general, to prevent any problems it is a good idea not to use more binder than absolutely necessary.

Research objective

In this introduction, two drawbacks of GFRUPs were mentioned. They are brittle and a binder is needed for their manufacturing, with all the problems that are associated with that. The aim of this research is to develop a binder that does not degrade the mechanical properties but improves the fracture toughness of the composite. We call this binder a *toughening binder*.

This di

In this : Since th

of fractu

other re

discuss

In cha

flexure

multiva

15 an

unidir

The

tough

made

mixtu

from

the :

eviG

the ;

size

In c:

peuil

This dissertation

In this work, the influence of binders on the properties of GFRUPs is shown. Since the property of primary interest is the fracture toughness, various aspects of fracture toughness will be addressed in chapter two. There, the attempts by other researchers to improve the fracture properties of composites will be discussed too.

In chapter three, a study of the effect of an ideal commercial binder on the flexure properties of unidirectional GFRUPs is presented. With the use of multivariate statistical tools, it is shown that for fiber volume fractions between 15 and 30 % the commercial binder does not affect the flexure properties of unidirectional GFRUPs.

The remaining chapters four through six deal with the development of a toughening binder. Chapter four describes the path that was chosen originally. It made use of different kinds of silicone rubber that dissolve in the uncured resin mixture. When the polyester network is formed, the silicone phase separates from the polyester to form small silicone particles. The chapter describes how the silicones were synthesized. During the course of the research, it became evident that the size of the silicone domains was not influenced by the nature of the silicone end group. Since it was impossible to control the silicone particle size, this approach was abandoned.

In chapter five, a new approach is described. An elegant and environmentally benign method to coat recycled tire rubber with a small amount of commercial

binder

rubber

in chap

describe

continu

is used

Refere

1. L.F sor

2 F. Yo

3 K./

4. P (

binder is developed. It is shown that the binding characteristics of these coated rubber particles are similar to those of the commercial binder itself.

In chapters six and seven, the toughening effect of the new rubber binder is described. It is demonstrated that the delamination fracture toughness of random continuous fiber composites increases by 75 % when 6 % of toughening binder is used. The toughening mechanism is crack bridging by the rubber particles.

References

- 1. L.H. Sperling, *Introduction to Physical Polymer Science, 2nd ed.*, Wiley and sons, New York, 1992
- 2. F. Rodriguez, *Principles of Polymer Systems, 2nd ed., McGraw-Hill, New York* 1982
- 3. K.A. Seroogy, W.N. Reed, S.L. Voeks, *Advanced Composites III, Expanding the Technology* (1987) 115-120
- 4. P.D. Emrich, Advanced Composites III, Expanding the Technology (1987) 163-165

Mecha: catego:

strengt

strain

differe

deal w

used f

A des

_

answe

desig parts

0n tt

what

prod.

Chapter 2

FRACTURE AND FRACTURE TOUGHNESS

Mechanical properties of materials can be divided into two categories. The first category contains the *static* properties. These include Young's modulus, yield strength and Poisson's ratio. The *dynamic* or *fracture* properties include critical strain energy release rate (G_c) and critical stress intensity factor (K_c). The difference between dynamic and static properties is that the static properties deal with the whole test specimen under stress, while the dynamic properties are used for stresses located near a crack.

A designer mainly uses the static properties. In design, the main questions to be answered are whether the part has the correct strength and stiffness. Few designers wonder what goes on when a part fails. In a sense, that is good, since parts are usually designed not to fail and the designer should aim for success. On the other hand, parts do have a limited life time and it is important to realize what happens before a product fails. One of the important properties of a product is whether you can see whether it is damaged or in good condition.

If the c

If a latheavily,

from the capacity

property

Stres

Figur

The

the

nec.

This falls

the

If the product contains a large crack, most people will notice that it is damaged. If a large amount of the fibers in a composite are broken, the composite is heavily damaged. Yet if the material is non-transparent the damage is invisible from the outside. There is no warning, and when the part is loaded to its design capacity, it will suddenly fail catastrophically. This is one of the reasons dynamic properties of materials need to be studied.

Stresses in the vicinity of a crack

The stresses near a crack can be very different from the macroscopic stress. Figure 2.1 demonstrates that the stresses near the crack tip can be much higher than the stress far away from it. The stress level increases when it approaches the crack tip. For a perfectly linear elastic material, the stress at the crack tip would even reach infinity, since there is a finite load, but no area that the load can work on.

This explains why, even when the macroscopic stress is much lower than the failure stress, the part will fail. At the crack tip, the point where it matters most, the stress is equal to the stress-to-failure and the crack grows.

Figure

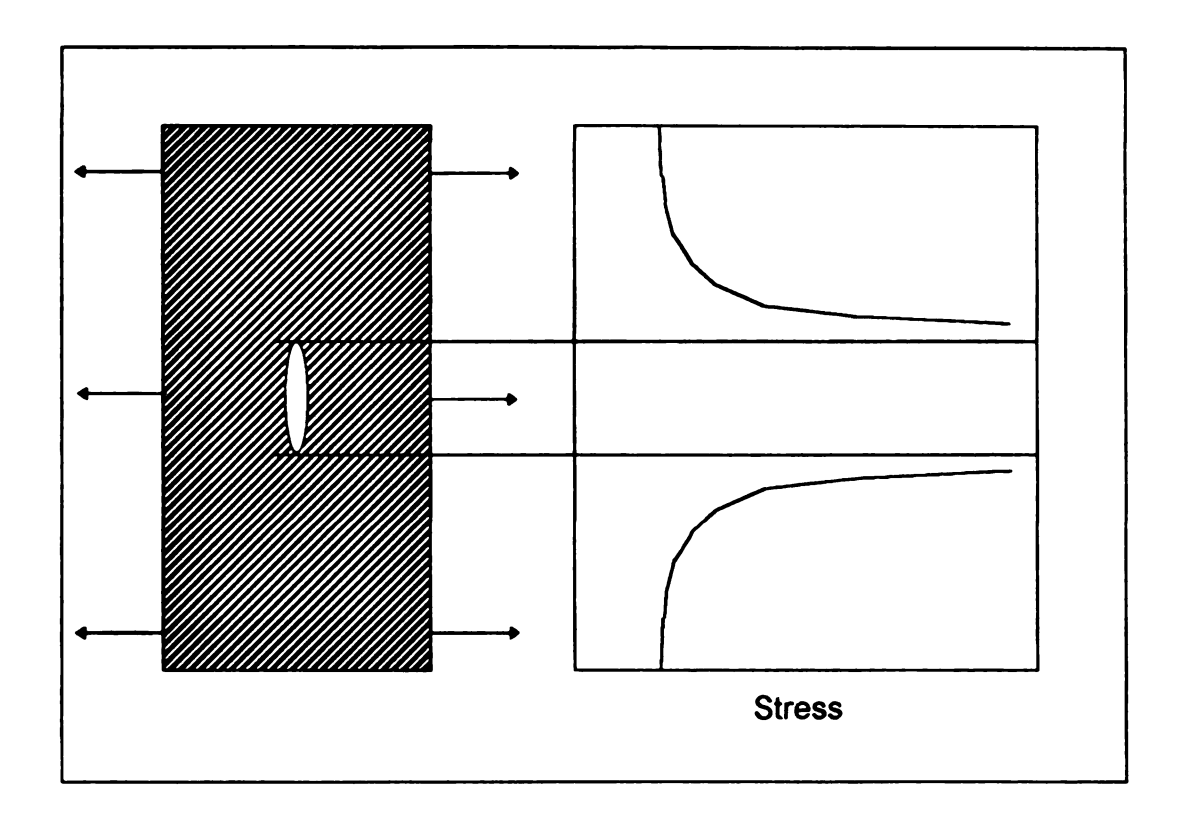


Figure 2.1 Schematic representation of stress levels in the vicinity of a crack

Fractur

deserv:

to desc

factor.

propert.

stress s

the crac

• The

• We

• We a

It can be

crack is

In this.

Futthern

Fracture is a complex process. Obviously, the field of fracture mechanics deserves its place in science [1,2]. Since the static properties are not sufficient to describe fracture, new properties have to be used such as the *Stress intensity factor*, *K*, the *Strain energy release rate*, *G*, and the *Plastic zone size*, *R*. These properties are all related. The stress intensity factor K is used to describe the stress situation around a crack. To be able to calculate the stress pattern around the crack in Figure 2.1, the following assumptions need to be made:

- The crack is small in a very large medium (no other cracks!).
- We have mode I loading only, i.e., the loading is in opening mode, without any shearing.
- We are very close to the crack.

It can be shown that the stress perpendicular to the crack and in the plane of the crack is given by:

$$\sigma = \frac{K_l}{\sqrt{2\pi r}}$$
 2.1

In this.

K_I = the mode I stress intensity factor

r = the distance from the crack tip

Furthermore, for this specific geometry (an elliptical crack in an infinite medium)

$$K_1 = \sigma_{\infty} \sqrt{\pi a}$$
 2.2

With

For this

In this

The fo

With

F_{Ina};

a mo

mate

mate

With

 σ_x = the stress far away from the crack

2a = total crack length

For this particular case, the relation between K and G is given by:

$$G = \frac{K_l^2}{F}$$

In this.

E = Young's modulus

The following relation between K and G is valid for all geometries:

$$G = \frac{\beta}{E} K_{l}^{2} + \frac{\beta}{E} K_{ll}^{2} + \frac{1+\nu}{E} K_{lll}^{2}$$
2.4

With

 β = 1 for plane stress conditions β = 1- v^2 for plane strain conditions

v = Poisson's ratio

Finally, we come to the relationship between K and R, the plastic zone size. For a mode III problem, this relation can be determined exactly assuming that the material behaves as an ideal elastoplastic material. An ideal elastoplastic material has a stress strain curve that looks like the one in Figure 2.2.

Figure

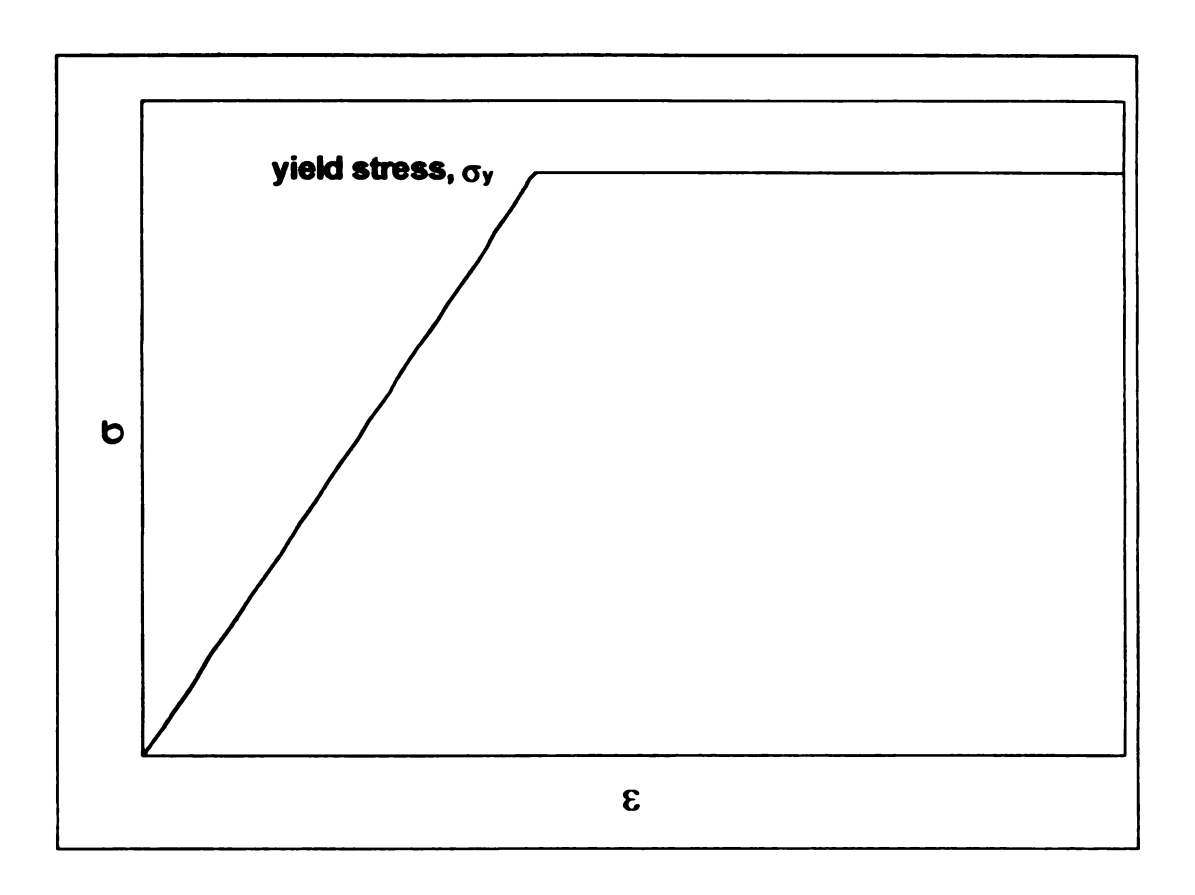


Figure 2.2 Stress strain curve for an ideally elastoplastic material

For th

,7

With

For a

and R

With

of a cra

For this material we find the following relation between K_{III} and R:

$$R = \frac{K_{|||}^2}{\pi r_v^2}$$
 2.5

With

 τ_v = yield shear stress of the material

For a mode I problem there is no exact solution for the relationship between K_I and R. However, with the Irwin [1,2] approximation we find:

$$R = \frac{K_l^2}{\pi \sigma_y^2}$$
 2.6

With

 σ_y = yield shear stress of the material

The higher the value for K, G and R, the better the material can resist the growth of a crack. Therefore, toughening research is aimed at increasing these values.

The t

Since

the in

have

Figu Surfa

Thou

back

usec

of a

The toughening of homogeneous thermosets

Since most thermosets are brittle materials many attempts have been made to increase their fracture toughness [e.g., 3-10]. Most of the attention has gone to the improvement of the fracture toughness of epoxies. Relatively few authors have focused on polyester thermosets [5, 10].

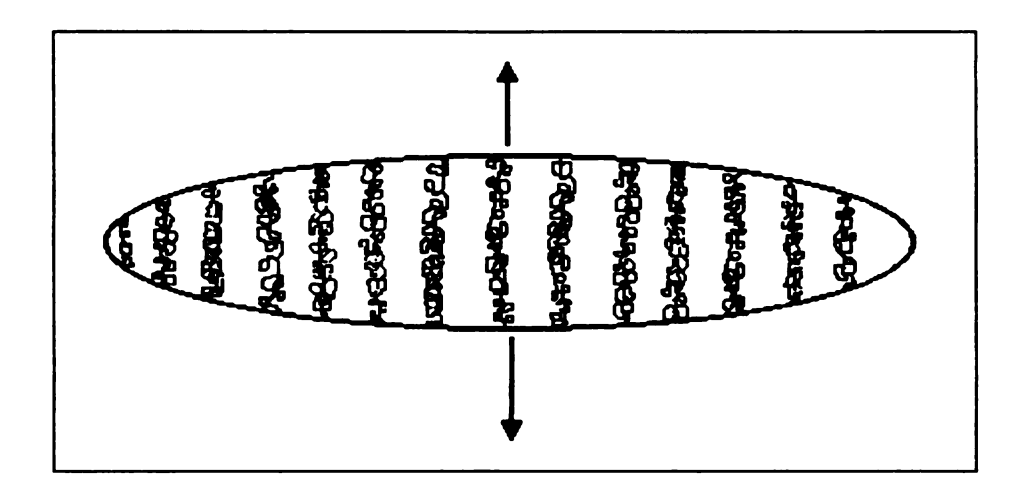


Figure 2.3 Schematic picture of a craze. Polymeric fibrils are bridging the surfaces of the craze.

Though there are other methods (such as changing the flexibility of the polymer backbone and the addition of thermoplastics to the thermoset), the most widely used method for improving the fracture toughness of thermosets is the addition of a rubbery phase. Various toughening mechanisms have been proposed.

Figu

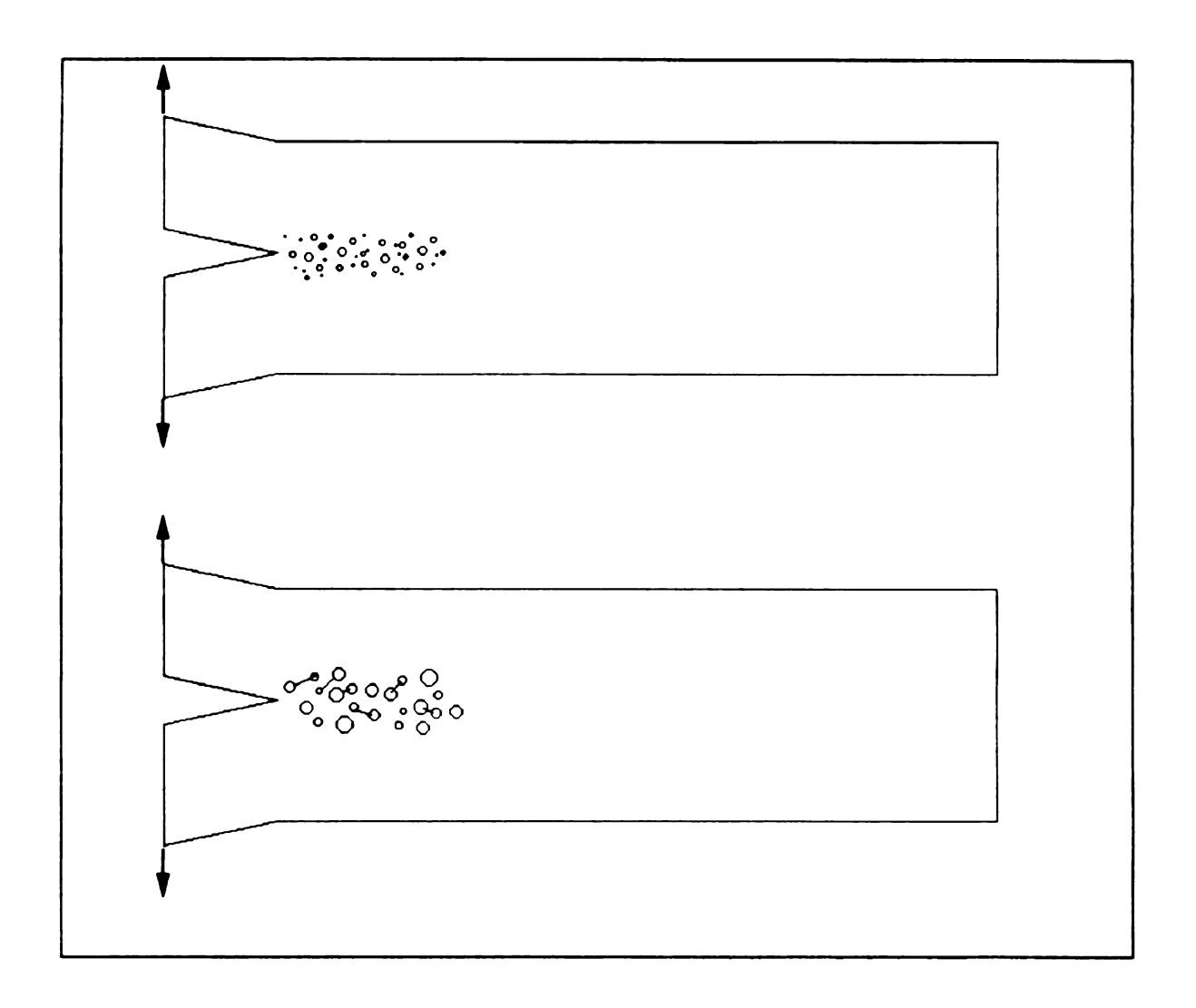


Figure 2.4 Schematic picture of the occurrence of cavitation

Tough

and coa

the ad

(Figure

Fibers

Sultan and McGarry proposed crazing as the dominating mechanism in rubber filled epoxy [3]. When a material crazes, a flat void is formed, that is bridged by polymeric fibrils (See Figure 2.3). The fibrils are oriented in the direction of the load. Since now the individual chains carry the load, crazing can make a large contribution to the toughness of the material. The classic example of a crazing polymer is polystyrene.

Yee and Pearson claim that cavitation is the dominating factor [6-8] (Figure 2.4). In this case, small cavities are formed within the rubbery particles that can grow and coalesce. When the cavities have grown, they can be connected by shear bands. In this way, large amounts of energy can be absorbed since the growth and coalescence of cavities require large amounts of material displacement.

Toughening mechanisms in fiber reinforced thermoset composites

Fibers in a composite can contribute to the fracture toughness in various ways. If the adhesion between the fiber and the matrix is very strong, it is possible that the crack runs through the fiber in the same plane as the matrix crack plane (Figure 2.5). In this case, the fracture toughness of the composite is low.

Figure

ة ر

Figure

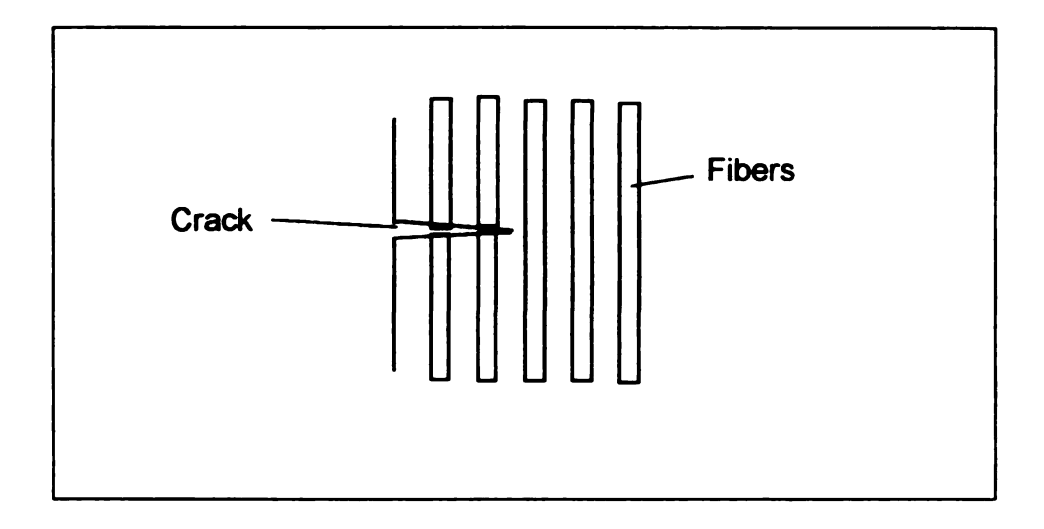


Figure 2.5 The fibers fracture in the same plane as the matrix

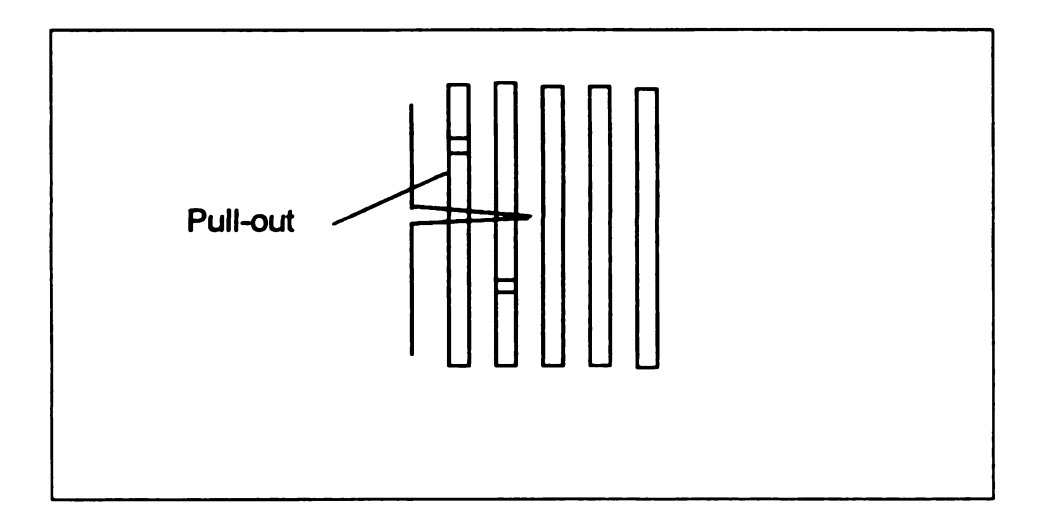


Figure 2.6 Fiber pull-out can increase the fracture toughness of a fibrous composite

j

Pull-

œm;

calc

W

V

C

Pull-out is a well-known toughening mechanism (Figure 2.6). In order for the crack to propagate, additional surface has to be created. For a unidirectional composite, the additional specific work of fracture due to fiber pull-out can be calculated [11]:

$$R_{PO} = \frac{V_f \sigma_f I_c}{12}$$
 2.7

With

R_{PO} = specific work of fracture (on a macroscopic fracture surface basis) due to pull-out

v_f = volume fraction of fiber

 $\sigma_f = \text{tensile strength of the fiber}$

l_c = critical fiber length, the length over which stress can be transferred along the fiber matrix interface

When the fibers can stretch, such as in glass fiber reinforced composites, an Outwater-Murphy debonding mechanism may occur (Figure 2.7). The crack passed around the fiber and the macroscopic crack is bridged by the fibers. In order for this mechanism to occur, the strain to failure of the matrix must be less than that of the fiber. This is true for most glass fiber reinforced thermosets.

Figure

Figure

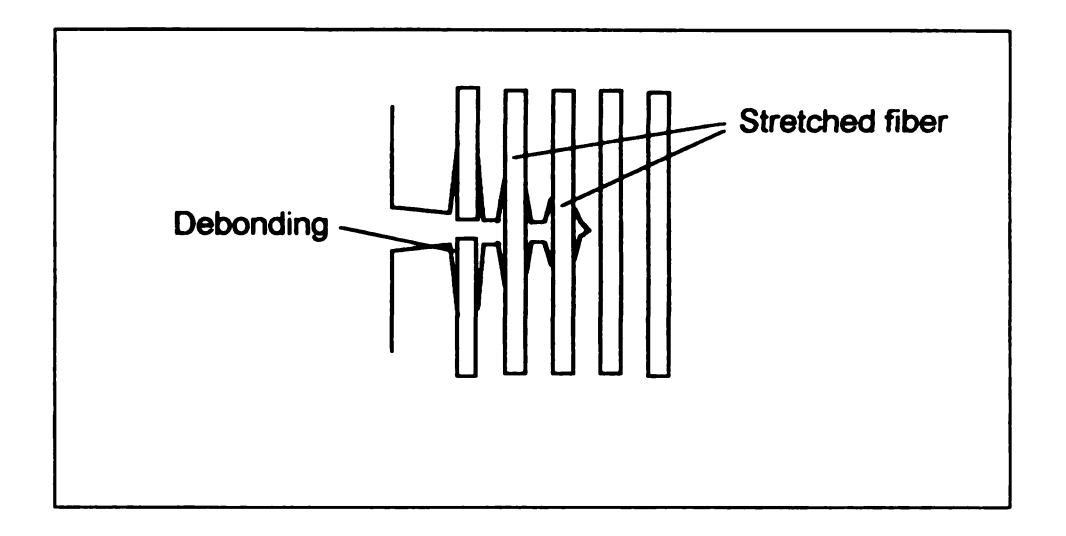


Figure 2.7 Schematic representation of Outwater-Murphy debonding

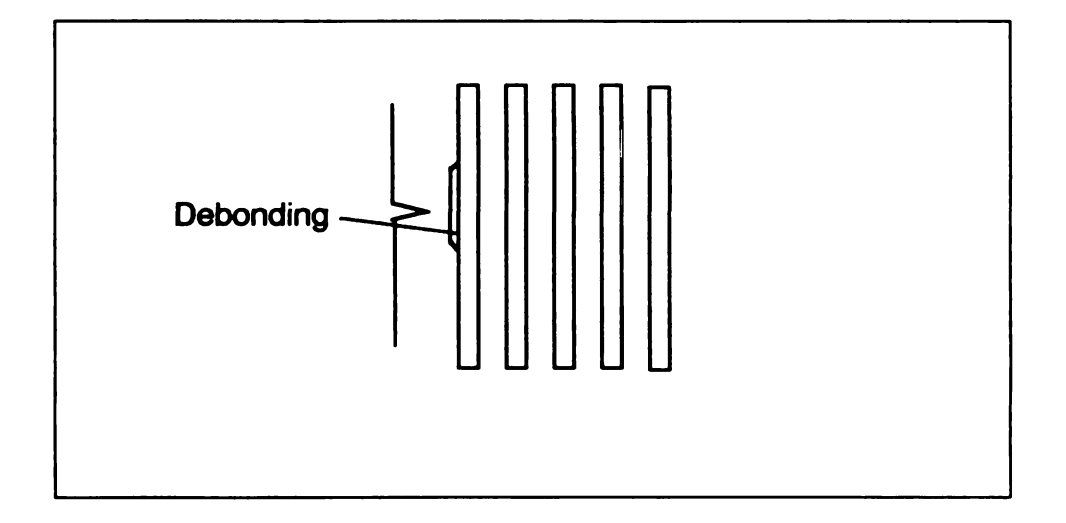


Figure 2.8 Schematic representation of Cook-Gordon debonding

The contribution of the Outwater-Murphy debonding to the work of fracture is given by:

$$R_{OM} = \frac{\sigma_f^2 v_f L}{2E_f}$$
 2.8

With

R_{OM} = specific work of fracture due to Outwater-Murphy debonding

L = debond length, approximately equal to I_c

 $E_f = modulus of the fiber$

If the strain to failure of the matrix is higher than that of the fiber, a Cook-Gordon debonding mechanism may be responsible for enhanced fracture toughness (Figure 2.8). In this case, the fiber-matrix interface fails before the macroscopic crack reaches the fiber. Marston, Atkins and Felbeck [11] developed an equation for the work of fracture due to Cook-Gordon debonding.

$$R_{CG} \approx v_f \frac{I_c}{d} R_m$$
 2.9

With

R_{cg} = specific work of fracture due to Cook-Gordon debonding

d = fiber diameter

R_m work of fracture of the matrix

of fract tougher mechan or stren As can irrelevat

Each of

the inte

artical

researd

To incr

decreas

Many r

interfac

field [1

rubber |

Each of the shown fracture mechanisms will lead to different values of the work of fracture of the unidirectional composite. Therefore, the research on toughening of fiber composites is geared towards manipulating the fracture mechanism of the material to maximize the work of fracture, rather than modulus or strength.

As can be seen from equations 2.7-2.9, the fracture toughness of the matrix is irrelevant except when toughening occurs through a Cook-Gordon mechanism. The parameter that is easiest to manipulate for a materials designer is the critical fiber length, I_c . That is why most of the composite fracture toughness research is focused on the manipulation of I_c . This critical length is a function of the interfacial shear strength, τ .

$$I_c = \frac{\sigma_f d}{2\tau}$$
 2.10

To increase the work of fracture, I_{c} has to be increased. Therefore, τ must decrease.

Many researchers work on the toughening of composites by weakening the interfacial shear strength. Labronici wrote an excellent review of the work in this field [12]. The weakening is usually done by coating the fibers with silicone rubber, silicone oil, SBS rubber or other elastomers or thermoplastics.

Table unidire

В

FI

Gr

•

U

5

Table 2.1 Improvements in fracture toughness or impact strength of unidirectional composites by fiber coating [12]

			Pro			
Fiber	Matrix	Coating	FT	Strength	Modulus	Ref.
Boron	Ероху	PU varnish	+550	-36	NR	13
Graphite	Ероху	PPS	298	-12	NR	14
Graphite	Ероху	PVOH	+213	-37	NR	14
Graphite	Ероху	AN	+202	0	NR	15
UD Short	Nylon	ATBN	+4556/	+62	NR	16
glass			+8907			

¹ polyurethane ² polyphenylenesulfide ³ polyvinylalcohol ⁴ acrylonitrile ⁵ amino terminated butadiene nitrile ⁶ Izod Impact ⁷ Drop dart

1

r

9

١

ı

i

f

ra

re

Labronici lists the methods that were used by various investigators and their results. The general trend in these results is that the fracture toughness increases by 0 to 100 %. At the same time, the strength and modulus decrease by 0 to 50 %. The best results obtained are listed in Table 2.1. Only in the case of ATBN modified short glass/nylon composites was the fracture toughness and strength improved simultaneously. The fracture toughness of the acrylonitrile modified graphite/epoxy improved significantly, while strength was retained. In all other cases the strength or modulus decreased when the fracture toughness was increased.

Toughening of random fiber reinforced composites

It should be noted that while all of the above toughening mechanisms may occur in random fiber materials, equations 2.7-2.9 are no longer valid. In the derivation of these equations, the assumption is made that the crack plane is perpendicular to unidirectional continuous fibers. This assumption cannot be valid for random fiber composites. This makes it much more difficult to understand the underlying principles for the toughening of random fiber reinforced composites. Therefore, less work has been done on the improvement of the fracture toughness in random fiber composites. The results of random fiber composite toughening research is summarized in Table 2.2

Table 2.2 Improvements in impact strength of random fiber composites

			Pro			
Fiber	Matrix	Modification	Impact	Strength	Modulus	Ref.
40 % Asbestos	Polystyrene	PEA ¹ mixed with fibers	+250 ²	NR	-30	17
35 % Glass	PP	SBS rubber ³	+1504	-20/+22	NR	18
30 % Glass	Ероху	Acryl latex	+513 ⁵	-5	-20	19

¹ polyethyl acrylate ² Izod ³ styrene butadiene styrene block copolymer

⁴ Weight drop impact ⁵ Notched Izod

It can be seen from Table 2.2 that the impact strength of a random fiber composite is a function of the matrix. This makes it worthwhile to try to improve the fracture toughness of random fiber composites by modification of the matrix. The direction of the load with respect to the fibers and the fiber volume fraction are important variables. If the load is in a direction in which most of the fibers are oriented, the effect of matrix toughening will be less. The fracture toughness will be determined by the fiber-matrix interaction. However, if the load is perpendicular to the plane with a preferred fiber orientation, the matrix properties will dominate, since the role of toughening mechanisms such as fiber pull-out and fiber-matrix debonding will be suppressed.

This means that there are possibilities to toughen random fiber composites by matrix modification. This is exactly what is investigated in this work. In this dissertation, research on matrix modification with rubber particles will be discussed. The delamination fracture toughness will be tested. In this case, the load is in the direction perpendicular to the fibers.

References

- 1. K. Hellan, Introduction to Fracture Mechanics, McGraw-Hill, 1984
- 2. M.F. Kanninen, C.H. Popelar, Advanced Fracture Mechanics, Oxford, 1985
- 3. J.N. Sultan, F.J. McGarry, *Polym. Eng. Sci.* **13** (1973) 29-34
- 4. S. Kunz-Douglass, P.W.R. Beaumont, M.F. Ashby, *J. Mater. Sci.* **15** (1980) 1109
- 5. G.A. Crosbie, M.G. Phillips, J. Mater. Sci. 20 (1985) 182-192
- 6. A.F. Yee, R. A. Pearson, J. Mater. Sci. 21 (1986) 2462-2474
- 7. R. A. Pearson, A.F. Yee, *J. Mater. Sci.* **21** (1986) 2475-2488
- 8. R. A. Pearson, A.F. Yee, J. Mater. Sci. 21 (1986) 2571-2580
- 9. R. Drake, Polymeric Materials: Science and Engineering, Proceedings of the ACS Division of Polymeric Materials: Science and Engineering **63** (1990)
- 10. R. Subramaniam, F.J. McGarry, J. Adv. Mater. 27 (1996) 26-35
- 11. T.U. Marston, A.G. Atkins, D.K. Felbeck, J. Mater. Sci. 9 (1974) 447-455
- 12. M. Labronici, H. Ishida, Composite Interfaces 2 (1994) 199-234
- 13. A.G. Atkins, *J. Mater. Sci.* **10** (1975) 819
- 14. J.H. Williams, Jr., P.N. Kousiounelos, Fibre Sci. Tech. 11 (1978) 83
- 15. R.V. Subramaniam, *Pure Appl. Chem.* **52** (1980) 1929
- 16. C.A. Rogg, *Mechanical Properties of Rubber Fiberglass/Epoxy Composites*, M.S. Thesis, M.I.T., 1988
- 17. M. Xanthos, T. Woodhams J. Appl. Polym. Sci. 16 (1972) 381
- 18. E.P. Plueddemann, SPI 29th Ann. Tech. Conf. Reinf. Plastics 24-A (1974)
- 19. D.G. Pfeiffer, L.E. Nielsen, J. Appl. Polym. Sci. 23 (1979) 2253

Chapter 3

THE INFLUENCE OF COMMERCIAL BINDER ON THE FLEXURE PROPERTIES OF UNIDIRECTIONAL GLASS FIBER REINFORCED UNSATURATED POLYESTERS

Introduction

The general belief in industry is that binders are deleterious to the composite properties [1,2]. That line of thinking is reasonable given that the binder has to be completely removed from the fibers to prevent weakening of the fiber-matrix interface. It cannot be present as a separate phase in the matrix, since that would be a flaw in the composite. Therefore, the binder has to dissolve completely into the matrix material. If the binder dissolves completely, it can still weaken the matrix if it does not take part in the curing reaction.

The aim of this research is to establish a correlation between the amount of binder used and the mechanical properties of the composite. We prepared unidirectional Glass Fiber Reinforced Unsaturated Polyesters (GFRUPs) with varying amounts of glass and binder and tested their flexure properties in the 0 and 90° direction in accordance with ASTM D 790.

Experimental

In the study, unsaturated polyester, styrene, benzoyl peroxide, dimethylaniline, glass fiber (sized with a polyester film former and a methacrylic coupling agent) and a polyester binder (very soluble in styrene) were used to manufacture panels. In the panels, the amount of binder as well as the amount of glass fiber were varied. The flexure properties of these panels were tested in the 0 and 90° direction. Appendix I contains more details about the materials used, the manufacturing of the panels as well as the test procedure.

Results and data treatment

The most common method to analyze data like this is shown in Figure 3.1. The measured data are averaged over each panel and plotted against the volume fraction of fiber. In this way, the data for each panel are reduced to two parameters: the mean and the standard deviation. Though it is generally well known that quantitative statistical analysis can be performed on raw data only, many authors process their data first and then perform their analyses, such as a regression analysis. For a linear analysis, in most cases, the error is relatively small. However, it is not very difficult to imagine how results can change if the data are fitted to an exponential curve.

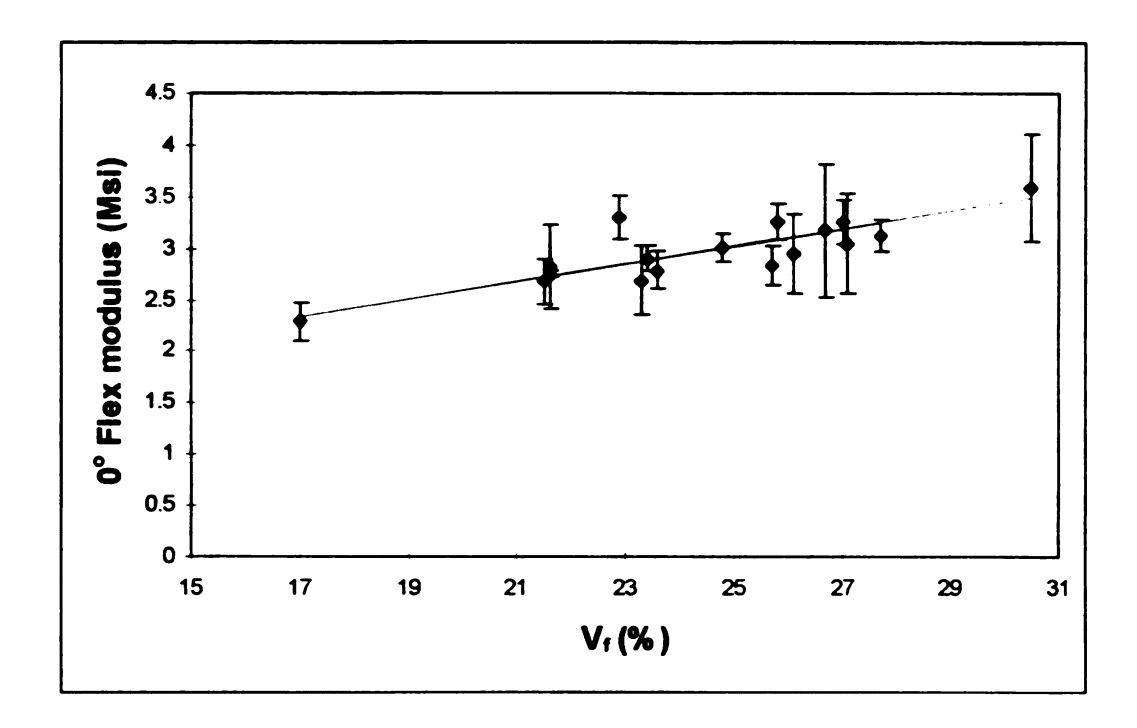


Figure 3.1 0° Flexure modulus averaged over each panel as a function of fiber volume fraction

In this research, two methods were used to establish whether there was a correlation between the amount of binder on the fibers and the mechanical properties of the composite. The residual analysis method is a two step method. First, a statistical analysis is done (in this case a linear regression). Then, the residual (a result of the regression analysis) is examined. Since this is a two step method, it can only be used to draw qualitative conclusions.

The multivariate approach is a one step method. Therefore, quantitative conclusions can be drawn. This approach has the drawback of giving numbers only, which are more difficult to interpret than graphs.

Residual analysis

The method of residual analysis assumes that there is a known linear relationship between fiber fraction and the property. Therefore, first, the linear relation between the fiber volume fraction and the property is determined by ordinary (absolute least squares) linear regression. Subsequently, the residuals are analyzed for a correlation with the binder percentage.

The raw data for the 0° flexure modulus are plotted against the fiber volume fraction, V_f in Figure 3.2.

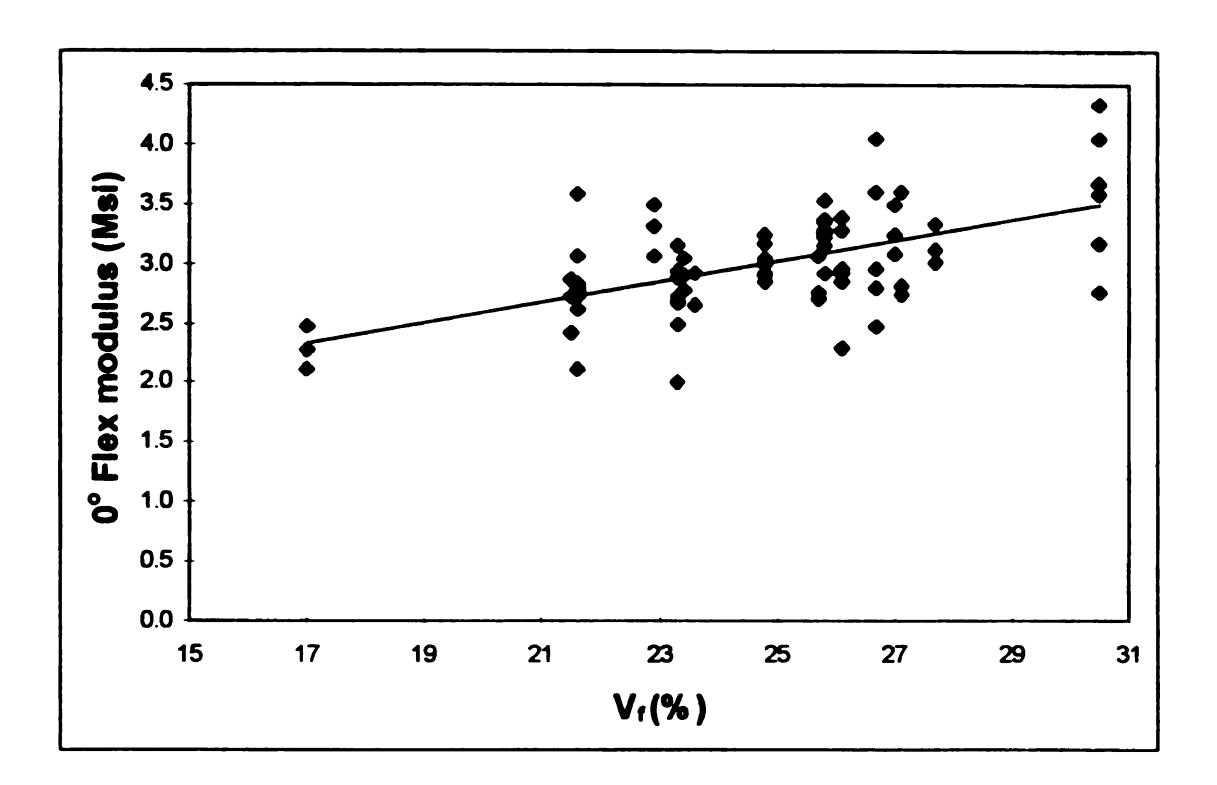


Figure 3.2 0° Flexure modulus plotted against the fiber volume fraction V_f

The data for the other properties (0° flexure strength, 90° flexure modulus and 90° flexure strength) were examined in a similar way. Table 3.1 shows the values for the coefficients in the relation $P = a + bV_f$ (P is the property under study). In this equation, V_f is given in percents. Table 3.1 also shows the correlation coefficient p. It was calculated using equation 3.1

$$\rho_{xy} = \frac{\sum (x_i - \bar{x}) \sum (y_i - \bar{y})}{\sqrt{\sum (x_i - \bar{x})^2 \sum (y_i - \bar{y})^2}}$$
3.1

With

 $(x_i, y_i) =$ individual data point $\bar{x} =$ average of x = average of y =

The value of ρ is always between -1 and 1. When the absolute value of ρ is larger than 0.8, the correlation is said to be strong.

Figure 3.3 shows the residual (= the experimental value - the value predicted by the correlation) of the 0° flexure modulus plotted against the percentage of binder on the fibers.

Table 3.1 Regression coefficients for the linear regression of the flexure properties with fiber volume fraction

Property	а	b	ρ
0° flexure strength (psi)	29810	2502	0.59
0° flexure modulus (ksi)	874	85.9	0.60
90° flexure strength (psi)	2833	43.4	0.17
90° flexure modulus (ksi)	256	20.0	0.47

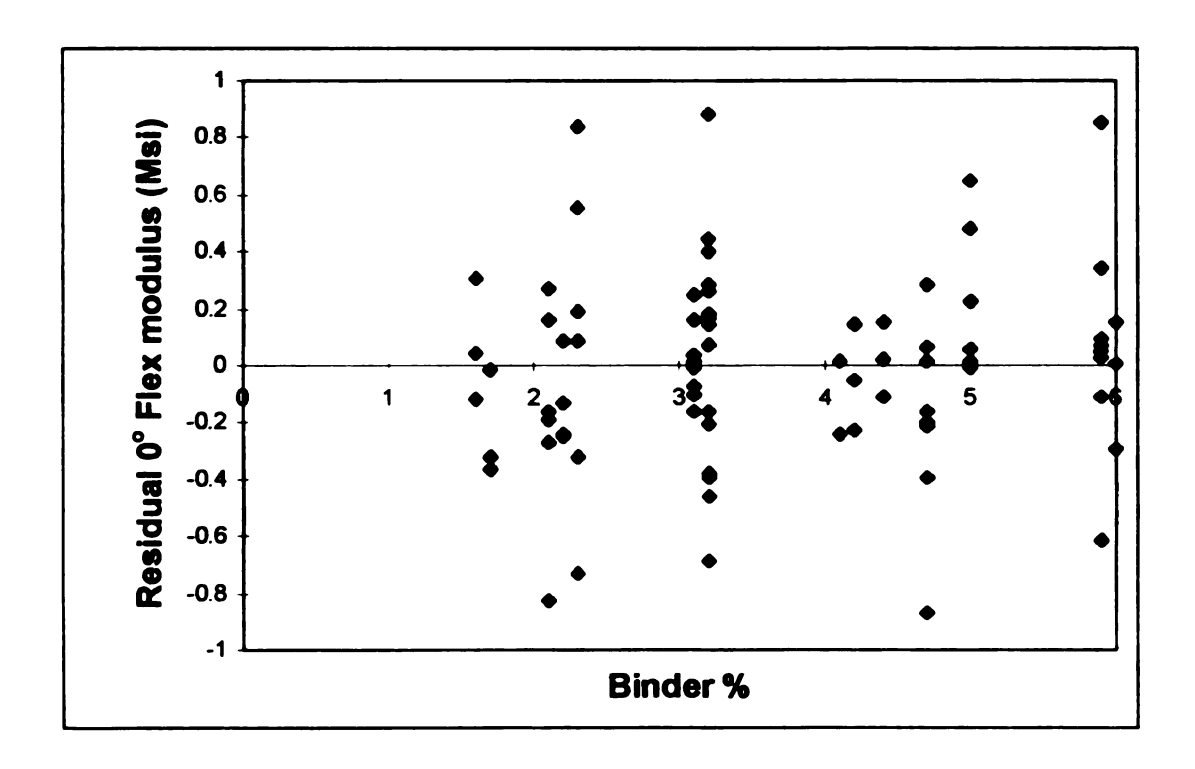


Figure 3.3 The residual of the 0° flexure modulus plotted against the percentage of binder on the fibers

Fig soi

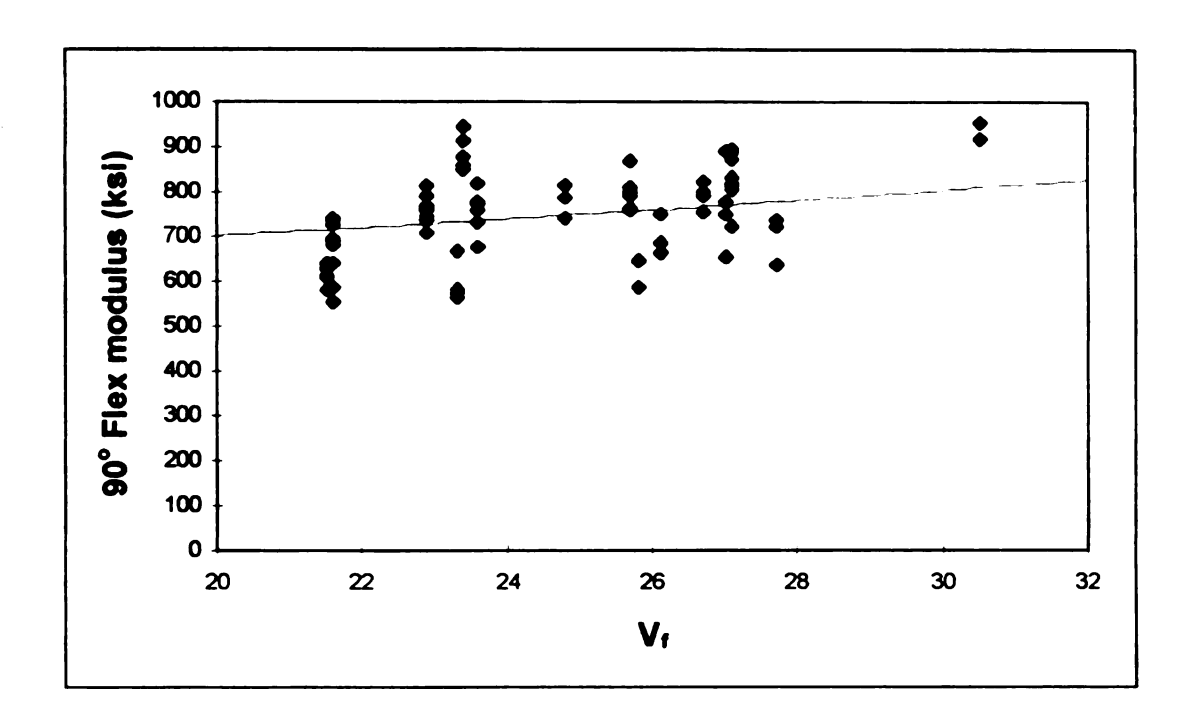


Figure 3.4 90° Flexure modulus plotted against the fiber volume fraction V_{f} . The solid line represents the 90° flexure modulus as calculated with equation 3.2

Fig:

Tab of th and

Pro Stre O' f. MO' Stre 90' Stre 90'

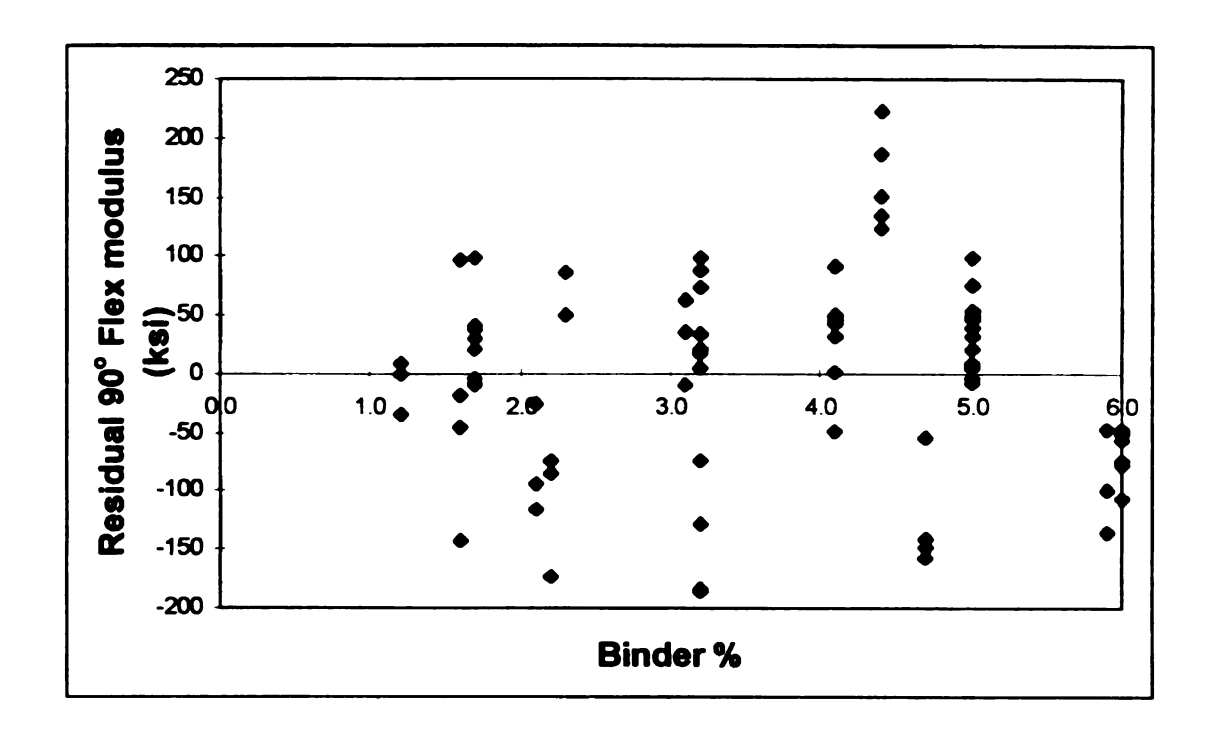


Figure 3.5 The residual of the 90° flexure modulus plotted against the percentage of binder on the fibers

Table 3.2 Regression parameters for the multivariate analysis: The dependence of the flexure properties on the fiber volume fraction and the binder percentage, and the correlation coefficients ρ

Property	а	b	С	$\rho (V_f, W_b)$	ρ (P,V _f)	ρ (P, w_b)
0° flexure strength (psi)	3396	2157	-386	0.8691	0.9909	0.8838
0° flexure modulus (ksi)	112	67.3	-13.2	0.8691	0.9908	0.8826
90° flexure strength (psi)	139	132	-16.2	0.8746	0.9822	0.8924
90° flexure modulus (ksi)	28.7	11.4	0.512	0.8746	0.9907	0.8817

The

Witt

Figure The

regio

Mult

The

mec

 $(V_f)_{\cdot}$

shov

COLLÉ

43

The 90° properties were also fit to a non-linear equation:

$$P = \frac{P_m}{1 - v_f}$$
 3.2

With

P = property under study

 $P_m = matrix property$

 $v_f = fiber volume fraction$

Figure 3.4 gives the 90° flexure modulus as a function of fiber volume fraction.

The solid line follows equation 3.2 with $E_{\rm m}$ = 561 ksi. As can be seen, in this

region of low fiber volume fraction, the deviation from linearity is very small.

Multivariate analysis

The second method consists of a multivariate regression analysis. For each

mechanical property the (linear) correlation between the fiber volume fraction

(V_f), the binder percentage (w_b) and property (P) was determined. Table 3.2

shows the parameters for the relation $P = aV_f + bw_b + c$ with the various

correlation coefficients.

Dis

Upo

exp

see

tens

Wit

A fi

sun For

Slig

eit

fib

ca

Discussion

Upon examination of the results in Figures 3.1 and 3.2 as well as Table 3.1, as expected, a reasonable correlation between the 0° properties and V_f can be seen. That is expected since for long, unidirectional fibers, in the 0° direction, tensile properties are given by the rule of mixtures:

$$E_c = V_f E_f + (1 - V_f) E_m = V_f (E_f - E_m) + E_m$$
 3.3

With

 E_c = tensile modulus for the composite

 $E_f =$ tensile modulus for the fiber

 E_m = tensile modulus for the matrix

A flexure test is not a tensile test. Nevertheless, the found correlation is not surprising.

For the 90° flexure strength, the correlation with V_f is very small, while there is a slight correlation between the 90° flexure modulus and V_f . This is not surprising either, since failure in the 90° direction is governed by the matrix properties. The fiber will influence those properties only at very high fiber volume fractions. This can be seen from the rule of mixtures for the 90° direction.

$$\frac{1}{E_C} = \frac{v_f}{Ef} + \frac{v_m}{E_m}$$
 3.4

Sm

Th

be a

Afte

the value

resi

prop

tren

prop The

resi

corr

90°

$$E_{c} = \frac{E_{f}E_{m}}{v_{f}E_{m} + v_{m}E_{f}} = \frac{E_{m}}{1 - (1 - \frac{E_{m}}{E_{f}})v_{f}}$$
3.5

Since $\frac{E_m}{E_f}$ << 1, equation 3.5 can be simplified to yield equation 3.6:

$$E = \frac{E_m}{1 - v_\ell}$$
 3.6

This is essentially the same as equation 3.2. The curve in Figure 3.4 appears to be a straight line. This is because for small values of v_f , $\frac{E_m}{1-v_f} \approx E_m(1-v_f)$.

After the dependence of the property on the fiber volume fraction is established, the effect of the fiber is eliminated. The residual is obtained by subtracting the value that the correlation predicts from the experimental value. Then, the residuals are plotted against w_B in Figure 3.3. If the binder has any effect on the properties, a trend in the residual should be observed. Since there is no such trend, it can be concluded that the binder does not have any effect on the flexure properties of the composite.

The second approach makes use of a linear multivariate analysis algorithm. The results of this method can be found in Table 3.2. After this analysis, a good correlation between the flexure properties and V_f is observed. Again, the 90° flexure strength correlates the least with V_f .

Wh

app

Hov V₁ a

inte

L

by

be:

₩_B

œr

When examining the correlation between the flexure properties and w_B , it appears that there is a strong positive correlation between these parameters. However, when reviewing our tests in further detail, a good correlation between V_f and w_B is also observed. In other words, our independent variables are interdependent. The correlation between the flexure properties and w_B is caused by their correlation with the fiber volume fraction. The correlation coefficient between properties and w_B is equal to the correlation coefficient between V_f and w_B . Therefore, it must be concluded that there is no evidence for an independent correlation between the flexure properties and binder percentage.

Conc

Unid

beer

with

betw

volu

anc

met

vo:

Bo:

ωr.

app

mu

car

Ωī

Conclusions

Unidirectional composite panels with varying glass and binder content have been manufactured. The 0° flexure properties of these composites vary linearly with the fiber volume fraction as could be expected. There is a slight correlation between 90° flexure modulus and the fiber volume fraction. Since the fiber volume fractions were relatively low, the relation between 90° flexure modulus and the fiber volume fraction is essentially linear. Therefore, the use of linear methods is appropriate. No correlation of the 90° flexure strength with fiber volume fraction was observed.

Both a residual method and a multivariate analysis approach were used to find a correlation between flexure properties and binder percentage. The multivariate approach is a direct method, while the residual method is indirect. Therefore the multivariate method should be preferred. From the results of both methods, it can be concluded that the binder does not affect the flexure properties of the composite.

References

- 1. B.J.R. Scholtens, A. de Koning, private communications, November, 1992
- 2. A. de Koning, private communication, February 26, 1993
- 3. H. Martens, T. Næs, *Multivariate Calibration*, John Wiley & Sons, Chichester, 1989
- 4. B.J.R. Scholtens, J.C. Brackman, J. Adhesion 52 (1995) 115-129

Chapter 4

FEASIBILITY STUDY FOR THE USE OF SILICONE RUBBER AS A TOUGHENING BINDER

Introduction

The first method that was tried to make a toughening binder made use of the fact that liquid silicone rubber (polydimethylsiloxane, PDMS) is soluble in styrene, the main ingredient of unsaturated polyester resin. However, when the unsaturated polyester cures, the solubility of the PDMS decreases, leading to phase separation.

Other researchers have tried similar methods using ATBN (Amino Terminated Butadiene Nitrile) or CTBN (Carboxy Terminated Butadiene Nitrile) rubbers in epoxy thermosets [e.g. 1-2]. These rubbers do not seem to be suitable for use in unsaturated polyesters, since they will react with styrene during crosslinking of the resin.

For PDMS to be an adequate toughening agent for unsaturated polyesters, it is necessary that small PDMS domains are formed within the resin. In this chapter, the influence of the PDMS end group on the particle size is studied.

Ex

In :

phe

Th

The

m:

res

A;

th P

ł

Experimental

In the study, silanol terminated as well as trimethylsilane terminated PDMS were used. The silanol end group was converted into different phenoxy end groups. The resulting end groups were the silanol ethers of nonyl phenol, cresol and phenol. Completion of the reaction was verified with FTIR.

The modified types of PDMS as well as the silanol terminated and the trimethylsilane terminated PDMS were mixed in with a resin mixture. The resin mixture was cured on a microscope slide. The PDMS phase separated from the resin during curing. The sizes of the PDMS domains were measured with a microscope.

Appendix I contains more details about the materials used, the modification of the silanol terminated PDMS, the FTIR analysis as well as the analysis of the PDMS domain size.

Results and Discussion

Estimation of the interchange cohesive pressure

A convenient parameter is needed to describe the different end groups. With the aid of solubility parameters, the interaction between the end group and styrene

can be modeled. The solubility parameter concept will be explained in detail in chapter 5 where it will be used in the development of a solubility model.

In this chapter, the interchange cohesive pressure, A_{12} , of the end group with styrene will be used as a parameter to characterize the end group. A_{12} is a parameter that describes the enthalpy of mixing between two components. When A_{12} is large, the enthalpy of mixing is large, leading to a small solubility. When A_{12} is small, the enthalpy of mixing is small, leading to a better solubility. A_{12} can easily be calculated from the solubility parameters of the components of the mixture:

$$A_{12} = (\delta_d^{S} - \delta_d^{E})^2 + (\delta_D^{S} - \delta_D^{E})^2$$
4.1

In this,

 δ_d^s = the dispersive contribution to the solubility parameter of styrene

 δ_d^E = the dispersive contribution to the solubility parameter of the end

 $\delta_{p}{}^{s}$ = the polar contribution to the solubility parameter of styrene

 δ_p^E = the polar contribution to the solubility parameter of the end group

In this chapter, the interaction is between the end group of the PDMS and styrene. Therefore, A_{12} can be calculated from the solubility parameters of these end groups and styrene.

Ta int st)

Table 4.1 Dispersive (δ_d) and polar (δ_p) solubility parameters and the interchange cohesive pressure with styrene for the various end groups and styrene

End group	δ _d (MPa ^½)	$\delta_{p} (MPa^{2})$	A ₁₂ (MPa)
-Si(CH₃)₃	4.649	0.0	230.5
-Si(CH₃)₂ OH	2.720	6.476	464.0
-Si(CH ₃) ₂ OC ₆ H ₅	10.819	0.832	104.2
-Si(CH ₃) ₂ OC ₆ H ₄ CH ₃	10.845	0.706	105.9
-Si(CH ₃) ₂ OC ₆ H ₄ C ₉ H ₁₉	13.392	0.383	87.4
Styrene	16.79	9.10	-

Ta PD the

es: pr:

K:

F

(M) sili

a

(S

te te

a

С

Table 4.1 shows the dispersive and polar solubility parameters of the various PDMS end groups as well as styrene and the interchange cohesive pressure for the end group with styrene. The dispersive and polar solubility parameters were estimated using the Matprop spreadsheet program and database [4]. This program is based on the group contribution theory as formulated by Van Krevelen [3, 5-6].

FTIR analysis

Figure 4.1 shows the FTIR spectra of silanol terminated PDMS (MW = 4200 g/mole) and the cresoxy terminated PDMS that was prepared. The silanol terminated PDMS shows characteristic peaks at 3260 (OH), 2964 and 2906 (CH₃), 1094 and 1022 (Si-O) and 1262, 864 and 802 cm⁻¹ (Si-C). The cresoxy terminated PDMS shows peaks at 2964 and 2906 (CH₃), 1094 and 1022 (Si-O) and 1262, 864 and 802 cm⁻¹ (Si-C) that are characteristic for the PDMS. However, there are two major differences between the spectrum of the cresoxy terminated PDMS and that of the silanol terminated PDMS. The cresoxy terminated PDMS spectrum shows small but very characteristic peaks at 1598 and 1492 cm⁻¹ (aromatic C-C). The other difference is the fact that the OH peak at 3260 cm⁻¹ has disappeared. This proves that the reaction product must be cresoxy terminated PDMS and that the product is at least reasonably pure.

Sim

term

Similar changes in the FTIR spectra were observed after reacting the silanol terminated PDMS with nonyl phenol and phenol.

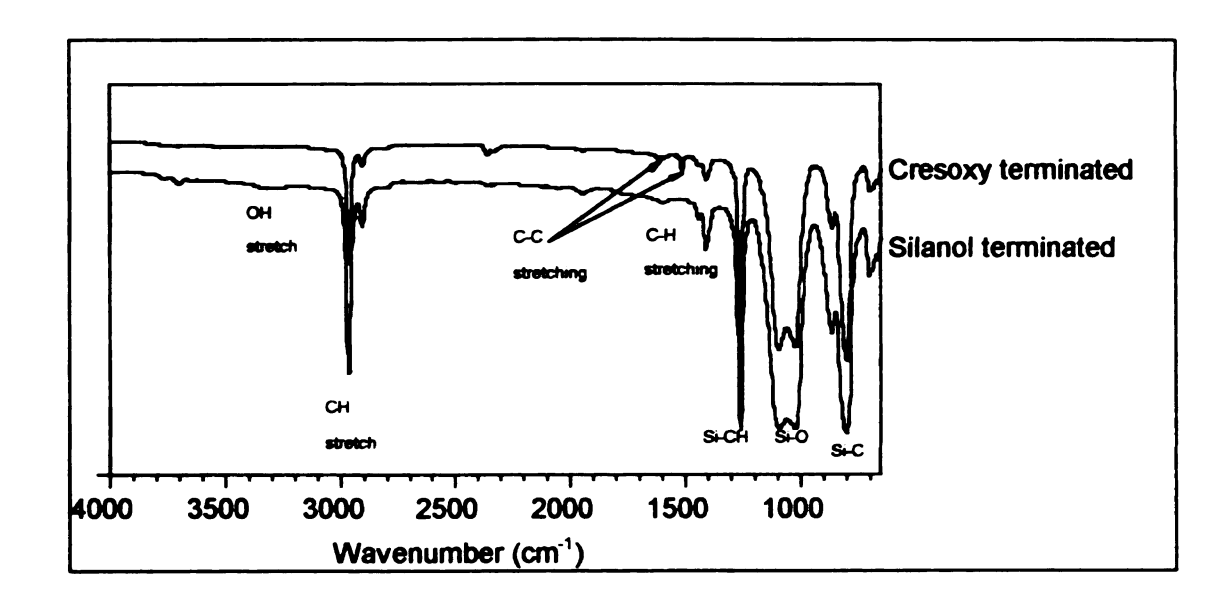


Figure 4.1 FTIR spectra for unreacted silanol terminated PDMS and for the same PDMS after reaction with cresol

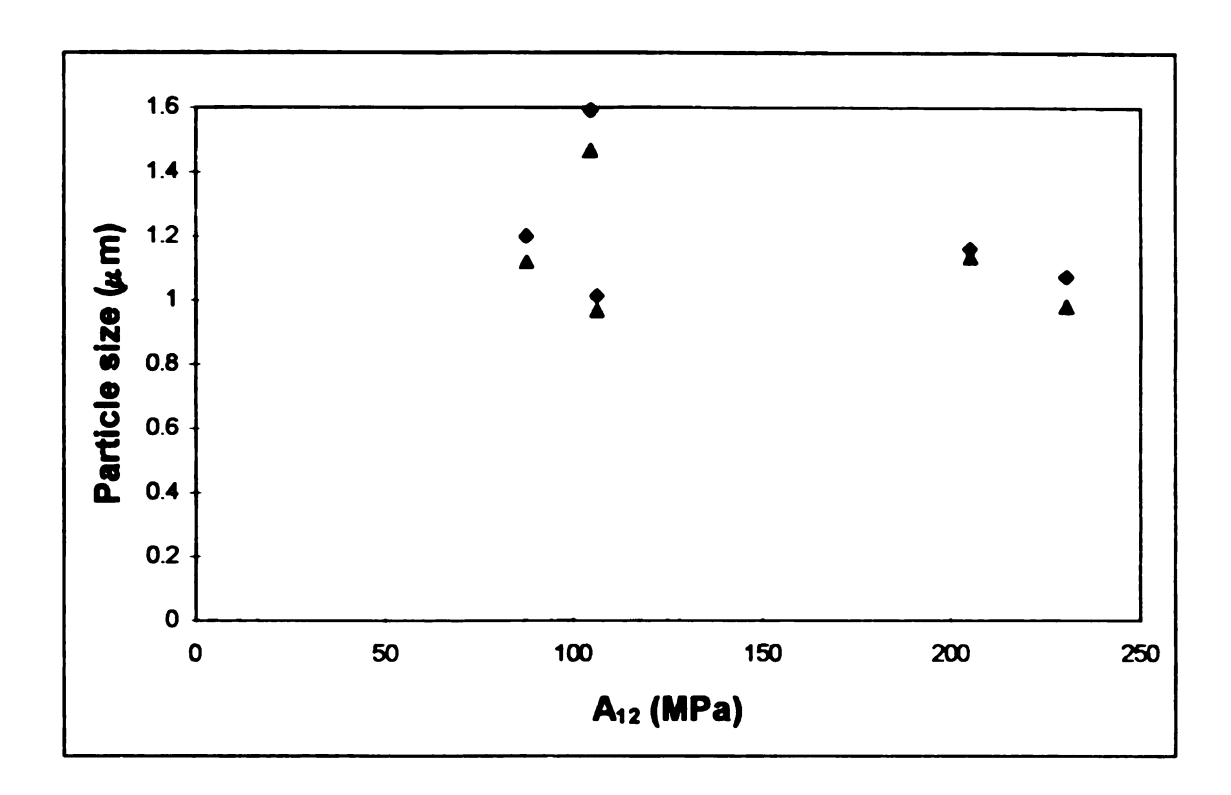


Figure 4.2 Number and volume average particle sizes of end group modified PDMS as a function of interchange cohesive pressure, A_{12} , between the end group and styrene

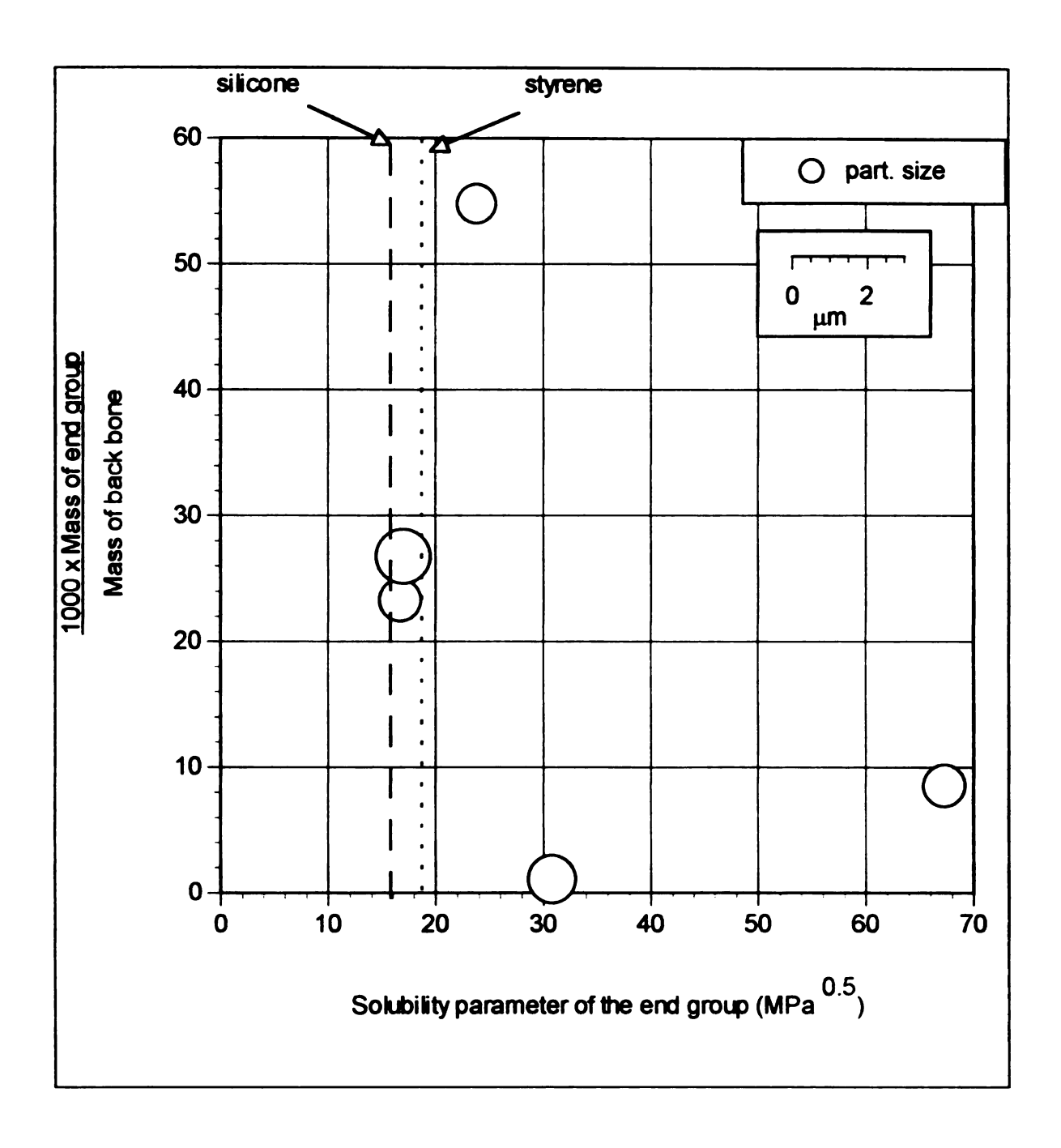


Figure 4.3 Silicone particle size as a function of the solubility parameter of the end group and of the relative mass of the end group

Parti
In F
unsa
size
diffe
figu
the
enti

Th

pa ki

re fr

٧

Particle size analysis

In Figure 4.2 the number and volume average particle size of the PDMS in unsaturated polyester are shown as a function of A₁₂. It appears that the particle size is not influenced by the interchange cohesive pressure. Figure 4.3 shows a different approach to model the interaction of the end group with styrene. In this figure, the particle size is plotted as a function of the total solubility parameter of the end group as well as the relative size of the end group with respect to the entire silicone molecule. It is reasonable to assume that when the end group is small, its influence will be less than when it is large.

The total solubility parameter of the end group is the Pythagorean sum of all the contributions to the solubility parameter:

$$\delta_{\text{total}}^2 = \delta_{\text{d}}^2 + \delta_{\text{p}}^2$$
 4.2

There is no trend in particle size in either Figure 4.2 or Figure 4.3. This despite the fact that such a trend was expected on the basis of thermodynamical parameters. An explanation for this is that the process of phase separation is kinetically controlled rather than thermodynamically. This explanation is reasonable since the phase separation has to take place within a short time frame. The thermodynamic driving force for phase separation is only present while the mixture is curing. Yet, when the mixture is gelled, the phase separation

must slow down considerably. It is very well possible that the particle size will never reach its equilibrium.

Conclusions

The synthesis of end capped PDMS was successful. FTIR did not detect any impurities.

The end group of the PDMS does not influence the particle size of the PDMS in unsaturated polyester resin. There was no correlation between the PDMS particle size and A₁₂, the interchange cohesive pressure of the end group with styrene. A possible explanation for this is that the phase separation of the PDMS in the curing polyester is kinetically controlled rather than thermodynamically. Since it was impossible to control the PDMS particle size by varying the PDMS end group chemistry, it was concluded that end group modified PDMS is not a good candidate for a toughening binder. Therefore, a different approach was chosen. This is described in chapters five, six and seven of this work.

1. 2

References

- 1. T.K. Chen, Y.H. Jan, *Polym. Eng. Sci.* **35** (1995) 778-785
- 2. H.R. Azimi, R.A. Pearson, R.W. Hertzberg, *Polym. Eng. Sci.* **36** (1996) 2352-2365
- 3. A.F.M. Barton, Handbook of Solubility Parameters and Other Cohesion Parameters, CRC Press, Boca Raton, 1983
- 4. Matprop, Materials Property Estimator and Database, Version 2.1, 1993
- 5. C.M. Hansen, A. Beerbower, Solubility parameters, in *Kirk-Othmer Encyclopedia of Chemical Technology*, Suppl. Vol., 2nd ed., A. Standen, Ed., Interscience, New York, 1971, 889
- 6. D.W. van Krevelen, P.J. Hoftyzer, *Properties of Polymers: Their Estimation and Correlation with Chemical Structure*, 2nd ed., Elsevier, Amsterdam, 1976
- 7. G.L. Larson et al., Silicon Compounds Register and Review, Hüls America, Piscataway, NJ, 1991

Chapter 5

PREPARATION OF A RUBBER BINDER USING A REVERSE ANTISOLVENT PHASE SEPARATION METHOD

Introduction

This chapter and the following chapters describe the approach that was taken after the toughening attempt with silicones (Chapter 4) did not work. The toughening binder that was developed was made by coating recycled tire rubber particles with commercial binder. To achieve this, an antisolvent process was used. This process is described in this chapter. In chapter 6 it is shown that the fracture toughness of the composite can increase by 75 % when 6 % of rubber binder is added to the glass fibers.

Chapter 7 shows how the adhesion between the rubber and the matrix can be improved. Before coating the rubber with the commercial binder, the rubber is subjected to a UV / ozone treatment and soaked in oleic acid. The ozone reacts with the rubber surface to yield hydroxyl groups. The acid group in the oleic acid reacts with the hydroxyl groups on the rubber surface. During the curing reaction, the matrix can react with the double bond in the oleic acid. This

provides a molecular link between the rubber and the matrix. This results in an additional 25 % increase in the fracture toughness of the composite.

Antisolvent processes

Antisolvent processes are most widely applied in food and pharmaceutical industries. Antisolvent crystallization is a technology that is used in the crystallization of temperature sensitive compounds such as pharmaceuticals [1,2]. The most common ways to crystallize a compound are evaporative crystallization and cooling crystallization.

In evaporative crystallization, the solvent is evaporated which increases the concentration of the solute. This continues until the solute concentration reaches its maximum (the solubility). Then, the solute can start to crystallize. After all the solvent is evaporated, all the solute has crystallized.

Cooling crystallization uses another method to get the solute concentration to reach the solubility. In this method, the solute concentration is kept constant, but the solubility is decreased, by lowering the temperature. Again, when the concentration is higher than the solubility, the solute can start to crystallize. After a filtration step, the crystals are obtained.

The physical principle for antisolvent crystallization is the same as for cooling crystallization. The solubility of the solute is reduced until the solubility is below

the solute concentration. In this method, the solubility is altered by the addition of an antisolvent. The antisolvent has the following characteristics:

- It is very soluble in the solvent.
- The solute has a very low solubility in the antisolvent.

Thus, addition of the antisolvent can reduce the solubility of the solute. Recently, the use of antisolvent methods has been applied in polymers. In these cases, however, a polymeric solution has always been sprayed in a supercritical antisolvent such as carbon dioxide, [3-7]. In this research we want to use a liquid-liquid antisolvent method.

One problem arises that has to be taken into account. Solubility is a thermodynamic property. As with all thermodynamic processes that take place at constant pressure and temperature, it is the Gibbs free energy (G) that determines what is happening. The change in Gibbs free energy is a function of the change in enthalpy H and entropy S:

$$\Delta G = \Delta H - T \Delta S$$
 5.1

When a compound is dissolved in a solvent, usually ΔH will be positive. This will be compensated for by the relative large increase in entropy. It is the entropy function that makes the compound dissolve. When an antisolvent is added to a solution many things happen at the same time. The ΔH will be much more positive, but at the same time the ΔS will increase because of the addition of a

new compound. This is why most antisolvent crystallizations involve the crystallization of a salt out of water. The salt is only soluble in water because of the high dielectric constant of water. Once a water soluble organic compound is added, the dielectric constant decreases rapidly and the salt crystallizes. The aim of this research is to phase separate a polymer out of a solution, using methods similar to antisolvent crystallization. In this case, the solvent is acetone. Water will act as the antisolvent. Since the effect of the antisolvent on the enthalpy and the entropy needs to be known, thermodynamic modeling is necessary to assess the viability of an antisolvent phase separation approach.

A thermodynamic model for antisolvent phase separation of a polymer

With the aid of a simple solubility parameter model, the solubility of polyester (solute) in acetone (solvent) can be calculated as a function of the amount of added water (the antisolvent).

The idea behind solubility parameter models is that mixing of components can be modeled as a three step process. First, the components evaporate, then they are mixed in the gas phase and finally the gas mixture condenses to a liquid mixture. In order for the components to evaporate energy has to be supplied to overcome the cohesive force. The mixing in the gas phase is assumed to be the

mi œ T SI mixing of ideal gases and therefore purely entropic. When the system condenses, new cohesive forces are in place.

The cohesive pressure, c, is defined to deal with these forces. For a pure substance, it is defined as:

$$c = \frac{U}{V}$$
 5.2

With

U = molar evaporation energy

V = molar volume

For a mixture of two components, it is difficult to define a cohesive pressure. It is common to use the geometric mean assumption:

$$c_{12} = \sqrt{c_1 c_2}$$
 5.3

Thus, the interchange cohesive pressure, A_{12} , can be calculated.

$$A_{12} = c_1 + c_2 - 2c_{12} 5.4$$

 A_{12} describes the energetic interactions between the two components in the mixture. From here, it is just a small step to the introduction of the solubility parameter, δ , of a component:

$$\delta = \sqrt{c}$$

Using δ , the equation for A_{12} reduces to:

$$A_{12} = c_1 + c_2 - 2c_{12} = \delta_1^2 + \delta_2^2 - 2\delta_1\delta_2 = (\delta_1 - \delta_2)^2$$
 5.6

Now A₁₂ is only a function of the properties of the components of the mixture, not of the mixture itself.

In the next part of this chapter, a model will be derived. It is important to note that this model, as well as many others, is based on certain assumptions. These are [8-9]:

- There is no volume change of mixing
- Interaction forces are between the centers of the molecules (or, in the case of polymers, between the centers of segments of equal volume as the volume of a solvent molecule).
- There are no ternary or higher order effects.
- The distribution of molecules in the solution is random. In other words, there
 is no structure in the solution.

 The geometric mean assumption is valid. This means that the cohesive pressure of a binary mixture can be described as the geometric mean of the cohesive pressures of its components.

For the calculation of the Gibbs free energy of the mixture for a two phase system, the following equations are used:

$$\frac{\Delta H_m}{RT} = \frac{A_{12} v_1 v_2 x_1 x_2}{RT (x_1 v_1 + x_2 v_2)} = \frac{A_{12} V^*}{RT} \phi_1 \phi_2$$
 5.7

$$\frac{\Delta S_m}{R} = x_1 \ln x_1 + x_2 \ln x_2$$
 5.8

$$\frac{\Delta G_m}{RT} = \frac{A_{12}v_1v_2x_1x_2}{RT(x_1v_1 + x_2v_2)} + x_1 \ln x_1 + x_2 \ln x_2$$
5.9

In this.

 $\Delta H_m =$ the enthalpy of mixing

 $\Delta S_m =$ the entropy of mixing

 ΔG_m = the Gibbs free energy of mixing

R = the gas constant

T = the absolute temperature

 A_{12} = exchange energy density

V = average molar volume of the mixture

 x_1 , x_2 = mole fraction of component 1 and 2, respectively

 v_1 , v_2 = molar volume of component 1 and 2, respectively

 ϕ_1 , ϕ_2 = volume fraction of component 1 and 2, respectively

The exchange energy density, A₁₂, can be calculated from solubility parameters. In this chapter, the polar, dispersive as well as the hydrogen bonding components of the solubility parameter are used:

$$A_{12} = (\delta_{d,1} - \delta_{d,2})^2 + (\delta_{p,1} - \delta_{p,2})^2 + (\delta_{h,1} - \delta_{h,2})^2$$
5.10

In this,

 $\delta_{d,i}$ = dispersive contribution to the solubility parameter of i

 $\delta_{p,i}$ = polar contribution to the solubility parameter of i

 $\delta_{h,i}$ = hydrogen bonding contribution to the solubility parameter of i

Figure 5.1 shows an example of a Gibbs free energy plot as a function of composition. In this case, a sample with an overall composition of 1:1 will separate into two different phases. The composition of those phases is given by the two points where the Gibbs free energy touches the broken line. Mathematically, the composition of phases A and B is given by:

$$\left(\frac{\partial \frac{\Delta G_m}{RT}}{\partial x_2}\right)_A = \left(\frac{\partial \frac{\Delta G_m}{RT}}{\partial x_2}\right)_B = \frac{\left(\frac{\Delta G_m}{RT}\right)_B - \left(\frac{\Delta G_m}{RT}\right)_A}{x_{2B} - x_{2A}}$$
5.11

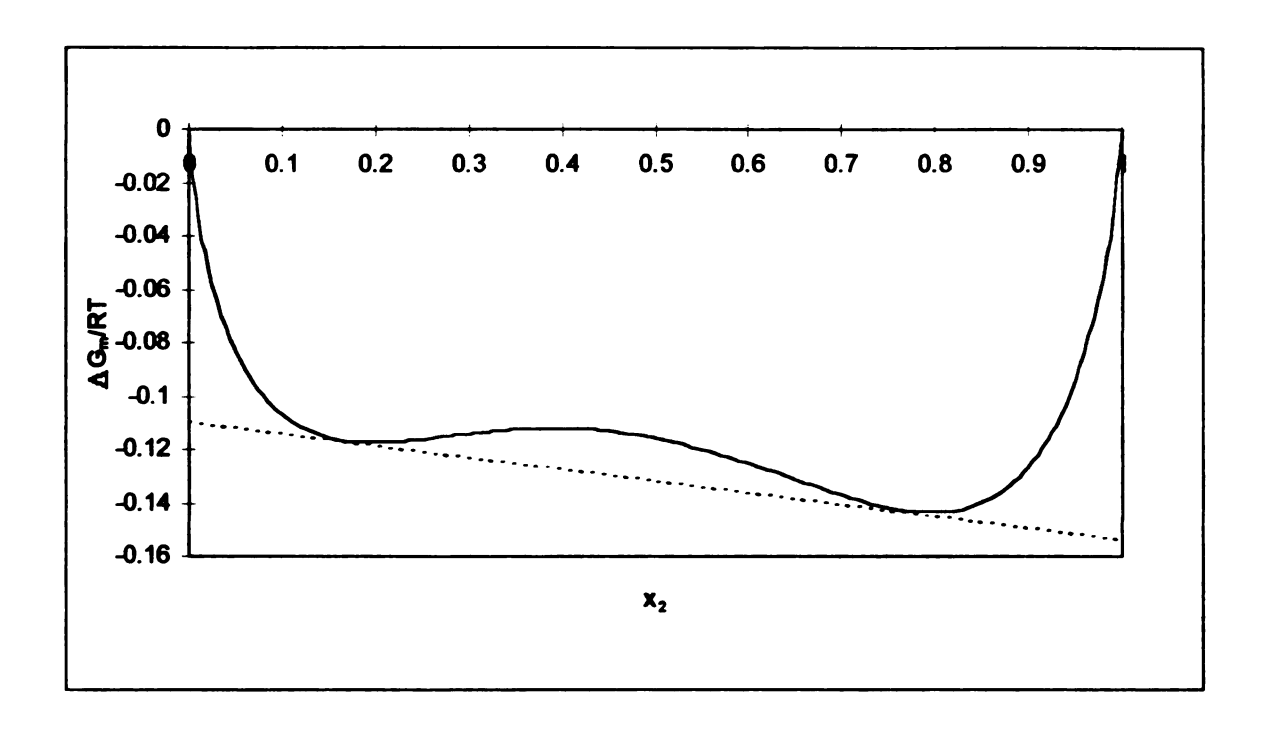


Figure 5.1 Example of a Gibbs free energy of mixing plot. The Gibbs free energy of mixing is given as a function of solute fraction. In this case, the mixture will separate into two phases. The composition of the two phases can be found from the points where the curve touches the straight line ($x_2 = 0.15$ and $x_2 = 0.78$).

For a multicomponent system, the equation for the Gibbs free energy of mixing becomes more complicated:

$$\frac{\Delta G_m}{RT} = \frac{1}{2RT \sum_{i=1}^{n} x_i v_i} \sum_{j=1}^{n} \sum_{j=1}^{n} A_{ij} v_i v_j x_i x_j + \sum_{j=1}^{n} x_j \ln x_j$$
 5.12a

or
$$\frac{\Delta G_m}{RT} = \frac{\sum_{i=1}^{n} x_i v_i}{2RT} \sum_{i=1}^{n} \sum_{j=1}^{n} A_{ij} \phi_i \phi_j + \sum_{i=1}^{n} x_i \ln x_i$$
 5.12b

In this.

n = the number of components

The factor $\frac{1}{2}$ is there to prevent counting the contribution of the interaction between i and j as well as j and i as two separate contributions. Obviously, $A_{ii} = 0$. Equation 5.12 only takes into account the effect of binary interactions. Ternary interactions are neglected.

In this research, the compound under study is polyester. The polymeric nature makes the situation more complex. Since the area of interest is that of concentrated solutions, a Flory-Huggins model should be more realistic than a standard model for low molecular weight materials. Using the Flory-Huggins correction for the entropy of mixing, equation 5.13 is obtained.

$$\frac{\Delta G_m}{RT} = \frac{\sum_{i=1}^{n} x_i v_i}{2RT} \sum_{i=1}^{n} \sum_{j=1}^{n} A_{ij} \phi_i \phi_j + \sum_{i=1}^{n} x_i \ln \phi_i$$
 5.13

If the polymer is taken to be component n, then

$$\chi_i = \frac{A_{\rm in} v_i}{RT}$$
 5.14

This yields the Flory-Huggins equation for a multicomponent system:

$$\frac{\Delta G_m}{RT} = \sum_{i=1}^{n-1} \chi_i x_i \phi_i \phi_n + \frac{\sum_{i=1}^{n} x_i v_i}{2RT} \sum_{i=1}^{n-1} \sum_{j=1}^{n-1} A_{ij} \phi_i \phi_j + \sum_{i=1}^{n} x_i \ln \phi_i$$
5.15

In this equation, the first term describes the enthalpic interaction between the polymer and the various solvents. The second term describes the enthalpic interaction between the various solvents. The third term describes the entropy of mixing.

Though the equations are getting more complicated, the procedure to find the solubility of one component in a mixture of two (or conceivably more) other components is still the same. Plot the Gibbs free energy of mixing for adding the last component with the mixture of a given composition. From that, determine the

solubility of the third component in the mixture. This research deals with ternary mixtures.

Since the composition of the binary mixture is given, the ratio $x_1/(x_1+x_2)$ remains constant. It is equal to $x_{1,0}$, the mole fraction of component 1 before addition of the third component.

To determine the solubility of component 3 in binary mixture $A(x_1,x_2)$, the Gibbs free energy of mixing due to the mixing of 3 and A needs to be calculated.

$$\left(\frac{\Delta G_m}{RT}\right)_{(1-2)-3} = \left(\frac{\Delta G_m}{RT}\right)_{1-2-3} - \left(1 - x_3\right) \left(\frac{\Delta G_m}{RT}\right)_{1-2}$$
5.16

In this equation the subscript (1 + 2) + 3 refers to the addition of component 3 to a binary mixture of component 1 and 2. The subscript 1 + 2 + 3 refers to mixing components 1, 2 and 3 simultaneously. The subscript 1 + 2 refers to mixing components 1 and 2. Equation 5.13 applied for a ternary mixture yields the first term (5.17), while equation 5.13 for a binary mixture gives the second term (5.18).

$$\left(\frac{\Delta G_m}{RT}\right)_{1-2\cdot3} = \frac{\sum_{i=1}^3 x_i v_i}{2RT} \sum_{i=1}^3 \sum_{j=1}^3 A_{ij} \phi_i \phi_j + \sum_{i=1}^3 x_i \ln \phi_i$$
 5.17

$$\left(\frac{\Delta G_m}{RT}\right)_{1+2} = \frac{A_{12}v_1v_2x_1x_2}{RT(x_1v_1 + x_2v_2)} + x_1 \ln \phi_1 + x_2 \ln \phi_2$$
5.18

When $\Delta G_m/RT$ is plotted as a function of x_3 for a constant ratio of x_1/x_2 , a curve similar to Figure 5.1 is obtained. The procedure for finding the solubility is as follows:

- The Gibbs free energy of mixing is plotted as a function of mole fraction of solute using an Excel spreadsheet.
- An initial solubility is estimated from the plot. Now the worksheet calculates a tangent line.
- The solubility estimate is changed until the line has two tangent points with the curve.

The two mole fractions that are obtained in this way, represent the solubility of the solute in the solvent (mixture) and the solubility of the solvent (mixture) in the solute.

The only problem left is to find good values for the solubility parameters. The data that are used in this research are given in Table 5.1. Reliable data for polyester are only available if group contribution theory is used. In group theory, the molecule is broken down into its components. It is assumed that each part of the molecule contributes to the solubility parameter. The volume of the group is used as a weight factor.

Table 5.1 Input parameters used to calculate the solubility of polyester in mixtures of acetone and water (from [8])

Component Name	Mol. wt. (g/mole)	(\mathbf{MPa}^{1})	δ_d (MPa $^{1/2}$)	δ_{p} (MPa ^{1/2})	v (cm³/mole)
Acetone	58.07	19.7	13	9.8	74
Water	18.01	48	12.2	22.8	18.1
Dimethyl phthalate	194.2	22.5	15.9	12.6	163.1

Figure 5.2 Molecular formulas of dimethyl phthalate and unsaturated polyester

Using group contribution theory, the solubility parameters for polyester would be very close (for practical purposes equal) to the solubility parameters for dimethyl phthalate. After all, the molecules are chemically very similar (see Figure 5.2 for the molecular formulas of dimethyl phthalate and unsaturated polyester). The unsaturated polyester is a random copolymer with parts that are phthalic in nature and parts that are maleic. The amount of maleic parts in the molecule is very small.

Thus, it is reasonable to use the experimental values for the solubility parameters for dimethyl phthalate as an estimate for the solubility parameters of polyester. The solubility parameters for water and acetone were taken from the same source.

The results of these calculations are given in Figure 5.3. For convenience, the axes are converted into units of weight fraction instead of mole fraction.

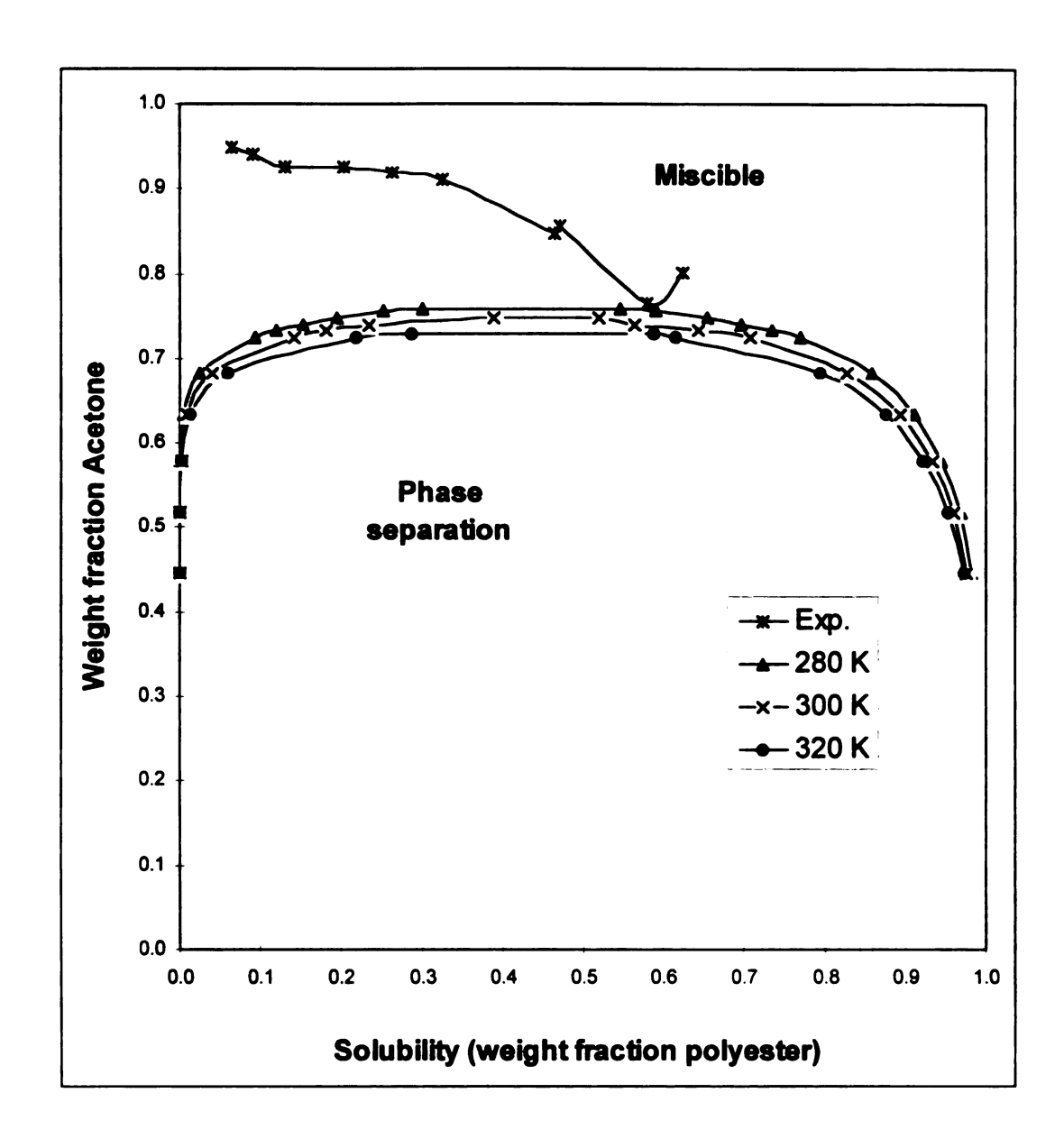


Figure 5.3 Phase diagram for a mixture of polyester and acetone/water from calculations for $T = 280 \text{ K} (\triangle)$, T = 300 K (X) and $T = 320 \text{ K} (\bigcirc)$. The graph also shows working data for the occurrence of phase separation (*). The working data may not represent thermodynamic equilibrium.

Experimental verification and discussion of the ternary mixing model

The ternary mixing model was verified by slowly adding a polyester solution in acetone of known composition to water. After a certain amount of solution had been added, the solution became unclear. The beaker was weighed to determine the amount of solution that was added. In this way, the composition of the mixture at the point where phase separation occurred could be determined. The results of these experiments are given in Figure 5.3 and compared to the calculated data. It must be noted that the results for the higher concentration of polyester are less reliable since the high viscosity of the polyester solution made proper mixing difficult.

As can be seen from Figure 5.3 the influence of the water is much larger than is predicted by theory. A relatively small amount of water in the acetone makes it an unsuitable solvent. It seems reasonable to assume that the unique properties of water are responsible for this. These make it difficult to describe with a solubility parameter model. Many of the assumptions that were listed at the beginning of this chapter do not hold for aqueous solutions. Some of the facts that were neglected in the model are:

 There is a substantial volume change of mixing for the mixing of acetone and water, as well as for the mixing of polyester and acetone.

- Because of hydrogen bonding, the structure of the solution is not random.
 Water will hydrogen bond with other water molecules. This lack of randomness reduces the entropy of mixing considerably.
- Interaction forces will not act between the centers of the molecules. Water will only interact with the carboxyl group of the polyester. Again, this order in the mixture, will reduce the entropy of mixing.

Manufacturing of a rubber binder with a reverse antisolvent phase separation process

In this research, rubber particles are coated with polyester with an antisolvent phase separation process. The fact that theory and experiment do not agree on the solubility of polyester in acetone/water mixtures does not make it impossible to use such a process. As a matter of fact, the unique properties of water make the process more effective than was anticipated theoretically. All the qualifications for a good antisolvent method are there: Polyester is very soluble in acetone. It is insoluble in mixtures of acetone and water.

The most obvious way to achieve phase separation would be to disperse rubber particles into a solution of polyester in acetone. While stirring the rubber particles, water would be added and the polyester would precipitate on the rubber particles.

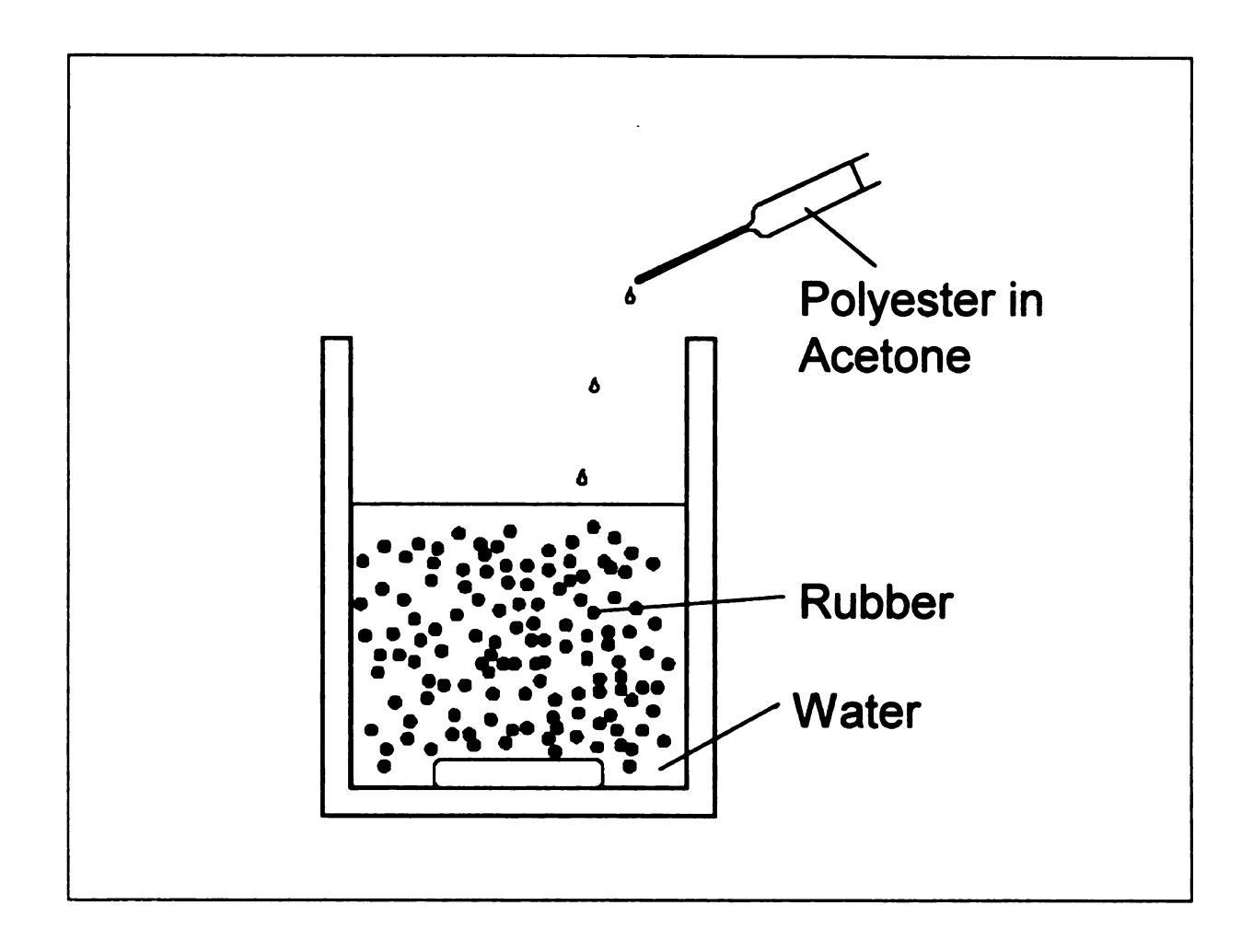


Figure 5.4 Schematic setup of the reverse antisolvent phase separation process

This process has a number of drawbacks. The acetone will swell the rubber. Since the particles will be used in a reaction injection molding process later, residual acetone in the rubber will be a problem. A problem associated with the swelling of the rubber is that the rubber will be sticky. Particles will be difficult to separate.

Another drawback is that after we separate the particles from the liquid we are left with a concentrated polyester solution in acetone, polluted with water. For a lab scale operation, this is not much of a problem. For an industrial scale production of rubber binder, however, this will be a major obstacle, both from a cost as well as an environmental perspective.

Because of these considerations, the reverse antisolvent phase separation process was investigated. With this process, the rubber is dispersed in water. A polyester solution is added to the dispersion until the polyester phase separates. This has the advantage that only tiny amounts of polyester and acetone are needed. Obviously, this is a vast improvement over the straightforward approach.

The setup that was used for our process is depicted in Figure 5.4. 35 grams of rubber particles are placed in a one liter beaker. Subsequently, approximately 430 g of water are added to the rubber. The mixture is stirred with a tongue blade to make sure that the rubber is wetted. Sometimes a few droplets of soap solution are added to aid the wetting of the rubber. When the rubber is dispersed, the mixture is stirred with a Teflon coated spin bar. Slowly, a solution

of 1 percent by weight polyester in acetone is added to the rubber dispersion.

After approximately 50 g of solution have been added, the polyester is immiscible in the acetone/water mixture and a white 'blob' is formed.

This blob contains the polyester rich phase, which still contains a large amount of acetone and water. Upon addition of a few more droplets of polyester solution, the blob grows and encapsulates virtually all (far more than 90 %) of the rubber particles. The blob can be separated from the water phase with a tongue blade and dried in an oven at 50 °C for a half hour. After drying, the rubber particles separate easily into a free flowing powder, by stirring a bit with a tongue blade. This may be caused by the relatively poor wetting of the rubber surface by the polyester.

Characterization of the rubber binder

The rubber binder was characterized by sieving, ESCA (Electron Spectroscopy for Chemical Analysis) surface analysis, and ESEM (Environmental Electron Scanning Microscopy). The rubber that was used was made out of recycled rubber tires. Appendix I contains more details about the sieving procedure, the ESCA analysis, the electron microscopy as well as the tire rubber, the acetone and the polyester that were used in the research.

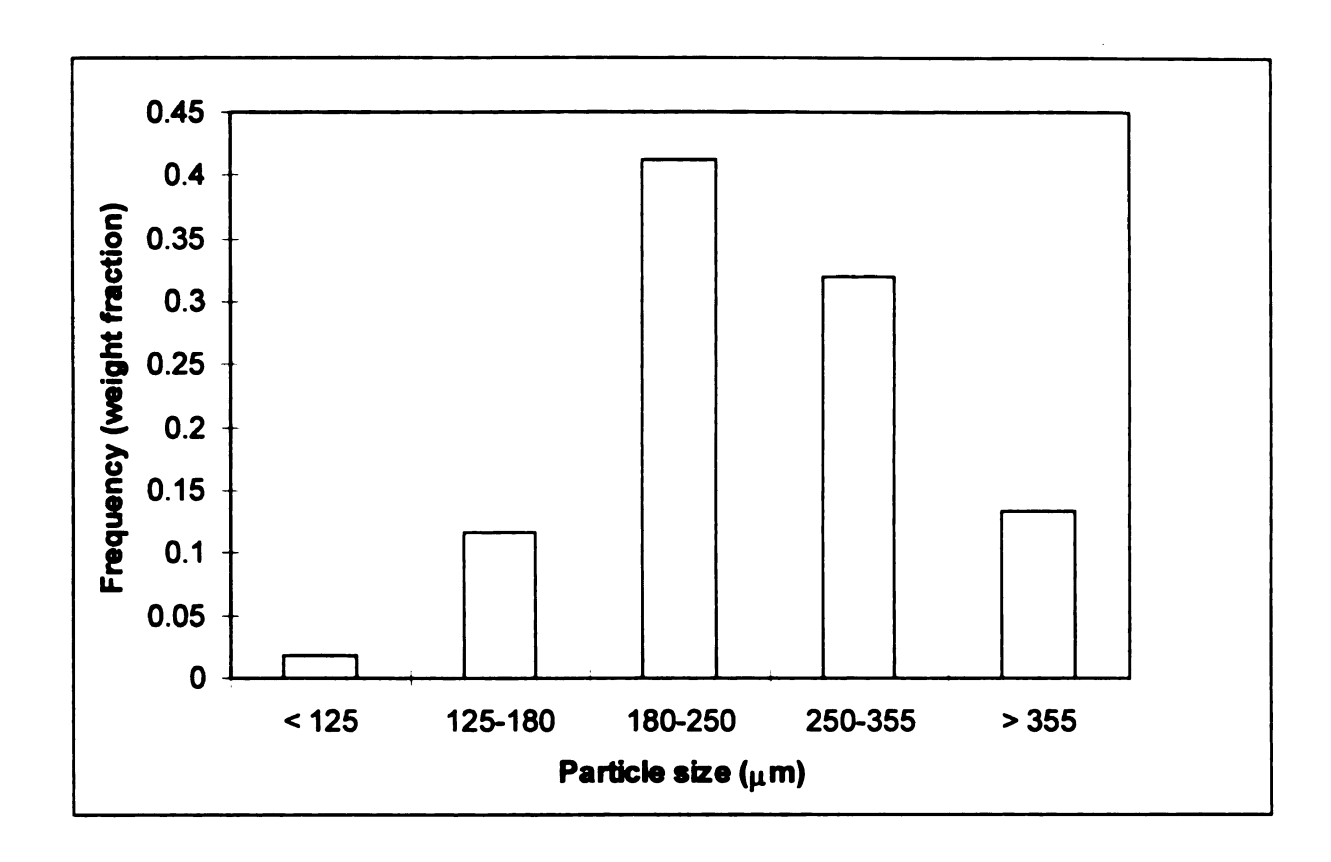


Figure 5.5 Weight based particle size distribution of the 40 mesh rubber particles

Table 5.2 Surface elemental composition in atom percent of uncoated rubber particles, rubber binder and polyester powder as determined by ESCA

Element	Uncoated rubber	Rubber binder	Polyester
Carbon	87.0	87.1	72.1
Oxygen	8.6	11.0	27.9
Silicon	4.4	1.9	-

Sieving

The weight distribution over the various sieves is shown in Figure 5.5. From the sieving data, it was calculated that the volume average particle size, d_V , was 260 μ m. The number average particle size, d_N , was 200 μ m.

Surface analysis

Before and after coating, the surface of the particles was analyzed by ESCA. Since ESCA is surface specific, it is an ideal tool to analyze whether the rubber particles were fully coated with polyester. The results of the ESCA analysis are given in Table 5.2.

The uncoated rubber contains a relatively large amount of oxygen. However, it is reasonable to assume that the oxygen is on the surface in the form of silica. Within experimental error, the amount of oxygen is exactly twice the amount of silicon. Similar observations were made on other types of tire rubber particles. The silica originated from sand in the tires. Therefore, the data was corrected for the presence of silica on the surface to compare the oxygen and carbon content of the rubber surface. Table 5.3 shows the data after correction for silica.

Now it is possible to make a direct comparison to find out how much of the surface is covered with polyester. Assuming that the surface contains X_{PE} of polyester and X_{nubber} of rubber, and given that the atomic concentrations of

oxygen on the rubber, polyester and coated rubber are $C_{O,nubber}$ $C_{O,PE}$ and $C_{O,nubber \, binder}$, respectively, the following equation must be satisfied:

$$C_{O,rubber\ binder} = X_{PE}C_{O,PE} + X_{rubber}C_{O,rubber}$$
 5.19

From that it is calculated that the rubber binder surface contains 27 % of polyester and 73 % of rubber.

Table 5.3 Surface elemental composition in atom percent of uncoated rubber particles, rubber binder and polyester powder as determined by ESCA, assuming that silicon is present in the form of silica.

Element	Uncoated rubber	Rubber binder	Polyester
Carbon	100.0	92.4	72.1
Oxygen	-	7.6	27.9

Environmental Scanning Electron Microscopy

Both the coated and the uncoated particles were examined by Environmental Scanning Electron Microscopy. Typical micrographs of the uncoated particles are shown in Figures 5.6 and 5.7. Figures 5.8-5.10 show typical micrographs of coated particles.

The surfaces of the untreated particles are clean except for some small amounts of dust or sand. On the treated particles in Figure 5.8, polyester droplets of approximately 5 μ m diameter can be seen clearly. Figure 5.9 shows that these droplets are present next to more irregular shapes, looking superficially like strings of droplets. After the magnification is increased (Figure 5.10), it turns out that these irregular shapes contain large amounts of very small spherical particles (0.2-2 μ m). The coverage seems to be of the same order of magnitude as found with ESCA.

The occurrence of small polyester droplets on the rubber binder surface indicates that the wetting of the rubber by the polyester is very poor. This was expected, since the particles are deposited on the rubber below the $T_{\rm g}$ of the polyester. The fact that the wetting and therefore the adhesion between the rubber and the polyester is poor, does not have any consequences for the binder function of the rubber binder since then, the rubber binder is heated above the $T_{\rm g}$ of the polyester. In addition, the surface free energy of the polyester will decrease when the temperature is raised. This will lead to a better wetting of the rubber particle by the polyester.



 $\textbf{Figure 5.6} \ \textbf{ESEM} \ \textbf{micrograph} \ \textbf{of untreated rubber particles}. \ \textbf{The box marks the} \ \textbf{field of view for Figure 5.7}.$



Figure 5.7 ESEM micrograph of untreated rubber particles

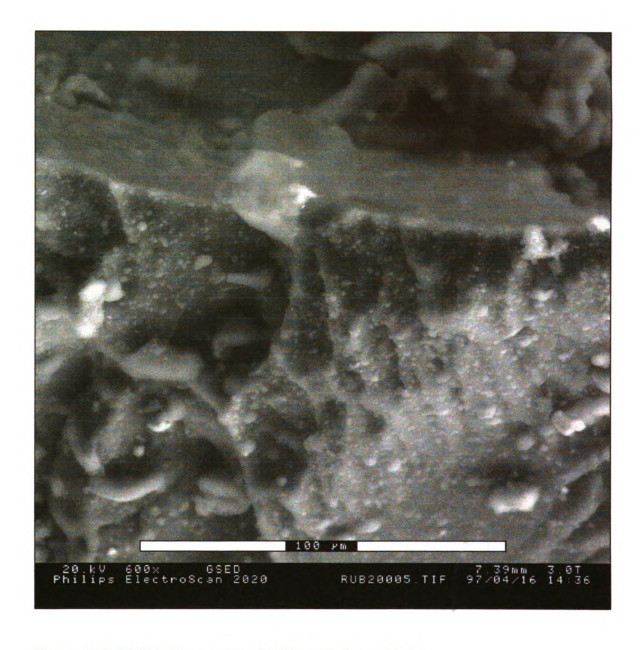


Figure 5.8 ESEM micrograph of rubber binder particles

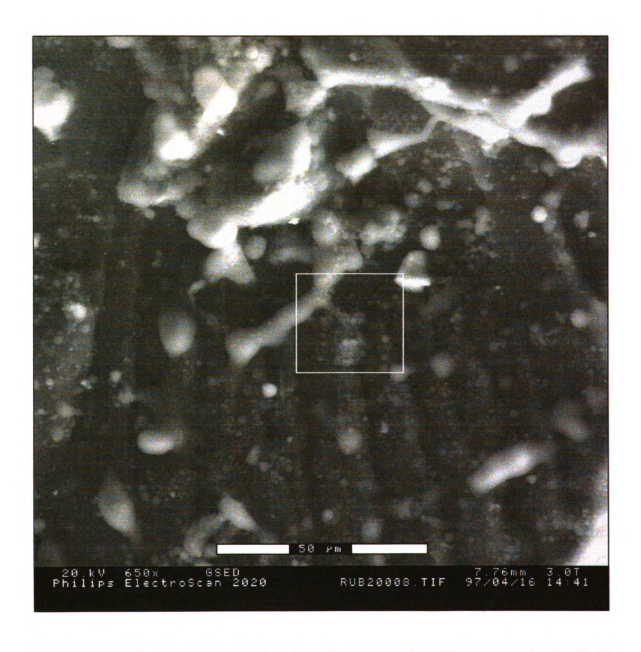


Figure 5.9 ESEM micrograph of rubber binder particles. The box marks the field of view for Figure 5.10.

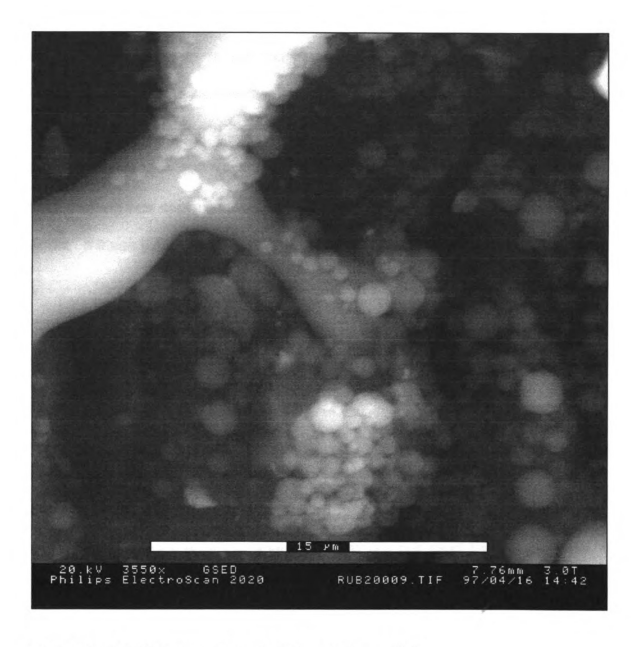


Figure 5.10 ESEM micrograph of rubber binder particles

Testing of the binding capacity

The binding capacity of the rubber binder was tested on aluminum foil and glass fiber preform, with rubber and the polyester (a commercial binder from DSM Italia) as a control. The experimental procedure is described in Appendix I. Both the rubber binder and the commercial binder were working when subjected to temperatures above 100 °C. The T_g of the binder that was already on the glass fiber preform was approximately 125 °C. Therefore, this binder did not have any effect on these experiments.

Conclusions

The polyester / acetone / water system is better suited to an antisolvent process than was predicted by thermodynamic modeling. The discrepancies between theory and experiment can be explained by considering the assumptions that were made in the theoretical analysis which are not valid for the polyester / acetone / water system. The most important assumptions that were made deal with the behavior of water. It was assumed that the distribution of molecules over the mixture was random, that interactions were between the center of molecules or polymer segments and that the volume change of mixing is zero. These assumptions are invalid, given that water will hydrogen bond with other molecules and specifically with the carboxylate group of the polyester. This

structuring of the mixture reduces the entropy of mixing, leading to a lower solubility of polyester in acetone / water than was anticipated.

The experiments have shown that rubber particles can be partially coated with polyester, using the reverse antisolvent phase separation process. This method is clean, and requires very little raw material, other than water.

ESCA analysis showed that 27 % of the surface of the particles is coated with polyester. From the Environmental Scanning Electron Microscopy experiments, it seems that this is a reasonable value for the coverage. Polyester is seen as clusters of small spheres $(0.2-2 \, \mu m)$ as well as larger droplets or irregular shapes. This indicates that the wetting of the rubber surface by the polyester was poor. This has no consequence for the binding behavior of the rubber binder, since the polyester was deposited below its T_g , while the binder function will be performed above T_g .

The binding behavior of the rubber binder was the same as that of commercial polyester powder.

References

- 1. M.S. Uusi-Penttilä, *Optimization of batch antisolvent crystallization*, Ph.D. Dissertation, Michigan State University, 1997
- 2. N.S. Tavare, M.R. Chivate, CSD Analysis from a batch dilution crystallizer, in *Handbook of Industrial Crystallization*, A.S. Myerson, Ed., Butterworth-Heinemann, USA, 1993.
- 3. W.J. Schmitt, M.C. Salada, G.G. Shook, S.M. Speaker, *AICHE J.* **41** (1995) 2476-2486
- 4. S.D. Yeo, P.G. Debenedetti, M. Radosz, R. Giesa, H.W. Schmidt, *Macromolecules* **28** (1995) 1316-1317
- 5. R. Bodmeier, H. Wang, D.J. Dixon, S. Mawson, K.P. Johnston, *Pharmaceutical Res.* **12** (1995) 1211-1217
- 6. S. Mawson, K.P. Johnston, J.R. Combes, J.M. Desimone, *Macromolecules* **28** (1995) 3182-3191
- 7. S. Mawson, K.P. Johnston, D.E. Betts, J.B. McClain, J.M. Desimone, *Macromolecules* **30** (1997) 71-77
- 8. A.F.M. Barton, Handbook of solubility parameters and other cohesion parameters, CRC Press, Boca Raton, FL,1983
- 9. L.H. Sperling, *Introduction to physical polymer science, second edition*, John Wiley and Sons, New York, 1992

Chapter 6

THE EFFECT OF THE RUBBER BINDER ON MECHANICAL PROPERTIES OF GLASS FIBER REINFORCED UNSATURATED POLYESTERS

Fracture toughness testing

Introduction

There are several tests to measure the fracture toughness of a composite specimen [1]. The two most important ones are the Double Cantilever Beam (DCB) test and the End Notch Flexure (ENF) test. These geometries are sketched in Figures 6.1 and 6.2.

There are some differences between the two geometries. The DCB test is a mode I test. The ENF test is a mode II test. The bending moment gives rise to a shear force at the crack tip.

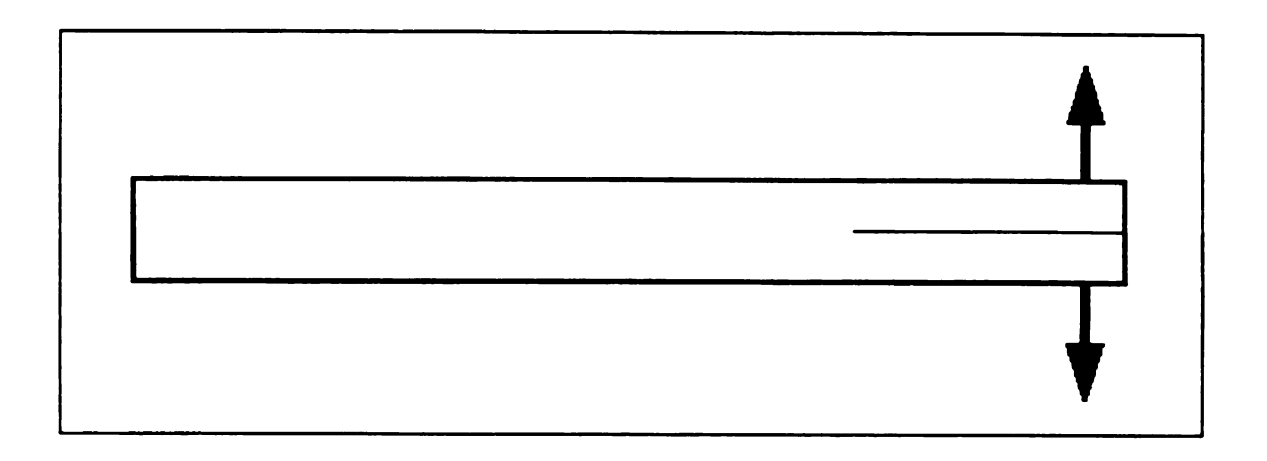


Figure 6.1 DCB geometry for fracture toughness testing

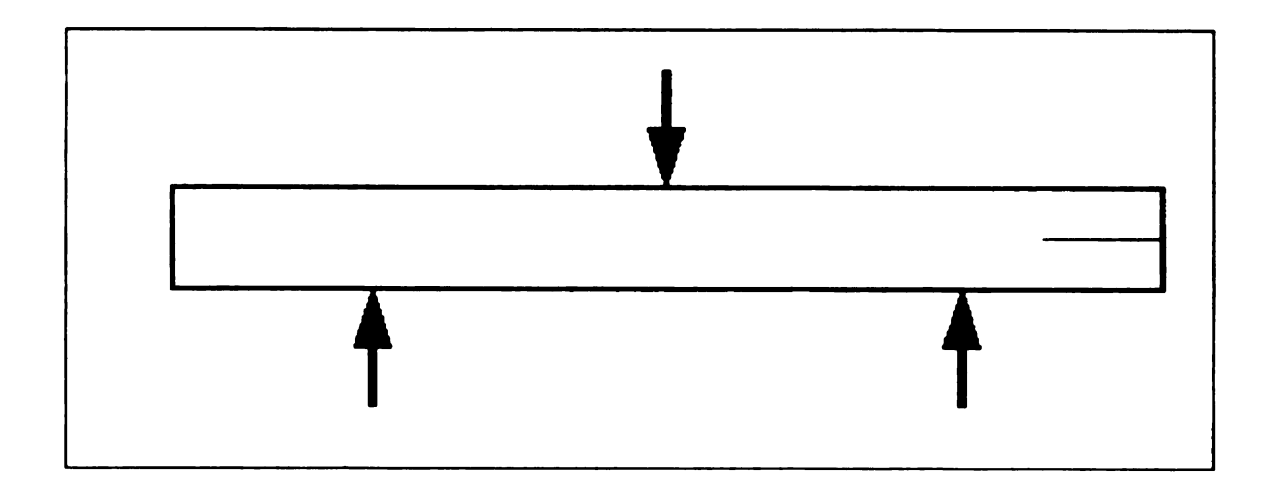


Figure 6.2 ENF geometry for fracture toughness testing

In the ENF test, the crack grows in an unstable manner. Once the crack starts to grow, it grows rapidly to the center of the specimen. The reason for this is that closer to the center, the shear stress will be larger. The fact that the crack grows unstably means that each test yields one data point only: the fracture toughness of the material at the tip of the crack starter. This is why the ENF test is not recommended for use in random fiber composites. The geometry at the crack tip is ill defined. The ENF test was not used in this research.

With the DCB test, there is stable crack growth. Every time the crack grows, the structure is relaxed and the stress at the crack tip decreases because of the increased compliance. In a DCB test the fracture toughness can be measured as a function of crack length. Now two fracture toughness values can be reported. These are the initial fracture toughness and the fracture toughness during crack growth. For random fiber composites, the initial fracture toughness value is not very meaningful because the crack tip geometry is ill defined. The fracture toughness values for the rest of the test can be used to obtain fracture toughness values for the specimen.

In an ideal test specimen, where the load would be applied exactly above and below the crack tip, the fracture toughness can be calculated using equation 6.1 [2].

$$G_{l} = \frac{3P\delta}{2ha}$$

With

 $G_I = mode I$ fracture toughness

P = load

 δ = load point displacement

b = specimen width

a = delamination length

Since a specimen is not ideal, three ways have been developed to overcome this. These are the Modified Beam Theory (MBT) [3], the Compliance Calibration method (CC) [4] and the Modified Compliance Calibration method (MCC) [5]. These three methods use a fit parameter to correct for non-ideality of the specimen.

In the MBT method, it is assumed that the experimental non-idealities can be corrected for by increasing the crack length by Δ . This leads to the following equations:

$$G_{I} = \frac{3P\delta}{2b(a+|\Delta|)}$$
 6.2

$$E_{1f} = \frac{64(a + |\Delta|)^3 P}{\delta h^3} = \frac{64(a + |\Delta|)^3 C}{hh^3}$$
 6.3

With

 $E_{1f} = modulus$

h = specimen thickness

C = compliance

Thus, when the $C^{1/3}$ is plotted versus a, a straight line is obtained. This line crosses the a-axis at - $|\Delta|$.

In the CC method, the power n for the relation between $C = c \cdot a^n$ is fitted. In the MBT method this power was fixed at 3. This parameter can be found by plotting log C vs. log a. The value of n gives a correction factor (rather than a shift):

$$G_{I} = \frac{nP\delta}{2ba}$$

A comparison with equation 6.1 shows that in the ideal case n = 3.

The MCC method also introduces a correction factor. This factor A_1 , can be found by plotting a/h as a function of $C^{1/3}$. Then, A_1 equals the slope of this line and G_1 can be calculated using:

$$G_{I} = \frac{3P^{2}C^{2/3}}{2A_{1}bh}$$
 6.5

Comparison with equation 6.1 shows that ideally A₁ is given by:

$$A_1 = \frac{a}{hC^{1/3}}$$

Experimental |

Random continuous fiber preforms were made with the rubber binder This rubber binder was made by the reverse antisolvent phase separation process that was described in chapter 5. At the center of the mat a Teflon sheet was inserted which functioned as a crack starter. The rubber binder content of the preform was varied between 0 and 10 weight percent. With these preforms, panels were made that were used in fracture toughness tests and flexure tests. Appendix I contains more details about the manufacturing of the preforms and the panels as well as the testing methods that were used.

For every specimen three curves were calculated for the critical strain energy release rate as a function of crack length using the MBT, CC and MCC correction methods. A typical set of curves is given in Figure 6.3

At the beginning of the experiment, when the crack length is small, there may be a region where the strain energy release rate is increasing. This is due to the fact that in that region crack growth is not self similar. The same is true for the end of the test. The tip of the damage zone may be too close to the edge of the specimen, leading to a rising curve. For this reason, the mean and standard deviation of the values on the plateau are taken to represent the strain energy release rate. All theories are averaged together.

The results of the fracture toughness test are given as a function of rubber binder content in Figure 6.4.

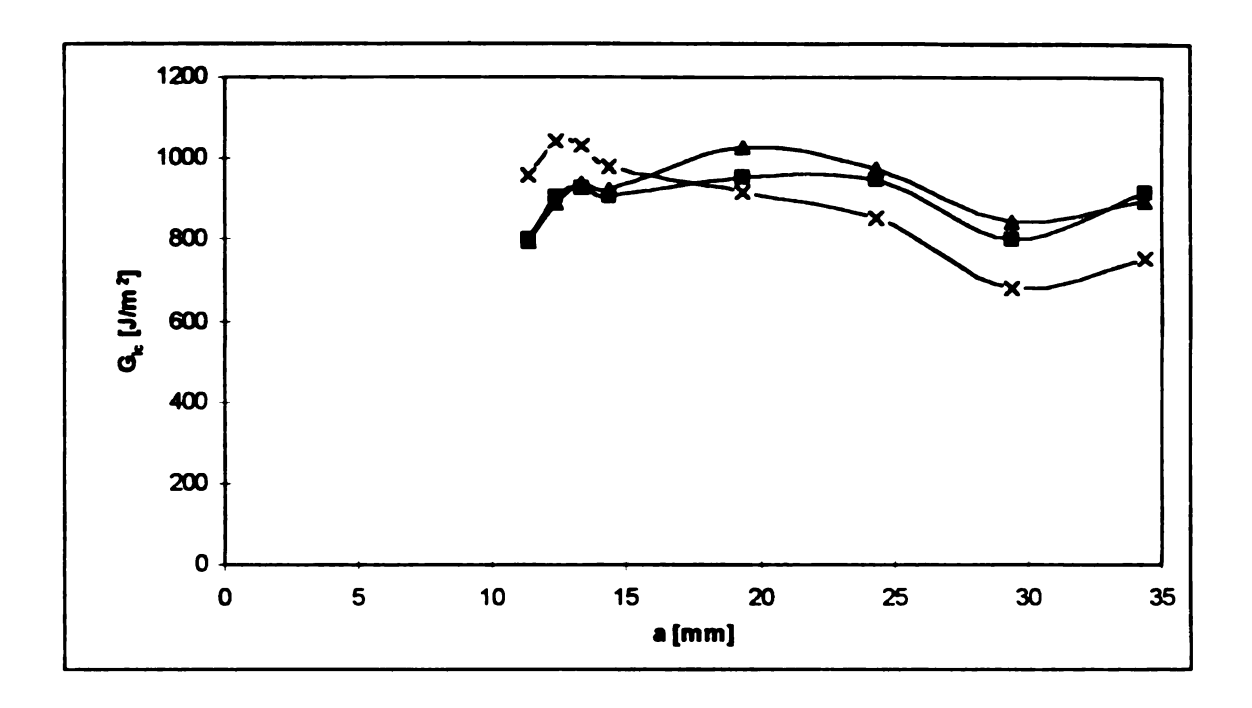


Figure 6.3 A typical set of strain energy release rate curves. Different theories were used to calculate these curves: -A- Modified Compliance Calibration theory, -X- Compliance Calibration theory, -M- Modified Beam Theory.

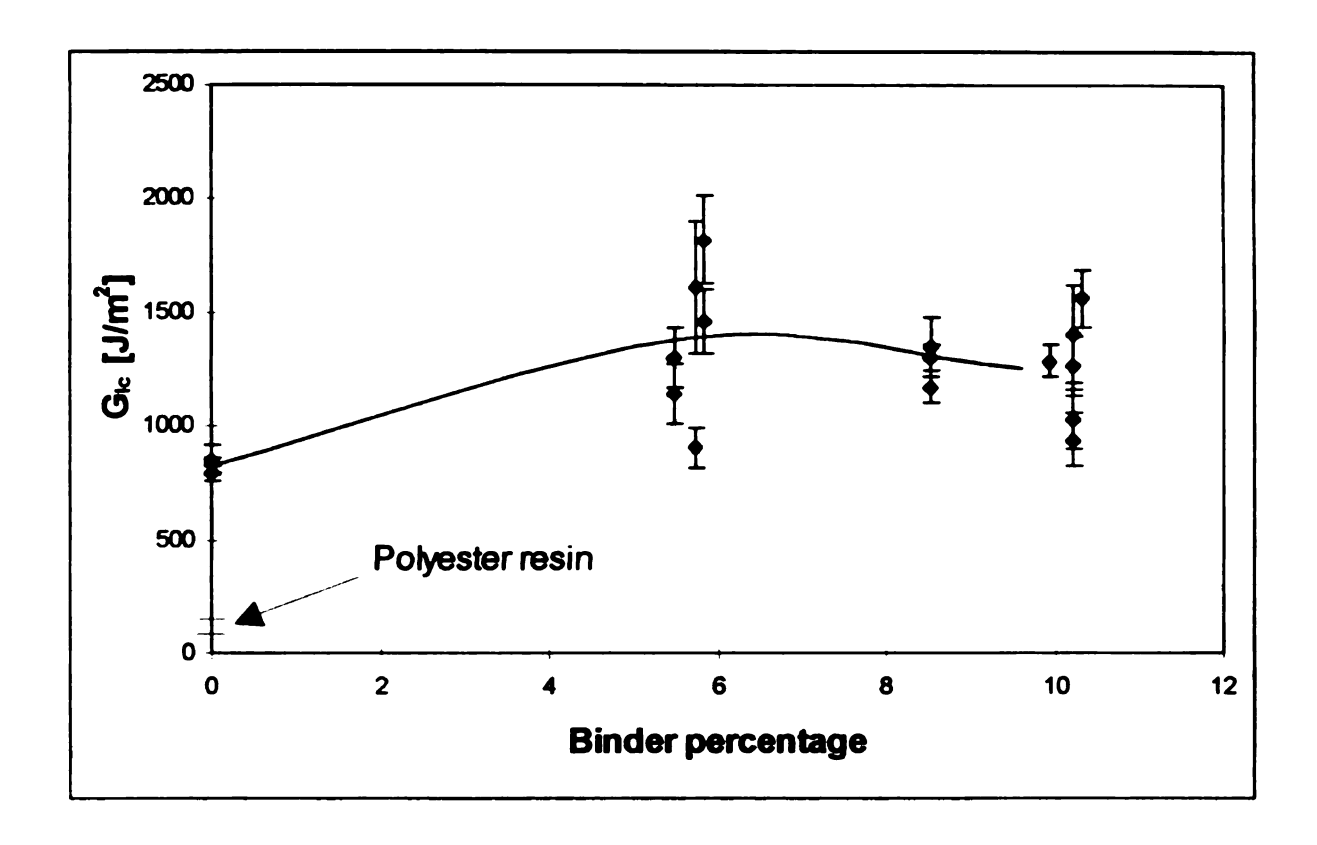


Figure 6.4 Strain energy release rate as a function of rubber binder percentage (solid line to guide the eye)

From Figure 6.4, two trends are apparent. The mean value of the strain energy release rate increases when the rubber binder percentage increases up to 6 %. After that the strain energy release rate remains constant or might decrease somewhat. At the same time, the standard deviation in the data increases with increasing rubber binder content. This standard deviation is depicted in Figure 6.5.

It can be seen that the standard deviation seems to follow the same trend as the strain energy release rate. It goes up initially and then seems to stabilize.

The large standard deviation in the test results is due to the non self similar nature of the fracture process. The number of rubber particles that are involved in the fracture process varies during the growth of the crack.

A work of fracture test method would have been better than the strain energy release rate test. The essential difference between the two tests is that in the strain energy release rate test, the fracture toughness is measured at various points in growth of the crack, while in the work of fracture test the fracture toughness is determined over intervals in the growth of the crack. The latter has the advantage that it averages the data over the distance of the interval, making the work of fracture test more accurate.

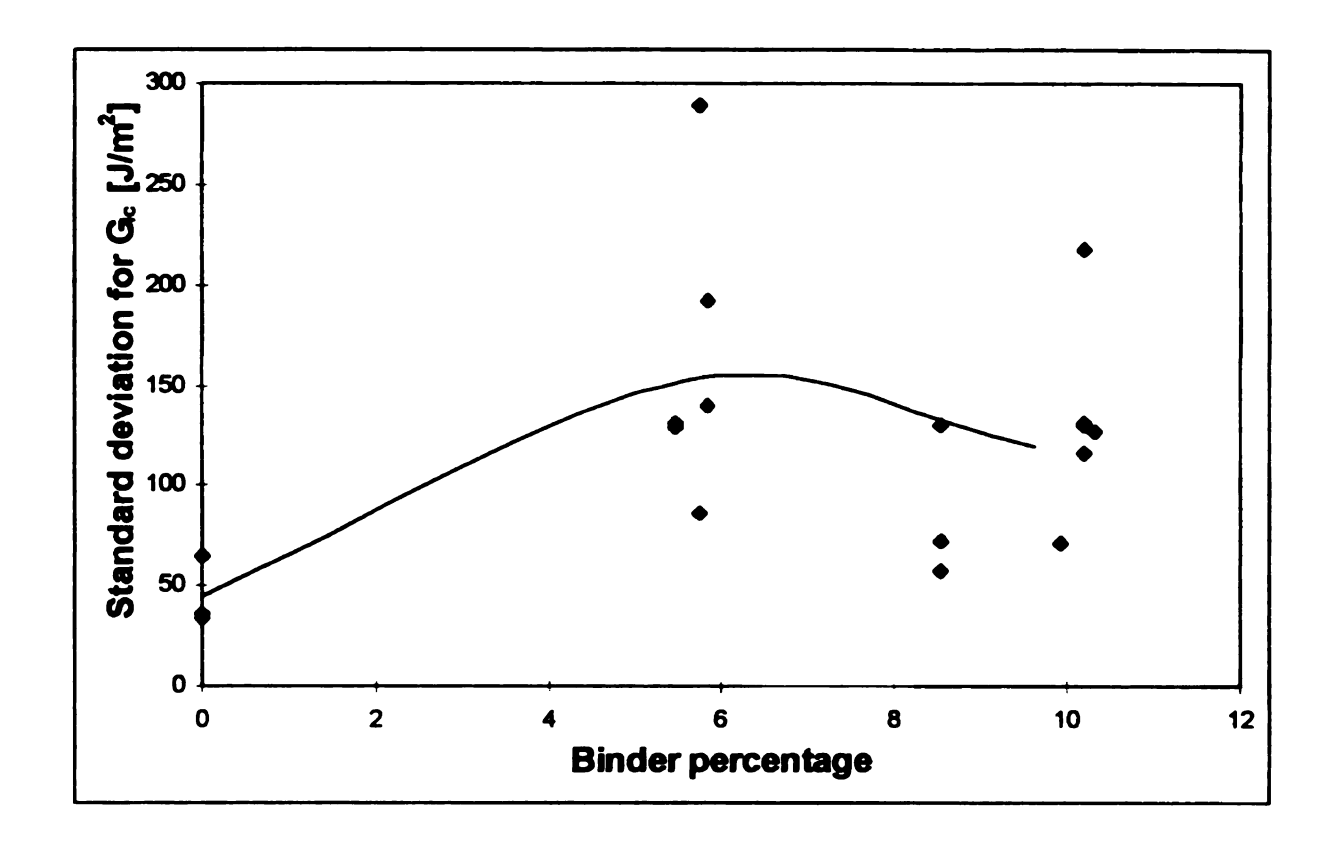


Figure 6.5 Standard deviation in the strain energy release rate as a function of rubber binder percentage (solid line to guide the eye)

Another important observation was made visually. During the test, rubber particles were bridging the crack. The particles seemed to be kept in place because they were clamped between fiber bundles. This was made possible by the irregular shape of the rubber particles. Once a fiber bundle failed the crack bridge failed too.

Environmental Scanning Electron Microscopy of fracture surfaces

The fracture surfaces were examined with Environmental Scanning Electron Microscopy. Typical micrographs are shown in Figures 6.6 - 6.8.

In the micrographs, smooth fiber surfaces can be seen. Though the fibers are optimized for Unsaturated Polyester applications, the fiber-matrix adhesion is poor. This can be explained by the fact that the bundles remain intact and do not spread. This is due to the nature of continuous fiber mats. The fibers in the bundle are entangled at the same position with the same lengths between entanglements. The entanglements between fiber bundles prevent the fibers from spreading.

Another observation is that there is no adhesion between the rubber and the matrix. The pull-out cavity left by a rubber particle is absolutely smooth (Figure 6.7). The same can be said of the rubber particle itself. There is no trace of matrix material on the particle (Figure 6.8). On top of that, not a single fractured rubber particle could be found.

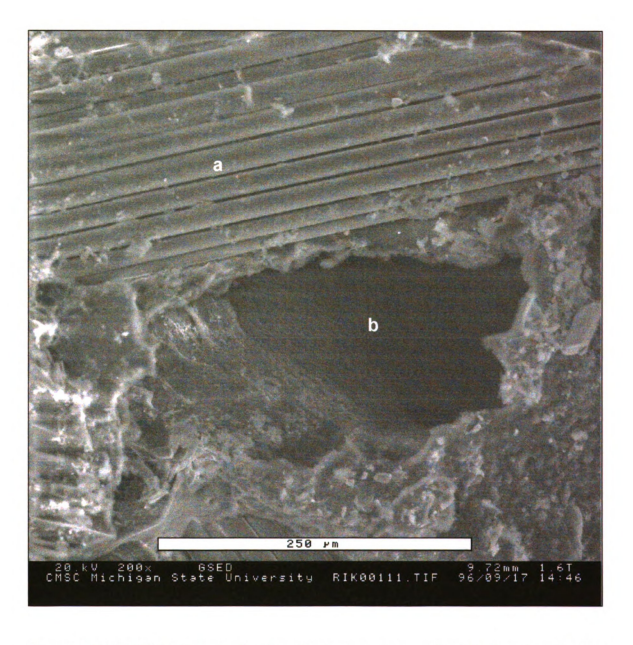


Figure 6.6 ESEM micrograph of a fracture surface after fracture toughness testing (a = glass fiber bundle, b = pull-out of rubber particle)



Figure 6.7 ESEM micrograph of a fracture surface after fracture toughness testing (a = pull-out of rubber particle, b = matrix side of fiber-matrix failure, c = fiber bundle)

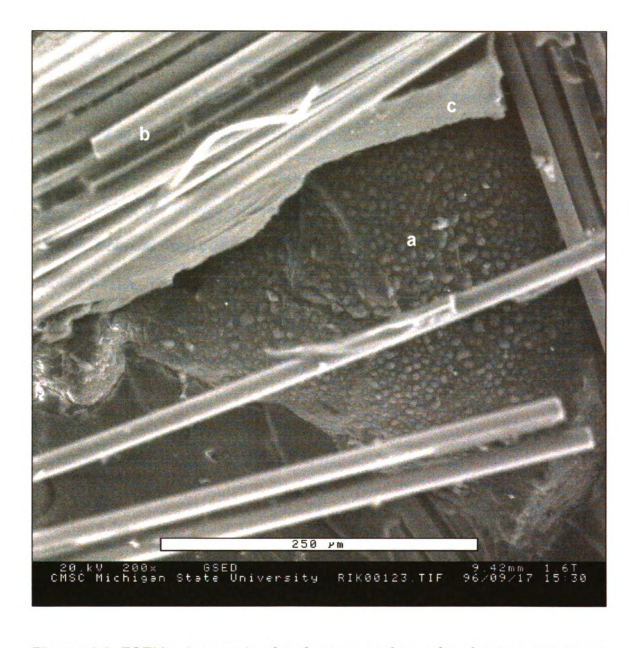


Figure 6.8 ESEM micrograph of a fracture surface after fracture toughness testing (a = rubber particle, b = fiber bundle, c = brittle matrix failure)

Flexure testing

From the same panels that were used for the fracture toughness testing, flexure specimens were cut. The specimen size was $3 \times 1/4 \times 1/8$ inch. The tests were performed as described in Appendix I. All specimens failed in tension.

The results of the flexure tests are given in Figures 6.9 and 6.10. From those figures, it can be seen that the flexure strength is not significantly affected by the rubber binder. The effect of the particles on the modulus is small. This was expected since the flexure test, is sensitive to the tensile properties in the fiber direction. The properties are dominated by the fibers, not by the matrix.

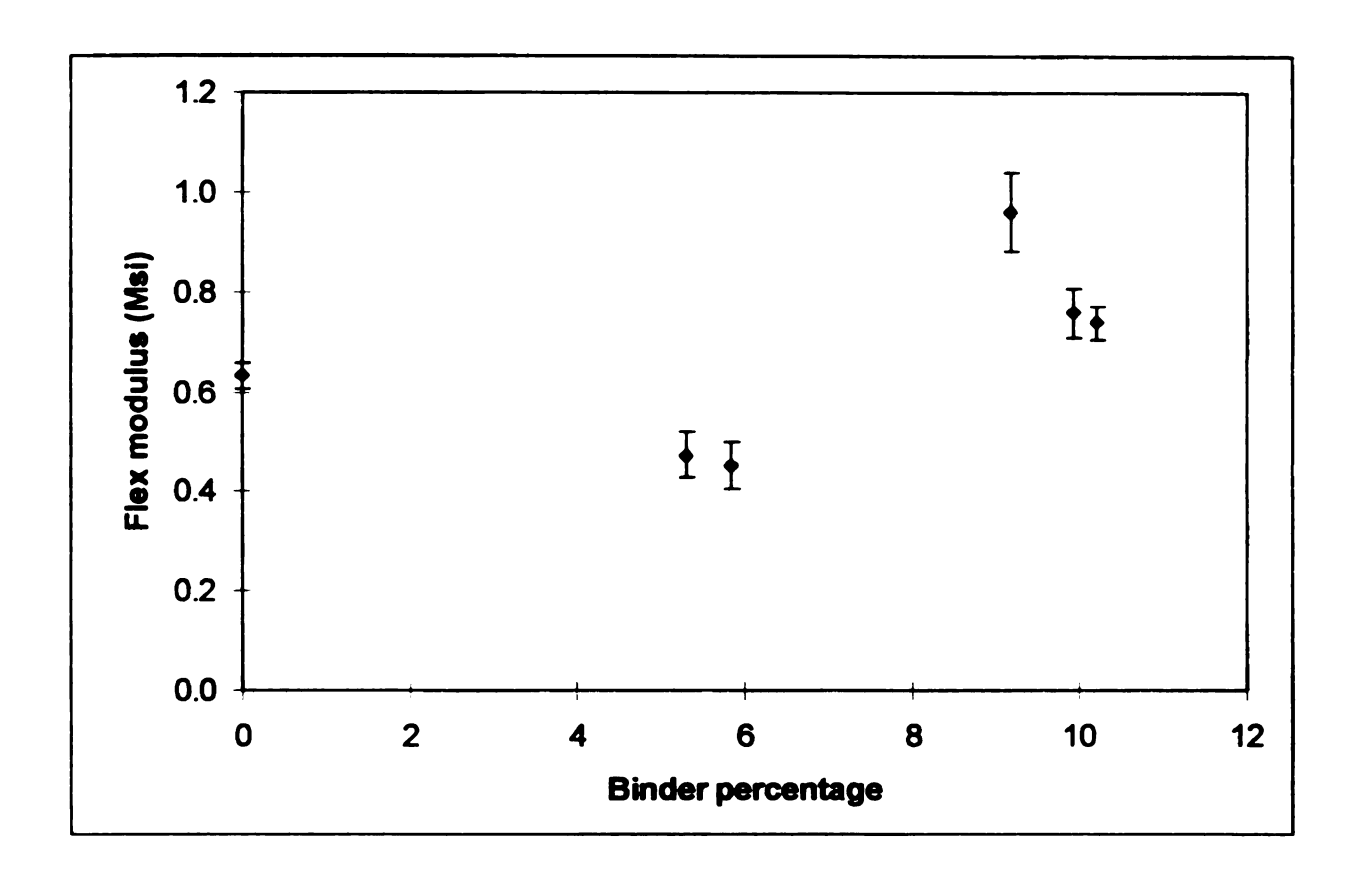


Figure 6.9 Flexure modulus of Random Continuous Glass Fiber Reinforced Unsaturated Polyester, modified with different levels of rubber binder

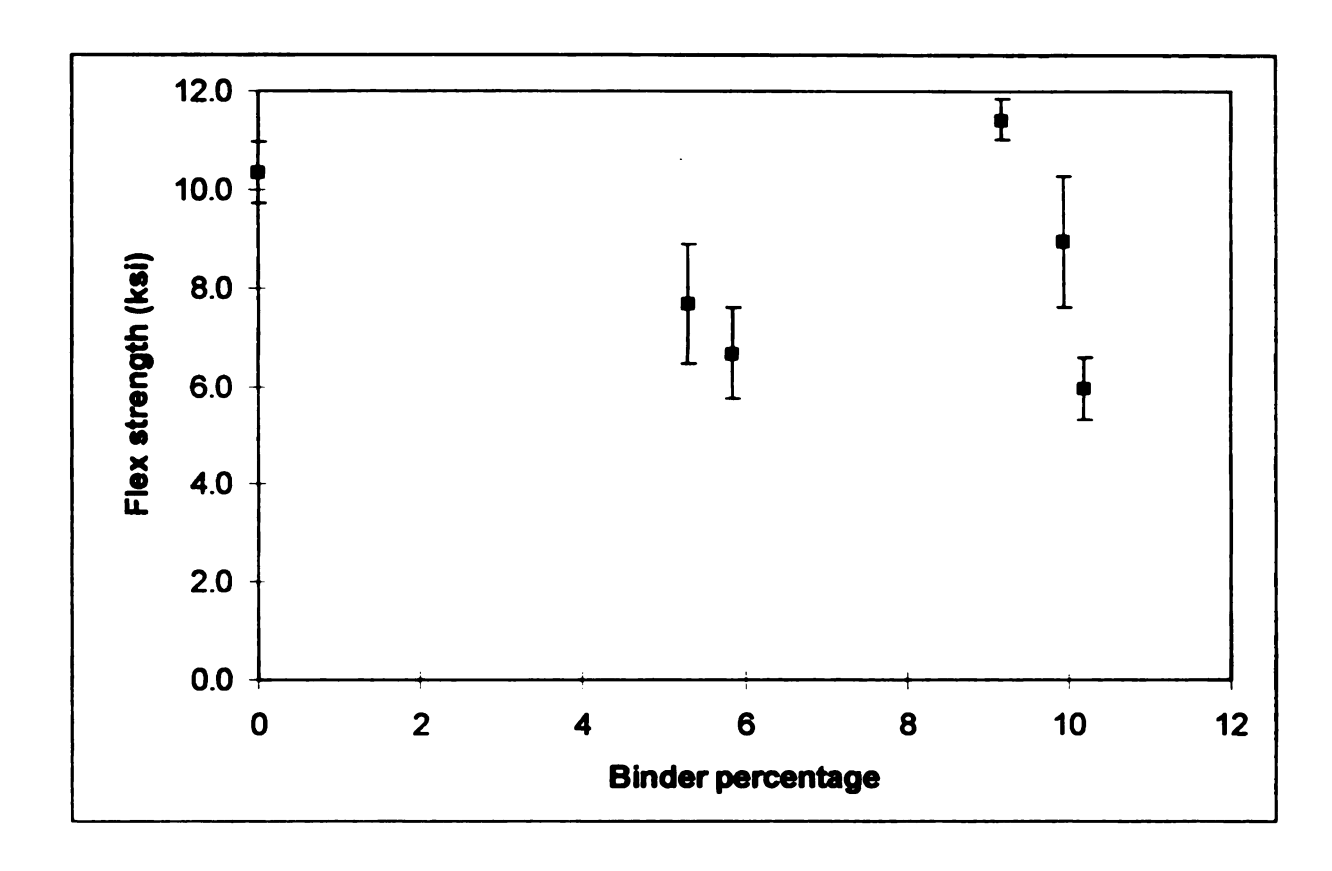


Figure 6.10 Flexure strength of Random Continuous Glass Fiber Reinforced Unsaturated Polyester, modified with different levels of rubber binder

Discussion

From the fracture toughness test, it can be seen that the fracture toughness increased from 800 J/m² to approximately 1400 J/m² for a specimen with 6 % rubber binder on the glass fiber. This is an increase of 75 %.

It is interesting that the standard deviation in the test follows a similar trend. The standard deviation for a specimen without rubber binder is approximately 50 J/m² (6 %). For a sample with 6 % rubber binder the standard deviation is 160 J/m² (12 %). The increase in standard deviation is caused by the increase in inhomogeneity of the sample. This could have been reduced if a work of fracture test method would have been used.

Another interesting observation is the particle bridging of the crack. This is the cause of the increase in fracture toughness. The crack bridging phenomenon is intriguing since from the ESEM micrographs it was clear that there was very little adhesion between the matrix and the rubber. Mechanical adhesion between the fiber bundles and the rubber particle made the crack bridging possible.

Conclusions

The delamination fracture toughness of Random Continuous Glass Fiber Reinforced Unsaturated Polyester is increased by the addition of rubber binder to the fiber mat. A rubber binder content of 6 % is optimal, leading to a 75 % increase in the delamination fracture toughness.

Crack bridging by the rubber particles is the mechanism responsible for this increase. The adhesion between the crack surface and the particle is that of mechanical interlocking of the particle between the fiber bundles.

The addition of up to 10 % rubber binder does not influence the flexure properties of Random Continuous Glass Fiber Reinforced Unsaturated Polyester. This is expected, since the flexure properties are governed by the fiber properties.

References

- 1. J.M. Whitney, I.M. Daniel, R.B. Pipes, 'Experimental Mechanics of Fiber Reinforced Composite Materials, Revised edition', Prentice-Hall, Englewood Cliffs, NJ, 1984, 234-244
- 2. ASTM D 5528 94a, Standard Test Method for Mode I Interlaminar Fracture Toughness of Unidirectional Fiber-Reinforced Polymer Matrix Composites
- 3. S. Hashemi, A.J. Kinloch, J.G. Williams, J. Mater. Sci. L. 8 (1989) 125-129
- 4. J.P. Berry, J. Appl. Phys. 34 (1963) 62-68
- 5. K. Kageyama, M. Hojo, *Proceedings of the 5th U.S./Japan Conference on Composite Materials*, Tokyo, 1990, 227-234

Chapter 7

THE EFFECT OF RUBBER SURFACE MODIFICATION ON THE MECHANICAL PROPERTIES OF GLASS FIBER REINFORCED UNSATURATED POLYESTERS

Introduction

The adhesion between the rubber particles and the matrix appeared to be minimal (see chapter 6). This chapter describes the attempt that was made to improve the rubber-matrix adhesion and the effect that it had on the mechanical properties of the composite.

Surface modification

Before the rubber particles were made into a binder, they were subjected to a surface treatment procedure. This procedure consists of two steps. In the first step, the surface is activated using a UV / ozone treatment procedure. In the

second step, oleic acid is grafted on the activated rubber surface. Details about the experimental procedure can be found in Appendix I

The idea behind this treatment is that the UV / ozone treatment will convert the aliphatic rubber surface into a surface rich in alcohol and acid groups [1,2]. The oleic acid can react with the alcohol groups on the surface. During the curing of the composite part, the double bond in the oleic acid can react with the styrene in the resin mixture to form a chemical link between the rubber and the matrix.

Alternatives for the UV / ozone treatment are flame treatment, corona treatment or plasma treatment. The UV / ozone treatment has the advantage that it is easy, relatively fast and environmentally benign. In addition, the UV / ozone treatment penetrates deeper into the surface than the other methods [2].

For a flat surface, a UV / ozone treatment time of a few minutes is usually optimal [9]. In that case, the treated surface area is approximately 5 cm² (5.10⁻⁴ m²). The surface area of 6 g of rubber is approximately 180.10⁻³ m². Therefore, longer treatment times were chosen.

The effect of the UV / ozone treatment time was studied with ESCA. Rubber samples were made with treatment times of 15 and 30 minutes and their surfaces were analyzed with ESCA.

The results of the ESCA analysis are given in Table 7.1. The presence of silicon distorts the picture. Table 7.2 gives the percentages of oxygen and carbon, assuming that all the silicon is present as silica. This method is the same as used in chapter 6.

Table 7.1 Atomic compositions of rubber particle surfaces as determined by ESCA

element	untreated	15 min UV	15 min UV	30 min UV	30 min UV
			+ oleic acid		+ oleic acid
carbon	87.0	87.8	88.0	88.8	89.0
oxygen	8.6	8.3	10.2	8.2	9.1
silicon	4.4	3.8	1.7	3.0	1.7

Table 7.2 Atomic compositions of rubber particle surfaces as determined by ESCA, after correcting for silica

element	untreated	15 min UV	15 min UV	30 min UV	30 min UV
			+ oleic acid		+ oleic acid
carbon	100	99	93	98	94
oxygen	0	1	7	2	6

As can be seen from Table 7.2, the difference between the 15 and 30 minute treatments is minimal. Unfortunately, the amount of oxygen on the surface is small. However, a large amount of the oleic acid remained on the surface. Part of that may have reacted with the surface oxygen. From the molecular formula of oleic acid (C₁₇H₃₃COOH), the percentage of oxygen and carbon in the molecule can be calculated. Since ESCA cannot detect hydrogen, for ESCA analysis purposes, oleic acid contains 10 % oxygen and 90 % carbon. Therefore, it can be concluded that approximately two thirds of the rubber surface is covered with oleic acid.

Fracture toughness testing

Panels were made with the surface treated particles and fracture toughness testing was performed as described in chapter 6. Figure 7.1 shows a comparison between the fracture toughness of samples with particles with and without surface treatment. Figure 7.2 shows the standard deviation in the test.

From the data in Figure 7.1, it can be seen that the fracture toughness values seem to be a little higher for the surface modified rubber binder. Now, the maximum value is 1600 J/m², which is a 100 % increase over the samples without rubber binder. Again, the maximum in the curve is for 6 % of rubber binder on a glass fiber basis. From Figure 7.2, it can be seen that the standard deviation in the fracture toughness appears to be a little less for the surface modified samples.

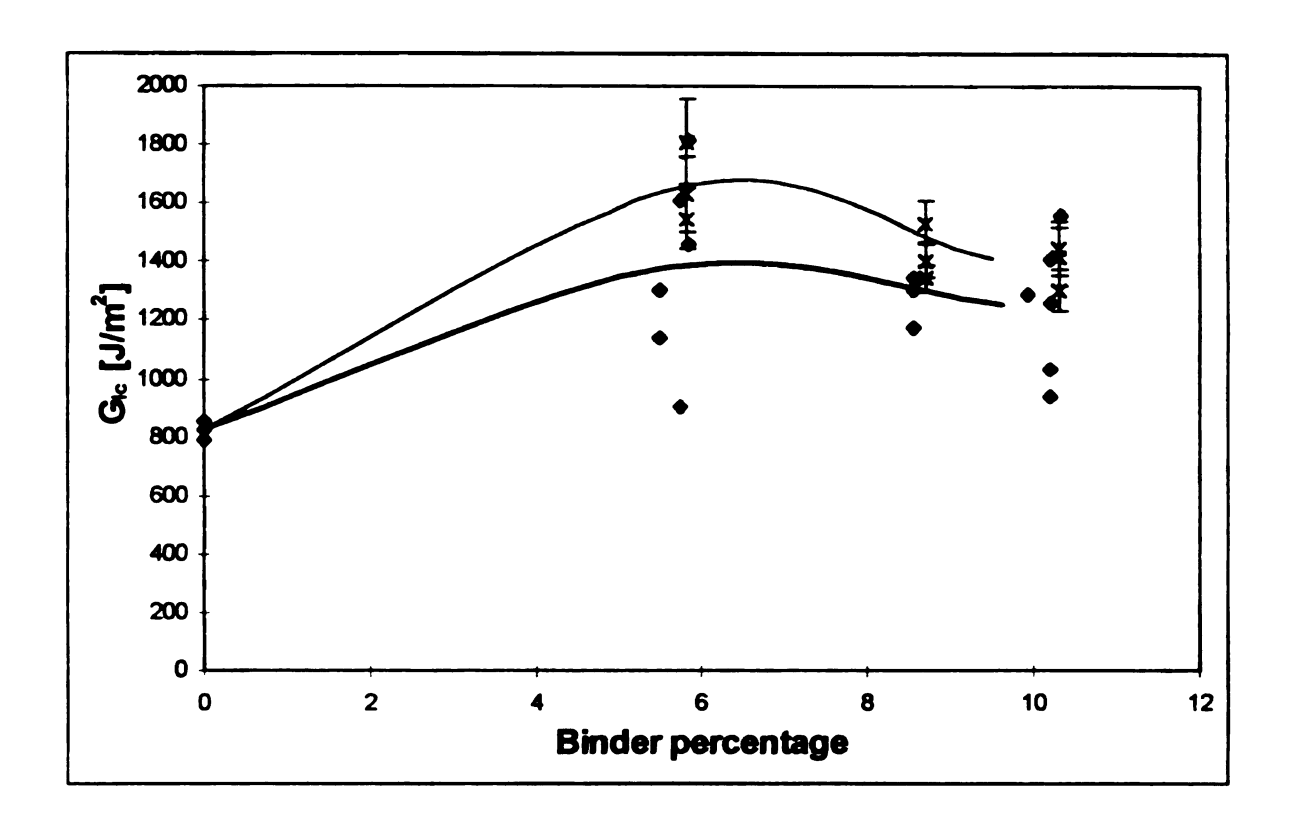


Figure 7.1 The fracture toughness of samples with surface modified rubber binder (x) compared with the fracture toughness of samples with standard rubber binder (♠). Error bars for the standard rubber binder have been removed for clarity.

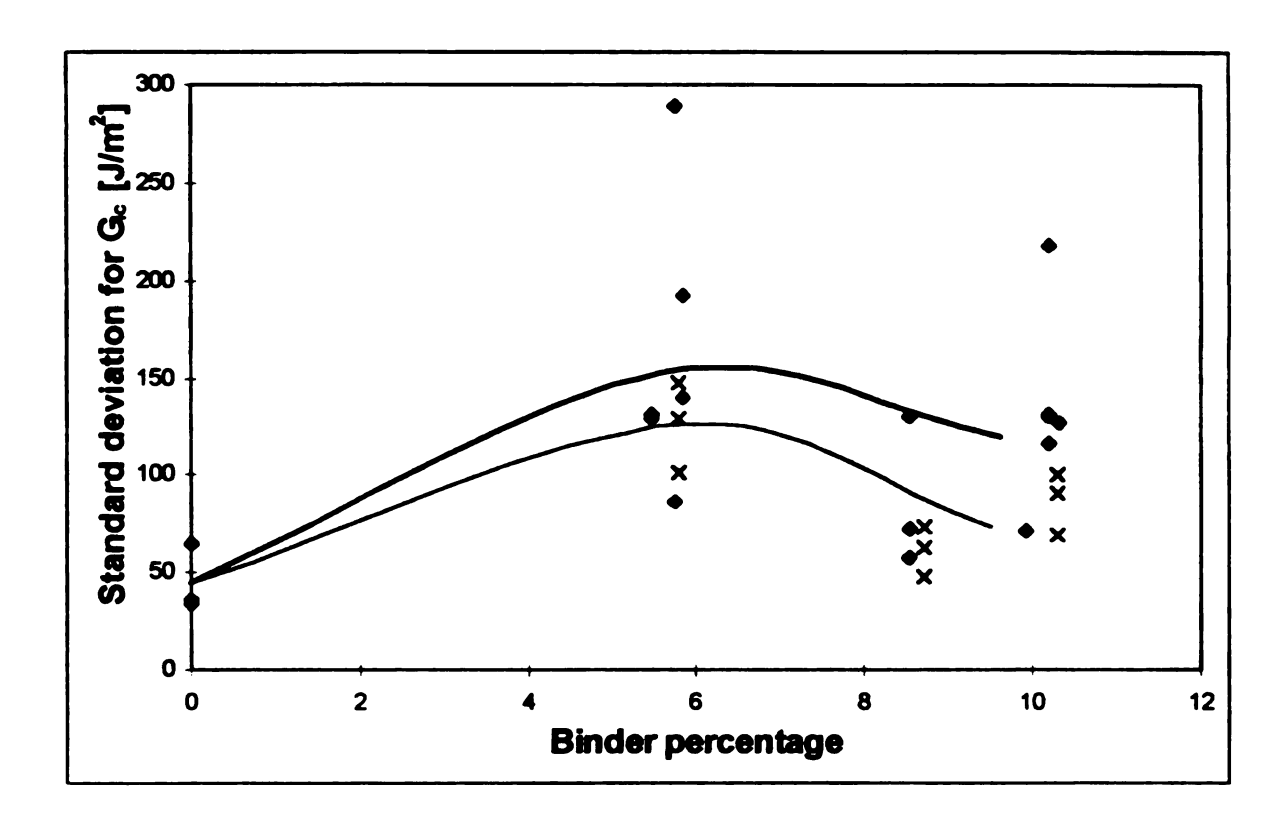


Figure 7.2 The standard deviation in the fracture toughness of samples with surface modified rubber binder (x) compared with the standard deviation in the fracture toughness of samples with standard rubber binder (\clubsuit)

Environmental Scanning Electron Microscopy of fracture surfaces

Micrographs were taken as described in Appendix I. Some typical micrographs are shown in Figures 7.3-7.7.

On these samples the same features can be found as on the samples with rubber without a surface treatment. These features are shown in Figures 7.3 and 7.4. Figure 7.3 shows a pull-out hole of a rubber particle. In Figure 7.4 a separate rubber particle is shown. Apparently, there is little adhesion between particle and matrix. These features are found in the vicinity of glass fibers.

Figures 7.5-7.7 show a feature that was not found in any sample with rubber that was not treated: fractured rubber particles. These particles are only found in relatively resin rich areas. The micrographs all show the same particle with different magnifications. This particle is typical for what can be seen on other fractured particles. Fractured particles were only found in resin rich areas. Figure 7.7 shows the particle-matrix interface. There seems to be a good contact between particle and matrix.

From the ESEM micrographs, it is clear that cavitation occurred in the rubber particle. The size of the cavities is in the order of 1 μ m. As discussed in chapter 2, cavitation is one of the major toughening mechanisms in rubber modified homogeneous polymers [3-5].



Figure 7.3 ESEM micrograph of a fracture surface after fracture toughness testing (a = pull-out of rubber particle)



Figure 7.4 ESEM micrograph of a fracture surface after fracture toughness testing (a = rubber particle, b = matrix)

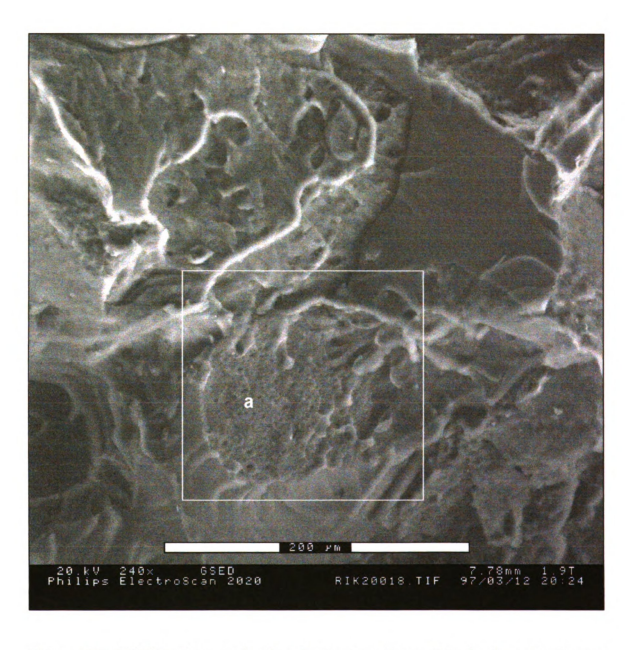


Figure 7.5 ESEM micrograph of a fracture surface after fracture toughness testing. (a = fractured rubber particle) The box indicates the view area for the micrograph in Figure 7.6.

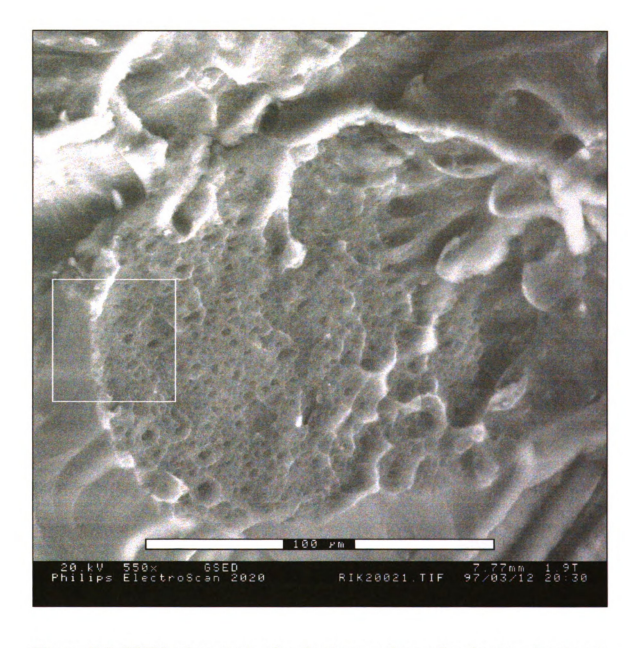


Figure 7.6 ESEM micrograph of a fracture surface after fracture toughness testing. The box indicates the view area for the micrograph in Figure 7.7.

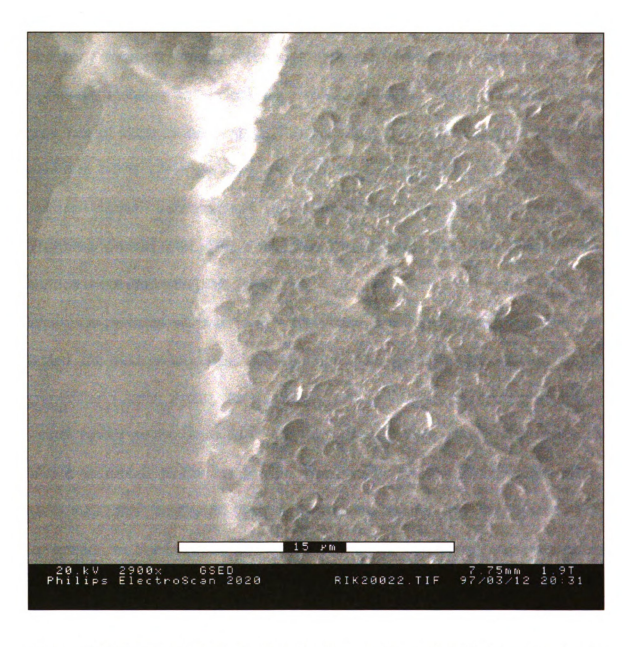


Figure 7.7 ESEM micrograph of a fracture surface after fracture toughness testing

Discussion

The UV / ozone treatment was moderately effective. There was a small, but significant increase in surface oxygen concentration after correcting for the presence of silica in the sample. The surface oxygen concentration increased from 0 to 1-2 %. Other treatment methods are usually capable of increasing the surface oxygen concentration up to approximately 10 %. The oleic acid treatment worked well. ESCA revealed that approximately two thirds of the surface is covered with oleic acid.

When the particles were used in a composite and the fracture toughness was tested, the fracture toughness values seem to be somewhat higher than for the unmodified rubber. Again, the maximum fracture toughness occurred at 6% of rubber binder on the glass fiber. The fracture toughness values for a specimen with 6 % rubber binder on a glass fiber basis has a fracture toughness of $1600 \pm 200 \text{ J/m}^2$. This a 100 % increase over the untoughened specimens.

In addition to the increase in fracture toughness, compared to the untreated rubber particles, there is a change in standard deviation. The standard deviation for the samples with treated particles seems to be somewhat lower. This could be caused by the fact that now more particles are involved in the toughening, since now there is good adhesion between matrix and particles.

The ESEM micrographs show an important new feature: the occurrence of fractured rubber particles, mainly in resin rich areas.

These observations seem to support a theory that in fiber rich areas mechanical interlocking of the particle between the fibers causes particle bridging. In that case, the mechanical adhesion is the weakest link in the chain, since the rubber does not fracture.

In resin rich areas, particle bridging can be caused by particle-matrix adhesion.

In this case, failure is adhesive only for non modified particles. For modified particles, cohesive failure of the rubber particle may occur.

This theory would explain the slight increase in fracture toughness since more particles are active in crack bridging. For the same reason, the standard deviation would decrease.

Conclusions

Surface modification of the rubber particles has been mildly successful. The UV / ozone treatment caused a slight but significant increase in surface oxygen. After treatment with oleic acid, approximately two thirds of the particle surface is covered.

The surface treatment of the rubber particles led to an additional increase in fracture toughness. The fracture toughness of a specimen containing 6% of rubber binder in the preform, is 100 % higher than the fracture toughness of the samples without rubber binder. With ESEM, fractured rubber particles could be

seen in resin rich areas, indicating particle-matrix adhesion. The mechanism of fracture of the rubber particles was cavitation. This was not the case for rubber particles that were not modified.

These data support the idea that the toughening effect is due to particle bridging. With good particle-matrix adhesion, more rubber particles can be active in crack bridging. That could explain the slight increase in fracture toughness for the modified rubber samples over the unmodified rubber samples.

References

- 1. N. Dontula, C.L. Weitzsacker, L.T. Drzal, *Proceedings of the 20th Annual "Anniversary" Meeting of the Adhesion Society*, L.T. Drzal, H.P. Schreiber, Eds., Hilton Head Island, SC, 1997, 97-99
- 2. M. Strobel, M.J. Walzak, J.M. Hill, A. Lin, E. Karbashewski, C.S. Lyons, J. Adhes. Sci. Technol. 9 (1997) 365-383
- 3. A.F. Yee, R. A. Pearson, J. Mater. Sci. 21 (1986) 2462-2474
- 4. R. A. Pearson, A.F. Yee, J. Mater. Sci. 21 (1986) 2475-2488
- 5. R. A. Pearson, A.F. Yee, J. Mater. Sci. 21 (1986) 2571-2580

Chapter 8

CONCLUSIONS

An approach has been developed for toughening Glass Fiber Reinforced Unsaturated Polyesters (GFRUPs) by using a toughening binder.

In chapter 3, it was shown that a well-designed commercial binder can perform the binder function without deteriorating the mechanical properties of the composite. Both a multivariate and a residual statistical analysis of 0 and 90° Flexure test results were used to prove this.

The initial attempt to make a toughening binder made use of silicone rubber (PDMS, polydimethylsiloxane). It was possible to modify the end group of the PDMS in such a way that the end group was a phenoxy, cresoxy or nonyl phenoxy group. These modifications were made in an attempt to control the size of the silicone phase in the unsaturated polyester. Completion of the reaction was proven with FTIR. The particle size of the silicone rubber in unsaturated polyester resin was between 0.8 and 2 μ m. The particle size was not influenced by the PDMS end group. An explanation for this is that the silicone phase separation is kinetically rather than thermodynamically controlled. Since the silicone phase size could not be controlled, this approach was abandoned.

The second attempt was successful. It is demonstrated that it is possible to deposit commercial binder on recycled tire rubber particles. The antisolvent method that was used is new in the field of polymer science. The method that was finally chosen is a reverse antisolvent phase separation. The rubber particles are dispersed in water. Then a binder solution in acetone is added to the dispersion. With this method, it was possible to coat the particle with approximately 27 % of polyester binder. This was shown by ESCA and ESEM. The binding characteristics of these modified rubber particles were the same as for the commercial binder that was used to modify the rubber.

The toughening effect of the binder was shown in chapters six and seven. Use of the binder increases the fracture toughness significantly. The maximum increase is when 6 % of binder is added to the glass fibers. Then, the fracture toughness increases by 75 %. The binder does not affect the flex properties of the composite. The fracture properties improve by an additional 25 % when the rubber surface is modified with a UV / ozone treatment followed by an oleic acid treatment.

The toughening mechanism is bridging of the crack by the rubber. If the rubber surface is not modified, there is no adhesion between the matrix and the rubber. The rubber is kept on the fracture surface because it is clamped between the fibers. This is made possible by the irregular shape of the rubber particles. In resin rich areas, crack bridging cannot occur. When the surface of the rubber is modified, the rubber particles in the resin rich areas can take part in the crack

bridging too. In this case, the rubber is kept on the fracture surface because of the particle-matrix adhesion. ESEM showed that the adhesion can be so strong that the rubber particle fractures. From the micrographs, it was also concluded that the rubber particle fracture was due to cavitation, which is a major toughening mechanism in rubber toughened thermosets.

For future research in this field, it is suggested that the influence of the particle size on the fracture toughness is studied. Work of fracture tests should be used rather than critical strain energy release rate tests because of their better accuracy.

Materials and experimental procedures

Materials

In the study, the following materials were used without further purification or analysis:

- Unsaturated polyester resin from DSM Resins, Zwolle, The Netherlands. The unsaturated polyester resin is based on ethylene glycol, propylene glycol, maleic anhydride and phthalic anhydride [1]
- Styrene, 98 %, benzoyl peroxide, 98 %, dimethyl aniline, 98 % from Aldrich. The styrene is the polymerizing species in the resin mixture, crosslinked by the unsaturated polyester. The benzoyl peroxide initiates the reaction while the dimethylaniline acts as an accelerator.
- Glass fiber with a polyester film former and a methacrylic coupling agent from PPG, Hoogezand, The Netherlands.
- Random continuous fiber mat was provided by OCF. The fibers had a methacrylic coupling agent and a polyester binder.
- Polyester binder from DSM Italia, Como, Italy.
- Silanol terminated (MW=4200) and trimethylsilane terminated (MW=14000) PDMS and tin octoate (50 % in PDMS) were purchased from United Chemical Technologies.
- Phenol and p-cresol were supplied by Aldrich.
- Nonyl phenol was obtained from TCI.
- Methyl ethyl ketone (MEK) was purchased from Malinckrodt.
- Micro detergent was supplied by MSU university stores.
- A 61 ± 1 wt-% solution of unsaturated polyester resin in styrene was provided by DSM Resins, Zwolle, The Netherlands.
- Recycled tire rubber was provided by Berends, Holland, MI. The rubber was specified as coming from regular automobiles and as a 40 mesh sieve fraction.

Experimental procedures

Manufacturing of unidirectional glass fiber reinforced panels (Chapter 3)

Preforms were made by winding the fiber around a rectangular plate. After winding, a known amount of binder was sprayed over the fibers. The fibers were heated to melt the binder and after cooling, the plate was removed. This yielded good fiber preforms.

Manufacturing of random continuous fiber preforms (Chapters 6 and 7)

Random continuous fiber preforms were made by cutting 6 x 6 inch pieces of continuous random fiber mat. Four layers of mat were stacked together, while rubber binder was applied between the layers. This rubber binder was made by the reverse antisolvent phase separation process that was described in chapter 5. The rubber particles had a diameter of 200 μ m and their surface contained 27 % polyester. At the center of the mat, between the second and the third layer, a 1 inch wide Teflon sheet was inserted to serve as a crack starter for the fracture tests. The ensemble was heated and slightly pressed with the aid of an iron. The temperature of the iron was approximately 100 °C.

Manufacturing of panels (Chapters 3, 6 and 7)

The panels were made by placing a preform into the mold. After the mold was closed, a vacuum was applied to the mold cavity to remove any volatile material. Subsequently, the resin mixture (see Table Al.1) was injected at a pressure of 10 psi for 5 minutes after which a packing pressure

of 100 psi was applied for 45 minutes. Injection was performed at room temperature. After removing the packing pressure, the mold was opened and the panel, a solid gel, was placed in an oven for the post cure cycle.

The panels were heated up to 120 °C in 30 minutes, after which the temperature was kept at 120 °C for 3 hours. After that, the oven was turned off and the panels cooled down slowly in approximately 1-3 hours.

Table Al.1 Composition of the resin mixture

Unsaturated Polyester resin	49.5 %
Styrene	49.4 %
Benzoyl peroxide	1.0 %
Dimethylaniline	0.13 %

Synthesis of end capped PDMS (Chapter 4)

The following procedure was typical for the synthesis of the end capped PDMS. 10 g of PDMS were placed in a round bottom flask. Then, a ten fold excess (on an equivalent basis) of phenol, p-cresol or nonyl phenol was added. Finally, 100 g of MEK and 0.2 g of tin octoate solution were added to the mixture.

Figure Al.1 Reaction equation for the end group modification of PDMS

The mixture was refluxed for 6 hours. During this time, the reaction in Figure Al.1 takes place. After the reaction, the mixture was distilled until approximately 75 % of the MEK was boiled off. The rest of the mixture was washed with methanol in a separatory funnel to remove excess MEK. The remaining liquid was clear.

Analysis of silicone domain size in unsaturated polyester (Chapter 4)

To obtain the particle size of the PDMS in the unsaturated polyester, 1 % of silicone was mixed with the unsaturated polyester resin mixture (Table Al.1). The mixture was spread on a microscope slide and cured using the standard curing cycle. Subsequently, particle sizes were measured using an Olympus microscope with a video camera and video caliper system. For each specimen, the particle size of at least 400 particles was measured. The sizes were sorted and ranked from small to large. Their rank number i ranged from 1 to N, the total number

$$F(i) = \frac{i}{N+1}$$

Most particle size distributions are log normal. The particle size distribution is given by:

of particles measured. Then, the cumulative particle size distribution, F(i) was calculated:

$$f(x) = \frac{1}{\sigma x \sqrt{2\pi}} e^{-\left[\frac{(\ln(x) - \mu)^2}{2\sigma^2}\right]}$$
 Al.2

The cumulative particle size distribution is given by:

$$F(x) = Erf(\frac{\ln(x) - \mu}{\sqrt{2}\sigma})$$
 Al.3

Therefore, the inverse error function of F(i) was plotted versus the logarithm of the particle size. A typical plot is given in Figure Al.2. The subsequent linear regression yields the parameters σ and μ . With this method it is easy to calculate the various average particle sizes.

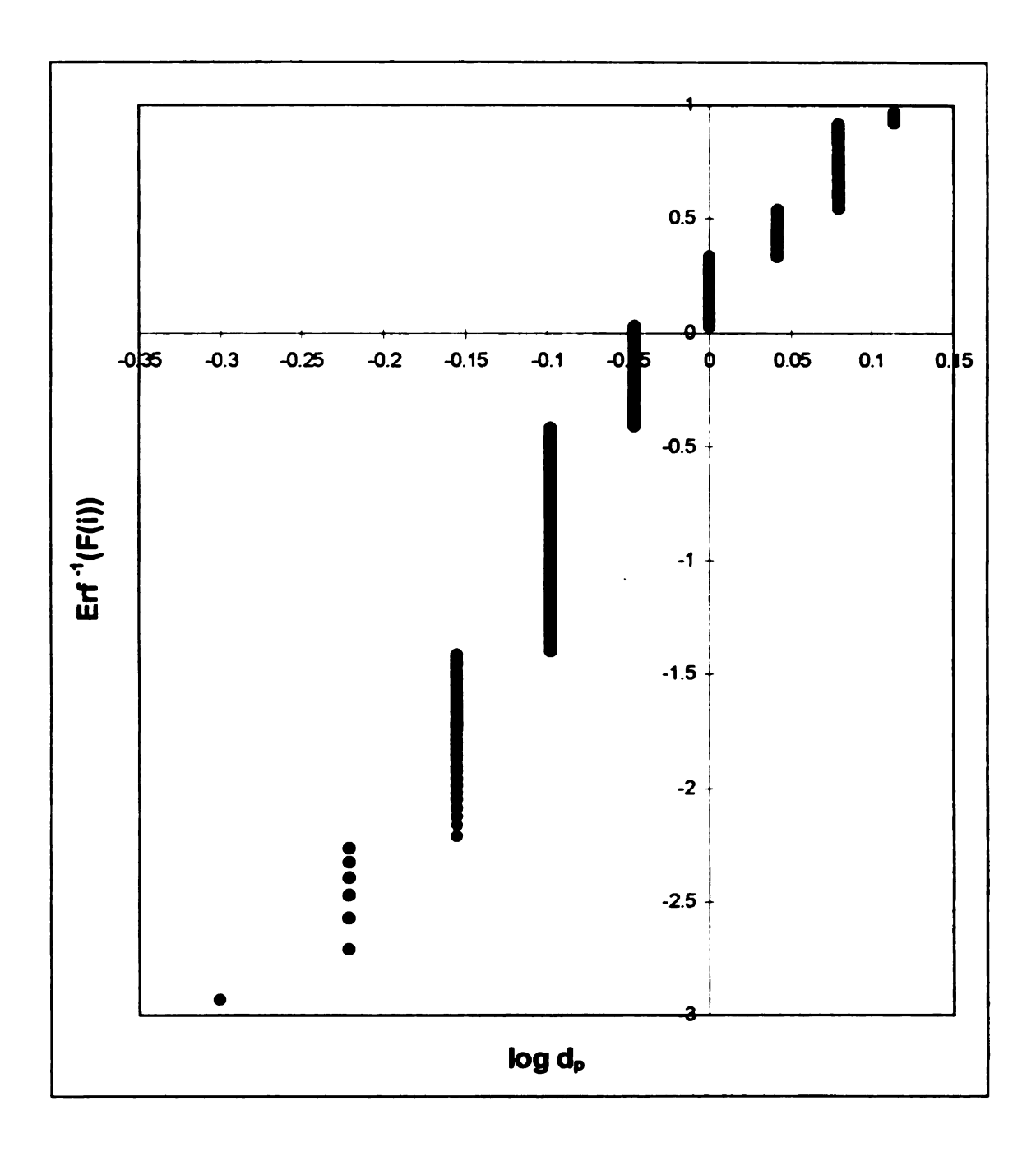


Figure Al.2 Cumulative distribution plot. The inverse of the error function of the cumulative distribution is plotted against the logarithm of the particle size, to obtain the distribution parameters σ and μ .

UV / ozone and oleic acid treatment of tire rubber particles (chapter 7)

The UV / ozone treatment was performed as follows:

Approximately 6 grams of rubber was placed in a 100 ml glass beaker. Water was added. The beaker was placed under a Xenon UV lamp and the dispersion was stirred with a Teflon spinbar. The rubber was irradiated during two minute intervals with pauses of two minutes to let the lamp and the sample cool down.

The distance between the lamp and the beaker was approximately 2.5 cm. The intensity of the lamp at this distance is 0.75 W/m². The lamp was pulsed at a rate of 120 pulses per second. The wavelength of the UV light is below 185 nm. [3]

After the UV treatment, the rubber is filtered and dried for approximately 15 minutes on filter paper at room temperature. Immediately after drying the rubber is soaked in oleic acid for 15 minutes. After the soaking, the rubber was filtered and washed with water. Then, the Polyester coating was applied using the reverse antisolvent phase separation process described in chapter 5.

Testing

Flexure testing (Chapters 3 and 6)

3 Point flexure tests were performed according to ASTM D 790 on a UTS test system. Sample dimensions and testing conditions are listed in Table Al.2.

Table Al.2 Sample dimensions and testing conditions for the 3 point flexure tests

	Chapter 3		Chapter 6	
Fiber orientation	0°	90°	Random	
Span (in)	2.25	2.25	2.25	
Thickness (in)	0.13	0.13	0.13	
Length (in)	3.0	3.0	3.0	
Width (in)	0.5	0.5	0.25	
Load cell (lbs)	1000	20	1000	
Preload (lbs)	2.0	0.04	1.0	

Fracture toughness testing

The specimen size was $3 \times 1/2 \times 1/8$ inch. The Teflon sheet was positioned at one end of the fracture toughness specimen, in such a way that it served as a crack starter. Metal hinges were glued to the specimen using "ELMER'S Wonderbond plus" cyanoacrylate adhesive. It should be noted that several other types of adhesives were tried but too often those glues failed. Both sides of the fracture toughness specimen were painted white using liquid paper and markings were made every 5 mm to monitor the crack growth.

The strain energy release rate was measured in accordance with ASTM D5528-94a on a UTS testing instrument. The load displacement curve was recorded. Each time the crack passed a crack length marker, the displacement was noted. With the aid of a computer program, the load displacement file was read, the displacements for the various crack lengths were put in and

curves for the fracture toughness as a function of crack length were generated. (For the Pascal source code, see Appendix II.) Three curves for the strain energy release rate as a function of crack length were calculated using the MBT, CC and MCC data reduction methods.

Testing of the binding characteristics

A small amount of rubber binder was spread on aluminum foil. The rubber binder was covered with another layer of foil. The ensemble was heated to 100 °C and pressed slightly. Control experiments were performed with uncoated rubber powder and with polyester powder (a commercial binder from DSM Italia).

Similar experiments were performed with glass fiber mats.

Analytical techniques

FTIR analysis (Chapter 4)

FTIR analysis was performed on a Perkin Elmer 1600. Spectra were taken between 4000 and 650 cm⁻¹.

Sieving (Chapter 5)

The particle size was measured by sieving a representative sample over a set of four sieves until the weight change on every sieve and in the cup was less than 1 percent as specified in ASTM 447B [2].

Electron Spectroscopy for Chemical Analysis (ESCA) (Chapters 5 and 7)

ESCA, also known as XPS (X-ray Photoelectron Spectroscopy), is a surface specific analytical technique. It yields the elemental composition of the outermost 10 nm of a specimen. In some cases, ESCA also gives information about atoms neighboring the detected element. ESCA is unable to detect hydrogen.

Spectra were taken on a Perkin Elmer PHI 5400 ESCA spectrometer using a standard 300 W Mg $K\alpha$ X-ray source. The pass energy of the electron analyzer was kept constant at 89.45 eV.

Environmental Scanning Electron Microscopy (ESEM) (Chapters 5, 6 and 7)

ESEM micrographs were taken on a Philips Electroscan 2020 Environmental Scanning Electron Microscope. The energy of the electron beam was 20 keV. A GSED detector was used with a water pressure of 1-3 Torr.

References

- 1. A. de Koning, personal communication, February 26, 1993
- 2. Manual on testing sieving methods, ASTM 447B, ASTM, 1985
- 3. N. Dontula, personal communication, 1997

	APPENDI)	C II	
Turbo Pascal 7.0 so	APPENDI) urce code for the fract		ion program
Turbo Pascal 7.0 so			ion program
Turbo Pascal 7.0 so			ion program
Turbo Pascal 7.0 so			ion program
Turbo Pascal 7.0 so			ion program
Turbo Pascal 7.0 so			ion program
Turbo Pascal 7.0 so			ion program

```
Program test(input,output);
Uses CRT, Graph, Printer,
type box=array[1..4] of integer;{xmin,ymin,xmax,ymax}
   head=array [1..2] of string[2];
   lead=array [1..15] of string[12];
   dat=array [1..15,1..2] of string[40];
   xdat=array [1..15] of real;
   da1=array [1..15,1..2] of real;
   TLegend=array[1..3] of string[7];
Var DriverPath,InputPath,OutputPath,PrinterPort:String;
Function Power (a,b:real):real;
var q:real;
begin
   q:=exp(b*In(a));
   Power:=q;
end;
Function log (x:real):real;
var q:real;
begin
    q:=ln(x)/ln(10);
    log:=q;
end;
Procedure scale(Var min,max,amin,amax:real);
var lmin,lmax,dlog,p:real;
   s,ss:string;
begin
    amin:=abs(min);
    amax:=abs(max);
    If min>=0 then
      begin
         amin:=0;
         p:=Round(log(amax)-0.5)+1;
         amax:=Power(10,p);
         p:=amax*(Round(10*max/amax-0.5)+1)/10;
         amax:=p:
      end
```

```
else If max<=0 then
          begin
             amax:=0;
             p:=Round(log(amin)-0.5)+1;
             amin:=-Power(10,p);
             p:=amin*(Round(10*min/amin-0.5)+1)/10;
             amin:=p;
          end
          else
          begin
             Imax:=Round(log(amax)-0.5)+1;
             Imin:=Round(log(amin)-0.5)+1;
             dlog:=lmax-lmin;
             If dlog<-1 then Imax:=Imin-1
                    else if dlog>1 then lmin:=lmax-1;
             amax:=Power(10,Imax);
             p:=amax*(int(10*max/amax)+1)/10;
             amax:=p;
             amin:=-Power(10,lmin);
             p:=amin*(int(10*min/amin)+1)/10;
             amin:=p;
          end;
end;
Function Max(n:integer;x:xdat):real;
var q:real;
  i:integer;
begin
   For i:=2 to n do if x[i]>q then q:=x[i];
   Max:=q;
end:
Function Min(n:integer;x:xdat):real;
var q:real;
  i:integer;
begin
   q:=x[1];
   For i:=2 to n do if x[i] < q then q:=x[i];
   Min:=q;
end;
Procedure drawbox(b:box);
begin
   Line (b[1],b[2],b[1],b[4]);
```

```
Line (b[1],b[4],b[3],b[4]);
   Line (b[3],b[4],b[3],b[2]);
   Line (b[3],b[2],b[1],b[2]);
end;
Function Rx(x:real):integer;
var V:ViewPortType;
begin
   GetViewSettings(V);
   Rx:=Round(x*(V.X2-V.X1));
end:
Function Ry(x:real):integer;
var V:ViewPortType;
begin
   GetViewSettings(V);
   Ry:=Round(x*(V.Y2-V.Y1));
end:
Procedure Regression (x,y:xdat; n:integer; Var slope,constant,r:real);
var i: integer;
sx,sy,sxx,syy,sxy:real;
begin
         sx:=0;
         sy:=0;
         sxx:=0;
         syy:=0;
         sxy:=0;
         for i:=1 to n do
         begin
                 sx:=sx+x[i];
                 sy:=sy+y[i];
                 sxx:=sxx+x[i]*x[i];
                 syy:=syy+y[i]*y[i];
                 sxy:=sxy+x[i]*y[i];
      end;
      slope:=(n*sxy-sx*sy)/(n*sxx-sx*sx);
      constant:=(sy-slope*sx)/n;
         r = (n*sxy-sx*sy)/sqrt(n*sxx-sx*sx)/sqrt(n*syy-sy*sy);
 end;
 Procedure Inputinit(var f:text;s:string);
 begin
```

```
Assign (f,s);
        Reset (f);
end;
Procedure Outputinit(var f:text;s:string);
begin
        Assign (f,s);
        Rewrite (f);
end:
Procedure Initialize;
var f:text;
begin
   Inputinit(f,'FT.ini');
   Readin(f);
   ReadIn(f);
   ReadIn(f);
   Readin(f, DriverPath);
   ReadIn(f);
   Readin(f,InputPath);
   Readin(f);
   Readin(f,OutputPath);
   Readin(f);
   Readin(f, PrinterPort);
   Close(f);
end;
Procedure Tableinput(col,row:integer;header:head;leader:lead;var data:dat);
var c,e:char;
  i,j,l,dummy:integer;
  s:string;
  b:boolean;
  grDriver,grMode,Errcode:integer;
  out:box;
  x,y,rowsize:real;
   TColor, EColor, DColor: byte;
  ht:word;
begin
   Tcolor:=White;
   EColor:=LightMagenta;
   DColor:=Yellow;
   for i:=1 to row do for j:=1 to col do data[i,j]:=";
   grDriver:=Detect;
   Initgraph(grDriver, grMode, DriverPath);
   ErrCode:=Graphresult;
```

```
if ErrCode=grOk then
  begin
     SetBkColor(1);
     SetColor(DColor);
     out[1]:=0;
     out[2]:=0;
     out[3]:=GetMaxX;
     out[4]:=GetMaxY;
     Drawbox(out);
     SetTextStyle(2, Horizdir, 6);
     Outtextxy(Rx(0.6),Ry(0.5),'Press <ESC> when done');
     rowsize:=0.7/row;
     out[1]:=Rx(0.03);
     out[2]:=Ry(0.03);
     out[3]:=Rx(0.55);
     out[4]:=Ry(0.9);
     SetColor(TColor);
     Drawbox(out);
     For i:=1 to row do
     begin
         Outtextxy(Rx(0.08),Ry(rowsize*(i-1)+0.15),leader[i]);
     For j:=1 to col do
      begin
         Outtextxy(Rx(0.1+j*0.15),Ry(0.04),header[j]);
      end:
     i:=1;
     i:=1:
     y:=0.15+rowsize*(i-1);
      x:=0.1+j*0.15;
      b:=False;
      c:=' ';
      SetFillStyle(SolidFill,GetBkColor);
      While (c<>chr(27)) do
      begin
         c:=readkey:
         If (c=\#0) or (c=chr(13)) or (c=chr(27)) then s:=data[i,j]
                else s:=":
                                   Esc
                                                Bkspce
       Special
                    Return
{
       While (c<> #0) and (c<>chr(13)) and (c<>chr(27)) and (c<>chr(9)) do
       begin
       If (c=chr(8)) then
       begin
         !:=Length(s);
         if I<>0 then
         begin
             Delete (s,I,1);
             SetFillStyle(SolidFill,GetBkColor);
             ht:=Textheight('Tg');
             Bar(Rx(x),Ry(y),Rx(x+0.12),Ry(y)+20);
```

```
Setcolor(EColor);
         Outtextxy (Rx(x),Ry(y),s+' ');
      end:
     c:=Readkey;
   end
   else
   begin
      If b then
      begin
          SetFillStyle(SolidFill,GetBkColor);
          Bar(Rx(x),Ry(y),Rx(x+0.12),Ry(y)+20);
          b:=false;
       end:
       s:=s+c;
       SetColor(EColor);
       Bar(Rx(x),Ry(y),Rx(x+0.12),Ry(y)+20);
       Outtextxy(Rx(x),Ry(y),s);
       c:=readkey;
   end;
end:
data[i,j]:=s;
If (c= #0) then
begin
   b:=True;
   SetFillStyle(SolidFill,GetBkColor);
   Bar(Rx(x),Ry(y),Rx(x+0.12),Ry(y)+20);
   SetColor(DColor);
   Outtextxy(Rx(x),Ry(y),data[i,j]);
   e:=readkey;
   If (e='H') and (i>1) then i:=i-1;
   If (e='P') and (i<row) then i:=i+1;
   If (e='M') and (j<col) then j:=j+1;
   If (e='K') and (j>1) then j:=j-1;
   y:=0.15+rowsize*(i-1);
   x:=0.1+j*0.15;
   SetColor(EColor);
   Bar(Rx(x),Ry(y),Rx(x+0.12),Ry(y)+20);
   Outtextxy(Rx(x),Ry(y),data[i,j]);
end;
If c=chr(13) then
begin
   SetColor(DColor);
   Bar(Rx(x),Ry(y),Rx(x+0.12),Ry(y)+20);
   Outtextxy(Rx(x),Ry(y),s);
   if (i<row) then i:=i+1;
   y:=0.15+rowsize*(i-1);
    SetFillStyle(SolidFill,GetBkColor);
    Bar(Rx(x),Ry(y),Rx(x+0.12),Ry(y)+20);
    SetColor(EColor);
    Outtextxy(Rx(x),Ry(y),data[i,j]);
```

```
end;
   If c=chr(9) then
   begin
      SetColor(DColor);
      Outtextxy(Rx(x),Ry(y),s);
      if (j<col) then j:=j+1;
      x:=0.1+j*0.15;
      SetColor(EColor);
      Outtextxy(Rx(x),Ry(y),data[i,j]);
   end:
end:
CloseGraph;
end:
end;
Function Screen1:byte;
var grDriver,grMode,Errcode:integer;
  out:box:
  c:char;
Begin
   grDriver:=Detect;
   Initgraph(grDriver, grMode, DriverPath);
   ErrCode:=Graphresult;
   if ErrCode=grOk then
   begin
      SetBkColor(1);
      SetColor(14);
      out[1]:=0;
      out[2]:=0;
      out[3]:=GetMaxX;
      out[4]:=GetMaxY;
      Drawbox(out);
       SetTextStyle(2,Horizdir,10);
       SetColor(15);
       Outtextxy(Rx(0.1),Ry(0.1),'Fracture Toughness');
       Outtextxy(Rx(0.1),Ry(0.2),'Analysis program');
       SetTextStyle(2,Horizdir,8);
       Outtextxy(Rx(0.1),Ry(0.4), Written by: Rik ter Veen');
       SetTextStyle(2, Horizdir, 6);
       out[1]:=Rx(0.05);
       out[2]:=Ry(0.55);
       out[3]:=Rx(0.95);
       out[4]:=Ry(0.95);
       Outtextxy(Rx(0.1),Ry(0.6),'F1: Analyze new file');
       Outtextxy(Rx(0.1),Ry(0.7),'F2: Analyze old file');
       Outtextxy(Rx(0.1),Ry(0.85),'F3: Quit this program');
       Drawbox(out);
       c:=' ':
```

```
While (c<>';') and (c<>'<') and (c<>'=') do
      begin
          While Readkey<>#0 do c:=' ':
          c:=Readkey:
      end:
      if c=';' then screen1:=1
            else if c='<' then screen1:=2
                     else screen1:=3:
      Closegraph;
   end
   else Writeln('Graphics Error: ', GraphErrorMsg(ErrCode));
end;
Procedure Screen2(var sample,inp,outp,rem,lc:string; var wg,wb:real;var np:byte);
var da:dat;
  Le:lead;
  he:head;
  i:byte:
  dummy:Word;
begin
     he[1]:=' ';
     Le[1]:='Sample:';
     Le[2]:='Input File:';
     Le[3]:='Output File:';
     Le[4]:='Points:';
     Le[5]:='Glass wt.:';
     Le[6]:='Binder wt.:';
     Le[7]:='Load Cell:';
     Le[8]:='Remarks:';
     Tableinput(1,8,he,le,da);
        sample:=da[1,1];
        inp:=da[2,1];
{
      inp:='c:\rik\tough\program\test.';}
        outp:=da[3,1];
      outp:='c:\rik\tough\program\test.out'; }
{
        Val(da[4,1],np,dummy);
        Val(da[5,1],wg,dummy);
     Val(da[6,1],wb,dummy);
        lc:=da[7,1];
        rem:=da[8,1];
end:
Function Screen4:byte;
var grDriver,grMode,Errcode:integer;
  out:box;
  c:char;
```

```
Begin
   grDriver:=Detect;
   Initgraph(grDriver, grMode, DriverPath);
   ErrCode:=Graphresult:
   if ErrCode=grOk then
   begin
      SetBkColor(1);
      SetColor(14);
      out[1]:=0;
      out[2]:=0;
      out[3]:=GetMaxX;
      out[4]:=GetMaxY;
      Drawbox(out);
      SetTextStyle(2, Horizdir, 8);
      SetColor(15);
      Outtextxy(Rx(0.1),Ry(0.1),'Analysis done');
      out[1]:=Rx(0.05);
      out[2]:=Ry(0.35);
      out[3]:=Rx(0.95);
      out[4]:=Ry(0.95);
      SetTextStyle(2, Horizdir, 6);
      Outtextxy(Rx(0.1),Ry(0.4),'F1: New file');
      Outtextxy(Rx(0.1),Ry(0.5), F2: Present graphs');
      Outtextxy(Rx(0.1),Ry(0.6),'F3: Show data');
      Outtextxy(Rx(0.1),Ry(0.7),'F4: Print data');
      Outtextxy(Rx(0.1),Ry(0.85),'F5: Quit');
       Drawbox(out):
      c:=' ':
      While (c<>';') and (c<>'<') and (c<>'>') and (c<>'?') do
          While Readkey<>#0 do c:=' ';
          c:=Readkey;
       end:
       if c=':' then screen4:=1
             else if c='<' then screen4:=2
                      else if c='=' then screen4:=3
                               else if c='>' then screen4:=4
                                        else screen4:=5:
       Closegraph;
    end
    else Writeln('Graphics Error: ', GraphErrorMsg(ErrCode));
end;
Function Screen5(sample,date,vf,bin,nn,delta,a1:string):byte;
var grDriver,grMode,Errcode:integer,
   out,gr,te,info:box;
   c:char;
```

```
begin
   grDriver:=Detect:
   Initgraph(grDriver, grMode, DriverPath);
   ErrCode:=Graphresult;
   if ErrCode=grOk then
   begin
      SetBkColor(1);
      SetColor(14);
      out[1]:=0;
      out[2]:=0;
      out[3]:=GetMaxX;
      out[4]:=GetMaxY;
      info[1]:=Rx(0.03);
      info[2]:=Ry(0.03);
      info[3]:=Rx(0.27):
      info[4]:=Ry(0.7);
      gr[1]:=Rx(0.3);
      gr[2]:=Ry(0.03);
      gr[3]:=Rx(0.97);
      gr[4]:=Ry(0.7);
      te[1]:=Rx(0.03);
      te[2]:=Ry(0.73);
      te[3]:=Rx(0.97);
      te[4]:=Ry(0.97);
      Drawbox(out);
      Drawbox(te);
      Drawbox(gr);
      Drawbox(info);
      SetTextStyle(2, Horizdir, 6);
      SetColor(White);
      Outtextxy(Rx(0.48),Ry(0.75),'INFO');
      Outtextxy(Rx(0.35),Ry(0.8),Vf [%]: );
      Outtextxy(Rx(0.35),Ry(0.85),'Rubber [%]: ');
      Outtextxy(Rx(0.05),Ry(0.85),'Date: ');
      Outtextxy(Rx(0.05),Ry(0.8),'Sample: ');
      Outtextxy(Rx(0.65),Ry(0.8),'Delta [mm]: ');
      Outtextxy(Rx(0.65),Ry(0.85),'n: ');
      Outtextxy(Rx(0.65),Ry(0.9),'A1: ');
      SetColor(Yellow);
      Outtextxy(Rx(0.52),Ry(0.8),Vf);
      Outtextxy(Rx(0.52),Ry(0.85),bin);
      Outtextxy(Rx(0.16),Ry(0.85),Date);
      Outtextxy(Rx(0.16),Ry(0.8),Sample);
      Outtextxy(Rx(0.82),Ry(0.8),Delta);
      Outtextxy(Rx(0.82),Ry(0.85),nn);
      Outtextxy(Rx(0.82),Ry(0.9),A1);
      SetColor(White);
      Outtextxy(Rx(0.5),Ry(0.3),'Pick a graph option');
      Outtextxy(Rx(0.05),Ry(0.05),'MENU');
```

```
Outtextxy(Rx(0.05),Ry(0.2),F1:FT = f(a)');
     Outtextxy(Rx(0.05),Ry(0.27),'F2: MBT plot');
     Outtextxy(Rx(0.05),Ry(0.34),'F3: CC plot');
     Outtextxy(Rx(0.05),Ry(0.41),'F4: MCC plot');
     Outtextxy(Rx(0.05),Ry(0.55),'F5: Quit');
     c:=' ':
     While (c<>';') and (c<>'<') and (c<>'>') and (c<>'?') do
      beain
         While Readkey<>#0 do c:=' ';
         c:=Readkey;
      end;
      if c=':' then screen5:=1
        else if c='<' then screen5:=2
           else if c='=' then screen5:=3
              else if c='>' then screen5:=4
                 else screen5:=7;
      SetFillStyle(SolidFill,GetBkColor);
      Bar (gr[1],gr[2],gr[3],gr[4]):
      Drawbox(gr);
   else Writeln('Graphics Error: ', GraphErrorMsg(ErrCode));
end:
Procedure Plot(where:box;n:integer;ix,iy:xdat;xlabel,ylabel:string;marker:char;Lin:boolean);
var xmin,xmax,ymin,ymax,xmin1,xmax1,ymin1,ymax1,sl,con,r,x1,x2,y1,y2:real;
  xp,yp,xp1,xp2,yp1,yp2,i:integer;
  b:box;
  s:string;
begin
   xmin1:=min(n,ix);
   xmax1:=max(n,ix);
   ymin1:=min(n,iy);
   vmax1:=max(n,iv);
   Scale(xmin1,xmax1,xmin,xmax);
   Scale(ymin1,ymax1,ymin,ymax);
   SetViewport(where[1],where[2],where[3],where[4],ClipOn);
   ClearViewPort;
   SetTextStyle(2,Horizdir,5);
   b[1]:=Rx(0.1);
   b[2]:=Ry(0.05);
   b[3]:=Rx(0.95);
   b[4]:=Ry(0.95);
   Drawbox(b);
   SetTextStyle(DefaultFont, Horizdir, 1);
   SetColor(White);
   For i:=1 to n do
   begin
```

```
xp:=Rx(0.1+0.85*(ix[i]-xmin)/(xmax-xmin))-4;
     vp:=Ry(0.95-0.9*(iy[i]-ymin)/(ymax-ymin))-4;
     outtextxy(xp,yp,marker);
 end:
  SetTextStyle(2,Horizdir,5);
  xp:=Rx(0.1)-8;
  yp:=Ry(0.95);
  Str(xmin:0:2.s):
  Outtextxy(xp,yp,s);
  xp:=Rx(0.95)-8;
  Str(xmax:0:2,s);
  Outtextxy(xp,yp,s);
  xp:=Rx(0.5)-8:
  Outtextxy(xp,yp,xlabel);
  xp:=Rx(0);
  yp:=Ry(0.95)-8;
  Str(ymin:0:2,s);
  Outtextxy(xp,yp,s);
  yp:=Ry(0.05)-8;
  Str(ymax:0:2,s);
  Outtextxy(xp,yp,s);
  yp:=Ry(0.5)-8;
  SetTextStyle(2, Vertdir, 5);
  Outtextxy(xp,yp,ylabel);
  If Lin then
  begin
     Regression (ix,iy,n,sl,con,r);
     y1:=xmin*sl+con;
     if (y1>ymax) or (y1<ymin) then
     begin
         if y1>ymax then y1:=ymax
                else y1:=ymin;
         x1:=(y1-con)/sl;
      end
      else x1:=xmin:
      y2:=xmax*sl+con;
      if (y2>ymax) or (y2<ymin) then
      begin
         if y2>ymax then y2:=ymax
                else y2:=ymin;
         x2:=(y2-con)/sl;
      end
      else x2:=xmax;
      xp1:=Rx(0.1+0.85*(x1-xmin)/(xmax-xmin));
      yp1:=Ry(0.95-0.9*(y1-ymin)/(ymax-ymin));
      xp2:=Rx(0.1+0.85*(x2-xmin)/(xmax-xmin));
      yp2:=Ry(0.95-0.9*(y2-ymin)/(ymax-ymin));
      Line(xp1,yp1,xp2,yp2);
   end:
end;
```

```
Procedure
Plot3(where:box;n:integer;ix,iy1,iy2,iy3:xdat;xlabel,ylabel:string;marker:string;L:TLegend);
var xmin,xmax,ymin,ymax,xmin1,xmax1,ymin1,ymax1,sl,con,r,x1,x2,y1,y2:real;
  xp,yp,xp1,xp2,yp1,yp2,i:integer;
  b:box;
  s:string;
begin
   xmin1:=min(n,ix);
   xmax1:=max(n,ix);
   ymin1:=min(n,iy1);
   ymax1:=max(n,iy1);
   If min(n,iy2)<ymin1 then ymin1:=min(n,iy2);
   If min(n,iy3)<ymin1 then ymin1:=min(n,iy3);
   If max(n,iy2)>ymax1 then ymax1:=max(n,iy2);
   If max(n,iy3)<ymax1 then ymax1:=max(n,iy3);
   Scale(xmin1,xmax1,xmin,xmax);
    Scale(ymin1,ymax1,ymin,ymax);
   SetViewport(where[1],where[2],where[3],where[4],ClipOn);
    ClearViewPort;
    SetTextStyle(2, Horizdir, 5);
   For i:=1 to 3 do Outtextxy(Rx(0.75),Ry(0.65+0.08*i),L[i]);
    b(1):=Rx(0.1);
    b(2):=Ry(0.05);
    b[3]:=Rx(0.95);
   b[4]:=Ry(0.95);
    Drawbox(b);
    SetTextStyle(DefaultFont, Horizdir, 1);
    SetColor(White);
    For i:=1 to n do
    beain
       xp:=Rx(0.1+0.85*(ix[i]-xmin)/(xmax-xmin))-4;
       yp:=Ry(0.95-0.9*(iy1[i]-ymin)/(ymax-ymin))-4;
       outtextxv(xp.vp.marker[1]);
       xp:=Rx(0.1+0.85*(ix[i]-xmin)/(xmax-xmin))-4;
       yp:=Ry(0.95-0.9*(iy2[i]-ymin)/(ymax-ymin))-4;
       outtextxy(xp,yp,marker[2]);
       xp:=Rx(0.1+0.85*(ix[i]-xmin)/(xmax-xmin))-4;
       yp:=Ry(0.95-0.9*(iy3[i]-ymin)/(ymax-ymin))-4;
       outtextxy(xp,yp,marker[3]);
    end:
    SetTextStyle(2,Horizdir,5);
    xp:=Rx(0.1)-8;
    yp:=Ry(0.95):
    Str(xmin:0:2,s);
    Outtextxy(xp,yp,s);
```

xp:=Rx(0.95)-8;

```
Str(xmax:0:2,s);
  Outtextxy(xp,yp,s);
  xp:=Rx(0.5)-8;
  Outtextxy(xp,yp,xlabel);
  xp:=Rx(0);
  yp:=Ry(0.95)-8;
   Str(ymin:0:2,s);
   Outtextxy(xp,yp,s);
   yp:=Ry(0.05)-8;
   Str(ymax:0:2,s);
   Outtextxy(xp,yp,s);
   yp:=Ry(0.5)-8;
   SetTextStyle(2, Vertdir, 5);
   Outtextxy(xp,yp,ylabel);
end;
Procedure Hightandwidth(var f:text; var h,b:real;var date:string);
var s,ss:string;
  i:integer;
begin
        for i:=1 to 9 do readln(f,s);
        date:=copy (s,14,10);
        for i:= 1 to 11 do readin (f,s);
        i:=length (s)-18;
        ss:=copy(s,18,i);
        val (ss,b,i);
        readIn(f,s);
        i:=length (s)-18;
        ss:=copy(s,18,i);
        val (ss,h,i);
        for i:=1 to 8 do readin (f,s);
end;
Procedure Findload(var f:text; ext:real; var load:real);
var est,loadst,estt,loadstt:real;
        s,ss:string;
         q:byte;
      dummy:integer;
begin
         est:=0;
         loadst:=0:
         while est<ext do
      begin
            loadstt:=loadst;
         estt:=est;
```

```
readin (f,s);
           q:=pos(',',s)-3;
           ss:=Copy(s,2,q):
           Val(ss,loadst,dummy);
        q:=q+5;
           dummy:=Length(s)-q;
           ss:=Copy(s,q,dummy);
           Val(ss,est,dummy);
        If Eof(f) then
        begin
            Writeln('Displacement not found.');
            Writeln('Press <Enter> to continue');
            readin:
            halt:
        end;
     load:=loadstt+(loadst-loadstt)*(ext-estt)/(est-estt);
     load:=4.448*load:
end:
Procedure Calc(var samp,inp,outp,rem:string;wg,wb:real;np:byte);
var
        f,g:text;
        p,e,a,c3,ic,la,ah:xdat;{array [1..15] of real}
        a1,rd,m,ra,b1,b2,delta,nn,MBT,CC,MCC,h,b,binp,vf:real;
        date:string;
        header:head:
        leader:lead;
        i,j,n,dummy:integer;
     data:da1;
     da:dat:
begin
        Inputinit (f,inp);
        Outputinit (g,outp);
     For i:=1 to n do Str(i,leader[i]);
        header [1]:='a':
        header [2]:='d';
        Tableinput(2,n,header,leader,da);
     For i:= 1 to n do for j:=1 to 2 do
     begin
        Val(da[i,j],data[i,j],dummy);
     end;
     For i:=1 to n do
        begin
        a[i]:=data[i,1];
           e[i]:=data[i,2];
        end;
```

```
Hightandwidth(f,h,b,date); {Forget File headers etc.}
For i:=1 to n do
   begin
           Findload (f,e[i],p[i]);
           c3[i]:=Power((e[i]/p[i]),(1/3));
           lc[i]:=log(e[i]/p[i]);
           la[i]:=log(a[i]);
           ah[i]:=a[i]/h;
   end:
   close(f):
   Regression (a,c3,n,b1,b2,rd);
   delta:=b2/b1;
   Regression (la,lc,n,nn,b2,m);
   Regression (c3,ah,n,a1,b2,ra);
Vf:=1.476*wg/h;
binp:=100*wb/wg;
Writeln(g,'number of datapoints');
WriteIn(g,n);
WriteIn(g,'sample');
WriteIn(q.samp):
Writeln(g,'date');
WriteIn(g,date);
Writeln(g,'Vf [%]');
WriteIn(g,Vf);
Writeln(g, 'Binder percentage');
WriteIn(g,binp);
Writeln(g,'Specimen width');
WriteIn(g,b);
Writeln(g,'Specimen hight');
WriteIn(g,h);
WriteIn(g,'n');
Writeln(g,nn);
Writeln(g,'n corr.');
Writeln(g,m);
Writeln(g,'delta');
Writeln(g,delta);
WriteIn(g,'delta corr.');
WriteIn(g,rd);
Writeln(g,'A1');
Writeln(g,a1);
WriteIn(g,'A1 corr.');
Writeln(g,ra);
WriteIn(g,'remarks');
WriteIn(g,rem);
Writeln(g,'a');
WriteIn(g,'e');
WriteIn(g,'p');
Writeln(g,'MBT');
WriteIn(g,'CC');
Writeln(g,'MCC');
```

```
For i:=1 to n do
        begin
                 MBT:=1500*e[i]*p[i]/b/(a[i]+abs(delta));
                CC:=500*nn*p[i]*e[i]/b/a[i];
                MCC:=1500*Power(p[i],(4/3))*Power(e[i],(2/3))/a1/b/h;
                Writeln(g,a[i]);
          Writeln(g,e[i]);
                Writeln(g,p[i]);
          WriteIn(g,MBT);
                Writeln(g,CC);
          WriteIn(g,MCC);
     end;
     close(g);
end:
Procedure Bye;
begin
   Writeln ('Bye');
end;
Procedure Plotdelta(filename:string);
Var f:text;
  i,n:integer;
  x,y:xdat;
  e,p:real;
  place:box;
  xlabel,ylabel:string;
  marker:char;
  L:Boolean;
Begin
   Inputinit(f,filename);
   Readin(f);
   Readin(f,n);
   For i:=1 to 32 do Readin(f);
   For i:=1 to n do
   begin
      ReadIn(f,x[i]);
      Readin(f,e);
      ReadIn(f,p);
      y[i]:=Power((e/p),(1/3));
      ReadIn(f);
      ReadIn(f):
      ReadIn(f);
   end;
   close(f);
   xlabel:='a';
```

```
ylabel:='C^1/3';
   place[1]:=Rx(0.32);
   place[2]:=Ry(0.05);
   place[3]:=Rx(0.95);
   place[4]:=Ry(0.68);
   marker:='X';
   L:=true;
   Piot(place,n,x,y,xlabel,ylabel,marker,L);
end;
Procedure Plotn(filename:string);
Var f:text;
  i,n:integer;
  x,y:xdat;
   a,e,p:real;
   place:box;
   xlabel,ylabel:string;
   marker:char;
   L:Boolean;
Begin
   Inputinit(f,filename);
   ReadIn(f);
   Readin(f,n);
   For i:=1 to 32 do Readln(f);
   For i:=1 to n do
   begin
       Readin(f,a);
       Readin(f,e);
       ReadIn(f,p);
       x[i]:=log(a);
       y[i]:=log(e/p);
       ReadIn(f);
       Readin(f);
       ReadIn(f);
    end;
    close(f);
    xlabel:='log [a]';
    ylabel:='log [C]';
    place[1]:=Rx(0.32);
    place[2]:=Ry(0.05);
    place[3]:=Rx(0.95);
    place[4]:=Ry(0.68);
    marker:='0';
    L:=true;
    Plot(place,n,x,y,xlabel,ylabel,marker,L);
 end;
```

```
Procedure Plota1(filename:string);
Var f:text;
  i,n:integer;
  x,y:xdat;
  a,h,e,p:real;
  place:box;
  xlabel,ylabel:string;
  marker:char;
  L:Boolean;
Begin
   Inputinit(f,filename);
   Readin(f);
   ReadIn(f,n);
   For i:=1 to 11 do ReadIn(f);
   ReadIn(f,h);
   For i:=1 to 20 do ReadIn(f);
   For i:=1 to n do
   begin
       ReadIn(f,a);
       ReadIn(f.e):
       ReadIn(f,p);
       y[i]:=a/h;
       x[i]:=Power((e/p),(1/3));
       ReadIn(f);
       Readin(f);
       ReadIn(f):
   end:
   close(f);
   ylabel:='a/h';
   xlabel:='C^1/3';
   place[1]:=Rx(0.32);
   place[2]:=Ry(0.05);
   place[3]:=Rx(0.95);
   place[4]:=Ry(0.68);
   marker:="";
   L:=true;
   Plot(place,n,x,y,xlabel,ylabel,marker,L);
Procedure PlotGlc (var filename:string);
Var f:text:
   i,n:integer;
   x,y1,y2,y3:xdat;
   a,e,p:real;
```

place:box;

```
xlabel,ylabel:string;
  marker:char:
  L:Boolean:
  Legend:TLegend;
Begin
   Inputinit(f,filename);
   ReadIn(f);
   ReadIn(f,n);
   For i:=1 to 32 do ReadIn(f);
   For i:=1 to n do
   begin
      ReadIn(f,x[i]);
      ReadIn(f):
      ReadIn(f);
      ReadIn(f,y1[i]);
      ReadIn(f,y2[i]);
      ReadIn(f,y3[i]);
   end;
   close(f);
   xlabel:='a';
   ylabel:='Glc';
   place[1]:=Rx(0.32);
   place[2]:=Ry(0.05);
   place[3]:=Rx(0.95);
   place[4]:=Ry(0.68);
   Legend[1]:='O = MBT';
   Legend[2]:='X = CC';
   Legend[3]:=" = MCC";
   Plot3(place,n,x,y1,y2,y3,xlabel,ylabel,'OX*,Legend);
end:
Procedure Presentgraphs (var filename:string);
var Choice:byte;
   f:text;
   r:real;
   i:integer;
   sample,date,vf,bin,nn,delta,a1:string;
   c:char;
begin
    Inputinit(f,filename);
    For i:=1 to 3 do ReadIn(f);
    ReadIn(f,sample);
    ReadIn(f);
    ReadIn(f,date);
```

```
Readin(f);
  Readin(f,r);
  Str(r:2:0,vf);
  Readin(f);
  ReadIn(f,r);
  Str(r:2:0,bin);
  For i:=1 to 5 do ReadIn(f);
  Readin(f,r);
  Str(r:2:2,nn);
  For i:=1 to 3 do ReadIn(f);
  ReadIn(f,r);
  Str(r:2:2,delta);
  For i:=1 to 3 do ReadIn(f):
  Readin(f,r);
  Str(r:2:2,a1);
  Close(f):
  Choice:=Screen5(sample,date,vf,bin,nn,delta,a1);
   If Choice=2 then plotdelta(filename)
    else if Choice=3 then plotn(filename)
        else if Choice=4 then plota1(filename)
           else If Choice=1 then plotGIC(Filename);
   While (Choice<>7) do
   Begin
      While (c<>';') and (c<>'<') and (c<>'>') and (c<>'?') do
      begin
         While Readkey<>#0 do c:=' ';
         c:=Readkey;
      if c=';' then Choice:=1
        else if c='<' then Choice:=2
           else if c='=' then Choice:=3
               else if c='>' then Choice:=4
                  else Choice:=7;
      ClearViewPort:
      SetViewPort(0,0,GetMaxX,GetMaxY,ClipOn);
      If Choice=2 then plotdelta(filename)
        else if Choice=3 then plotn(filename)
           else if Choice=4 then plota1(filename)
               else If Choice=1 then plotGIC(Filename);
   end:
end;
Procedure Printdata(var filename:string);
var f.g:text;
  i,j,n,l:integer;
  s.ss:string;
  r:real:
```

```
begin
   Inputinit(q,filename):
   Inputinit(f, 'ft.ini');
   For i:= 1 to 9 do ReadIn(f):
   ReadIn(f,PrinterPort);
   Close (f):
   Outputinit(f,PrinterPort);
   Readin(a):
   ReadIn(q,n);
   ReadIn(q):
   ReadIn(g,s);
   l:=Length(s);
   ReadIn(g);
   Readin(q.ss):
   s:='Sample: '+s;
   For i:=1 to 20-I do s:=s+' ':
   s:=s+'Date: '+ss:
   Str(n,ss);
   Writeln(f, 'Fracture Toughness Analysis');
   WriteIn(f,'_
                                                 _);
   WriteIn(f,s);
   Writeln(f,'Points: ',ss);
   ReadIn(g);
   Readin(g,r);
   Str(r:5:2,ss);
   s:='Fiber fraction: '+ss+' %';
   For i:= 1 to 5 do s:= s+' ';
   Readin(a):
   Readin(g,r);
   Str(r:5:2.ss):
   s:=s+'Binder percentage: '+ss+' %';
   WriteIn(f.s):
   ReadIn(g);
   Readin(g,r);
   Str(r:5:2,ss);
   s:='Specimen Width: '+ss+' mm':
   For i:= 1 to 4 do s:= s+' ';
   ReadIn(g):
   ReadIn(g,r);
   Str(r:5:2,ss);
   s:=s+'Specimen Thickness: '+ss+' mm';
   WriteIn(f,s);
   ReadIn(g);
   Readin(g,r);
   Str(r:5:2,ss);
   s:='n: '+ss;
   For i:= 1 to 20 do s:= s+' ':
   Readin(g);
   Readin(g,r);
```

```
Str(r:6:4,ss);
   s:=s+'Correlation: '+ss:
   WriteIn(f,s):
   ReadIn(g);
   ReadIn(g,r);
   Str(r:5:2,ss);
   s:='delta: '+ss:
   For i:= 1 to 16 do s:= s+' ';
   Readin(q):
   ReadIn(q,r);
   Str(r:6:4,ss);
   s:=s+'Correlation: '+ss;
   WriteIn(f,s);
   ReadIn(g);
   Readin(g,r);
   Str(r:5:2,ss);
   s:='A1: '+ss;
   For i:= 1 to 19 do s:= s+' ';
   Readin(g);
   Readin(g,r);
   Str(r:6:4,ss);
   s:=s+'Correlation: '+ss;
   Writein(f,s);
   ReadIn(g);
   Readin(g,ss);
   s:='Remarks: '+ss;
   WriteIn(f,s);
   for i:= 1 to 6 do Readin(g):
   WriteIn(f);
   Writeln(f,' a
                                       MBT
                                                CC
                       disp. Load
                                                        MCC');
   For i:=1 to n do
   begin
      s:=";
      For j:=1 to 6 do
      begin
          Readin(g,r);
          Str(r:8:2,ss);
          s:=s+ss+' ';
      end:
      WriteIn(f,s);
   end:
   WriteIn(f,'_
                                                _);
   Close(f);
end:
Procedure Showdata(var filename:string);
var f:text;
  grDriver,grMode,Errcode:integer;
  out:box;
```

```
i.n:byte;
  r:real:
  s:string;
begin
   Inputinit(f,filename);
   grDriver:=Detect;
   Initgraph(grDriver, grMode, DriverPath);
   ErrCode:=Graphresult;
   if ErrCode=grOk then
   begin
      SetBkColor(1):
      SetColor(14);
      out[1]:=0;
      out[2]:=0;
       out[3]:=GetMaxX;
       out[4]:=GetMaxY;
       Drawbox(out);
       SetTextStyle(2,Horizdir,8);
       out[1]:=Rx(0.03);
       out[2]:=Ry(0.03);
       out[3]:=Rx(0.97);
       out[4]:=Ry(0.3);
       SetTextStyle(2,Horizdir,6);
       ReadIn(f):
       ReadIn(f,n);
       Str(n:2,s);
       Outtextxy(Rx(0.5),Ry(0.05),s);
       Readin(f);
       ReadIn(f,s);
       Outtextxy(Rx(0.2),Ry(0.05),s);
       ReadIn(f);
       ReadIn(f,s);
       Outtextxy(Rx(0.8),Ry(0.05),s);
       ReadIn(f);
       ReadIn(f,r);
       Str(r:5:2,s);
       Outtextxy(Rx(0.2),Ry(0.1),s);
       ReadIn(f);
       Readin(f,r);
       Str(r:5:2,s);
       Outtextxy(Rx(0.2),Ry(0.15),s);
       ReadIn(f);
       ReadIn(f,r);
       Str(r:5:2,s);
       Outtextxy(Rx(0.2),Ry(0.2),s);
       Readin(f);
       ReadIn(f,r);
       Str(r:5:2,s);
```

```
Outtextxy(Rx(0.2),Ry(0.25),s);
ReadIn(f):
ReadIn(f.r):
Str(r:5:2,s);
Outtextxy(Rx(0.5),Ry(0.1),s);
Readin(f):
ReadIn(f.r):
Str(r:2:4.s):
Outtextxy(Rx(0.8),Ry(0.1),s);
Readin(f):
ReadIn(f.r):
Str(r:5:2,s);
Outtextxy(Rx(0.5),Ry(0.15),s);
ReadIn(f):
Readin(f,r);
Str(r:2:4,s);
Outtextxy(Rx(0.8),Ry(0.15),s);
Readin(f):
Readin(f.r):
Str(r:5:2,s);
Outtextxy(Rx(0.5),Ry(0.2),s);
ReadIn(f):
Readin(f.r):
Str(r:2:4,s);
Outtextxy(Rx(0.8),Ry(0.2),s);
Readin(f);
ReadIn(f,s);
Outtextxy(Rx(0.5),Ry(0.25),s);
SetColor(15);
Outtextxy(Rx(0.05),Ry(0.92),'Press any key to continue');
Outtextxy(Rx(0.05),Ry(0.05),'Sample:');
Outtextxy(Rx(0.05),Ry(0.1),'Vf:');
Outtextxy(Rx(0.05),Ry(0.15),'B%:');
Outtextxy(Rx(0.05),Ry(0.2),'Width:');
Outtextxy(Rx(0.05),Ry(0.25),'Thickness:');
Outtextxy(Rx(0.35),Ry(0.05),'Points:');
Outtextxy(Rx(0.35),Ry(0.1),'n:');
Outtextxy(Rx(0.35),Ry(0.15),'delta:');
Outtextxy(Rx(0.35),Ry(0.2),'A1:');
Outtextxy(Rx(0.35),Ry(0.25),'Remarks:');
Outtextxy(Rx(0.65),Ry(0.05),'Date:');
Outtextxy(Rx(0.65),Ry(0.1),'R:');
Outtextxy(Rx(0.65),Ry(0.15),'R:'):
Outtextxy(Rx(0.65),Ry(0.2),'R:');
Drawbox(out);
out[1]:=Rx(0.03);
out[2]:=Ry(0.33);
out[3]:=Rx(0.97);
out[4]:=Ry(0.97);
Drawbox(out);
```

```
For i:=1 to 6 do readln(f);
     Outtextxy(Rx(0.06),Ry(0.34),' a');
     Outtextxy(Rx(0.21),Ry(0.34),'e');
     Outtextxy(Rx(0.36),Ry(0.34),' P');
      Outtextxy(Rx(0.51),Ry(0.34),'MBT');
      Outtextxy(Rx(0.66),Ry(0.34),'CC');
      Outtextxy(Rx(0.81),Ry(0.34),'MCC');
      SetColor(14);
      For i:=1 to n do
      beain
         ReadIn(f,r);
         Str(r:5:2,s);
         Outtextxy(Rx(0.05),Ry(0.35+i*0.04),s);
         Readin(f,r);
         Str(r:5:2,s);
         Outtextxy(Rx(0.2),Ry(0.35+i*0.04),s);
         ReadIn(f,r);
         Str(r:5:2,s);
         Outtextxy(Rx(0.35),Ry(0.35+i*0.04),s);
         Readin(f,r):
         Str(r:4:0,s);
         Outtextxy(Rx(0.5),Ry(0.35+i*0.04),s);
         ReadIn(f,r);
         Str(r:4:0,s);
         Outtextxy(Rx(0.65),Ry(0.35+i*0.04),s);
         Readin(f,r);
         Str(r:4:0,s);
         Outtextxy(Rx(0.8),Ry(0.35+i*0.04),s);
      end;
      close(f);
      While not KeyPressed do;
      Closegraph;
   end;
end;
var choice,np:byte;
  sa,inp,outp,lc,rem:string;
  wg.wb:real;
  b:boolean;
  he:head;
  le:lead;
  da:dat:
begin
   Initialize;
   b:=true;
   Choice:=Screen1;
   If (Choice=3) then Bye
```

```
else while b do
  begin
     if (Choice=1) then
     begin
        Screen2(sa,inp,outp,rem,lc,wg,wb,np);
        Calc(sa,inp,outp,rem,wg,wb,np);
     end
     else
     begin
        if (choice=2) then
        begin
            Cirscr;
            Le[1]:='File name:';
            He[1]:=";
            Tableinput(1,1,he,le,da);
            if da[1,1]<>" then outp:=da[1,1];
         end;
     end:
      Choice:=Screen4;
      If (Choice=5) then b:=false
       else if (Choice=2) then
       Begin
           PresentGraphs(outp);
           Choice:=Screen1;
           If (Choice=3) then b:=false;
        end
           else if (Choice=3) then
           Begin
              Showdata(outp);
              Choice:=Screen1;
              If (Choice=3) then b:=false;
           end
              else if (Choice=4) then
              Begin
                 Printdata(outp);
                  Choice:=Screen1;
                  If (Choice=3) then b:=false;
              end;
   end;
end.
```

Data for chapter 3

Table AllI.1 0° Flexure data for statistical analysis as described in chapter 3

V _f	Binder Strength		Modulus
(%)	(%)	(ksi)	(Msi)
21.6	5.9	105	3.58
21.6	5.9	92	3.07
21.6	5.9	86	2.83
21.6	5.9	88	2.76
21.6	5.9	80	2.80
21.6	5.9	65	2.12
21.6	5.9	88	2.78
21.6	5.9	77	2.62
24.8	3.1	94	3.04
24.8	3.1	88	2.90
24.8	3.1	91	2.99
24.8	3.1	94	3.17
24.8	3.1	88	2.85
24.8	3.1	90	2.93
24.8	3.1	108	3.25
24.8	3.1	92	3.02
27.7	2.2	88	3.01
27.7	2.2	91	3.02
27.7	2.2	98	3.12
27.7	2.2	107	3.34
26.1	2.1	101	3.39
26.1	2.1	86	2.85
26.1	2.1	94	2.93
26.1	2.1	101	3.27
26.1	2.1	87	2.96
26.1	2.1	69	2.29
27.0	1.6	104	3.50
27.0	1.6	94	3.24
27.0	1.6	95	3.08
23.3	4.7	57	2.01
23.3	4.7	89	2.89
23.3	4.7	97	3.16
23.3	4.7	87	2.72
23.3	4.7	77	2.48
23.3	4.7	88	2.68
23.3	4.7	82	2.66
23.3	4.7	94	2.94
30.5	2.3	135	4.33
30.5	2.3	111	3.68
30.5	2.3	107	3.58

V _f	Binder	Strength	Modulus
(%)	(%)	(ksi)	(Msi)
30.5	2.3	105	3.58
30.5	2.3	120	4.05
30.5	2.3	83	2.76
30.5	2.3	99	3.17
27.1	3.2	102	3.60
27.1	3.2	91	2.81
27.1	3.2	86	2.74
26.7	3.2	81	2.48
26.7	3.2	123	4.05
26.7	3.2	94	2.96
26.7	3.2	113	3.61
26.7	3.2	86	2.79
17.0	4.2	78	2.48
17.0	4.2	72	2.28
17.0	4.2	67	2.11
23.4	4.4	88	2.91
23.4	4.4	85	2.77
23.4	4.4	91	3.04
23.6	4.1	82	2.66
23.6	4.1	90	2.92
25.7	1.7	82	2.76
25.7	1.7	80	2.71
25.7	1.7	98	3.07
22.9	5.0	90	3.07
22.9	5.0	94	3.32
22.9	5.0	107	3.49
25.8	3.2	100	3.26
25.8	3.2	102	3.54
25.8	3.2	90	2.93
25.8	3.2	104	3.27
25.8	3.2	101	3.38
25.8	3.2	94	3.16
25.8	3.2	105	3.35
25.8	3.2	99	3.23
21.6	5.0	87	2.79
21.6	5.0	85	2.72
21.6	5.0	85	2.74
21.5	6.0	76	2.43
21.5	6.0	83	2.73
21.5	6.0	86	2.88

Table AllI.2 90° Flexure data for statistical analysis as described in chapter 3

Vf	Binder	Strength Modul	
(%)	(%)	(ksi)	(ksi)
21.6	5.9	3.70	641
21.6	5.9	3.76	553
21.6	5.9	3.80	588
24.8	3.1	4.05	742
24.8	3.1	4.20	788
24.8	3.1	3.58	814
27.7	2.2	3.65	637
27.7	2.2	3.41	737
27.7	2.2	3.63	725
26.1	2.1	4.11	684
26.1	2.1	3.67	752
26.1	2.1	3.48	663
27.0	1.6	2.98	750
27.0	1.6	3.75	778
27.0	1.6	3.75	892
27.0	1.6	4.36	653
23.3	4.7	3.27	566
23.3	4.7	3.06	575
23.3	4.7	3.01	669
23.3	4.7	2.84	581
30.5	2.3	4.11	952
30.5	2.3	5.48	916
27.1	3.2	4.08	803
27.1	3.2	4.29	871
27.1	3.2	4.54	818
27.1	3.2	3.51	896
27.1	3.2	4.32	887
27.1	3.2	4.04	816
27.1	3.2	2.99	723
27.1	3.2	4.23	832
26.7	3.2	4.14	824
23.4	4.4	4.05	848
23.4	4.4	6.13	859
23.4	4.4	6.20	912
23.4	4.4	4.11	876
23.4	4.4	3.49	947
23.4	4.4	4.76	875
23.6	4.1	3.91	820

Vf	Binder	Strength	Modulus
(%)	(%)	(ksi)	(ksi)
23.6	4.1	4.46	730
23.6	4.1	3.91	774
23.6	4.1	3.52	760
23.6	4.1	3.57	771
23.6	4.1	3.62	779
23.6	4.1	3.93	678
23.6	4.1	3.77	761
25.7	1.7	3.97	791
25.7	1.7	5.26	868
25.7	1.7	3.55	762
25.7	1.7	4.08	766
25.7	1.7	4.03	811
25.7	1.7	3.91	801
25.7	1.7	3.73	760
25.7	1.7	3.92	807
22.9	5.0	5.00	736
22.9	5.0	3.58	710
22.9	5.0	4.24	812
22.9	5.0	3.27	760
22.9	5.0	3.16	767
22.9	5.0	3.64	762
22.9	5.0	4.19	789
22.9	5.0	3.41	747
25.8	3.2	3.97	586
25.8	3.2	4.04	645
25.8	3.2	2.85	588
21.6	5.0	3.71	680
21.6	5.0	4.00	698
21.6	5.0	4.05	738
21.6	5.0	3.69	692
21.6	5.0	3.76	696
21.6	5.0	4.00	742
21.6	5.0	3.82	696
21.6	5.0	3.72	727
21.5	6.0	3.21	638
21.5	6.0	3.77	636
21.5	6.0	3.69	635

Table All.2 (cont'd)

V _f	Binder	Strength	Modulus
(%)	(%)	(ksi)	(ksi)
21.5	6.0	4.03	609
21.5	6.0	3.24	580
21.5	6.0	4.29	612
21.5	6.0	3.43	639
21.5	6.0	3.33	629
26.7	1.2	4.07	799
26.7	1.2	4.26	790
26.7	1.2	4.16	756

Data for chapter 4

Table AIV.1 Particle size data for Figure 4.2

A ₁₂ (MPa)	Particle size (µm)				
	Number Volume				
	average average				
104.2	1.464	1.596			
204.8	1.134 1.163				
105.9	0.968 1.014				
87.4	1.122 1.198				
230.5	0.98	1.073			

Table AIV.2 Particle size data for Figure 4.3

End group mass	Backbone mass	δ _{total} (MPa ^{1/2})	Volume average size
(g/mole)	(g/mole)	(MPa ^{1/2})	(μ m)
219	4200	21.9	1.198
107	4200	17.1	1.014
93	4200	16.4	1.596
15	14000	31.0	1.073
17	2000	67.8	1.163

APPENDIX V

Data for chapter 5

APPENDIX V

Table AV.1 Miscibility data for Figure 5.3

280 K		30	0 K	32	0 K	expe	riment	
	Polyester	Acetone	Polyester	Acetone	Polyester	Acetone	Polyester	Acetone
	3.53E-07	0.446315	1.25E-06	0.446315	4.02E-06	0.446315	0.064576	0.948817
	2.67E-05	0.51802	0.000068	0.51802	0.000159	0.51802	0.090106	0.940582
	0.000557	0.580159	0.00112	0.580159	0.002132	0.580159	0.130605	0.925889
ı	0.004928	0.634526	0.00846	0.634526	0.014039	0.634526	0.202922	0.925967
	0.025141	0.682494	0.0392	0.682494	0.060386	0.682494	0.264091	0.918999
	0.093493	0.72513	0.142	0.72513	0.220005	0.72513	0.32586	0.910189
	0.118815	0.733094	0.181	0.733094	0.287432	0.729134	0.463822	0.848616
	0.152209	0.740886	0.234	0.740886	0.587557	0.729134	0.470588	0.856889
	0.194737	0.74851	0.389	0.74851	0.615499	0.72513	0.57916	0.765835
	0.253301	0.755971	0.5208	0.74851	0.795113	0.682494	0.623053	0.801653
	0.299791	0.759643	0.563294	0.740886	0.876603	0.634526		
	0.546247	0.759643	0.644481	0.733094	0.922651	0.580159		
	0.591246	0.755971	0.708284	0.72513	0.952742	0.51802		
	0.654958	0.74851	0.8264	0.682494	0.972874	0.446315		
	0.697498	0.740886	0.8938	0.634526			_	
	0.734288	0.733094	0.9331	0.580159				
	0.770155	0.72513	0.9591	0.51802				
	0.857646	0.682494	0.9766	0.446315				
	0.910647	0.634526			-			
	0.944999	0.580159						
	0.969256	0.51802						
i	0.983339	0.446315						

Table AV.2 Sieve data for Figure 5.5

sieve size	weight fraction
< 125 μm	0.017551
125-180 μm	0.117632
180-250 μm	0.412397
250-355 μm	0.319063
> 355 µm	0.133357

Data for chapter 6

Table AVI.1 Fracture toughness data for Figures 6.4 and 6.5

V _f	Rubber	Gic	Standard
(%)	(%)	(J/m ²)	deviation
			(J/m ²)
19.6	5.7	905	87
18.5	5.5	1305	131
18.0	5.5	1141	129
19.1	8.5	1345	131
18.8	8.5	1175	73
19.3	8.5	1301	58
20.2	5.8	1818	192
19.9	5.8	1460	140
19.2	5.7	1607	289
19.7	10.2	938	117
20.8	10.2	1263	132
20.0	10.2	1031	130
22.4	10.3	1559	127
19.0	9.9	1287	71
19.4	10.2	1406	218
20.6	0.0	829	37
20.8	0.0	792	34
21.7	0.0	852	65
17.5	5.3	3014	416
21.1	10.3	2367	738

Table AVI.2 Data for Figures 6.9 and 6.10

	Modulus (Msi)		Streng	th (ksi)
Binder (%)	Average	Standard deviation	Average	Standard deviation
0.0	0.63	0.02	10.4	0.6
5.3	0.47	0.04	7.7	1.2
5.8	0.45	0.05	6.7	0.9
9.2	0.96	0.08	11.4	0.4
9.9	0.76	0.05	8.9	1.3
10.2	0.74	0.03	6.0	0.6

Data for chapter 7

Table AVII.1 Fracture toughness data for Figures 7.1 and 7.2

V _f	Rubber	Gic	Standard
(%)	(%)	(J/m ²)	deviation
			(J/m ²)
19.7	5.8	1629	129
19.6	5.8	1547	101
19.6	5.8	1809	147
19.9	8.7	1405	63
20.0	8.7	1531	74
20.1	8.7	1343	48
19.8	10.3	1443	91
19.7	10.3	1415	100
19.8	10.3	1302	69

ı	
)	•
ı	ı
•	!
	• ;
,	i
	٠
•	•
	ý.
	,
	,
	•
	:
	1
	•
	•
	1
	,
	:
	:
	÷
	,
	•
	,
	;
•	
	:
	÷
	,
	A.
	•